



Measurement of long-range multi-particle azimuthal correlations with the subevent cumulant method in pp and $p+Pb$ collisions with the ATLAS detector at the LHC

The ATLAS Collaboration

A detailed study of multi-particle azimuthal correlations is presented using pp data at $\sqrt{s} = 5.02$ and 13 TeV, and $p+Pb$ data at $\sqrt{s_{NN}} = 5.02$ TeV, recorded with the ATLAS detector at the LHC. The azimuthal correlations are probed using four-particle cumulants $c_n\{4\}$ and flow coefficients $v_n\{4\} = (-c_n\{4\})^{1/4}$ for $n = 2$ and 3, with the goal of extracting long-range multi-particle azimuthal correlation signals and suppressing the short-range correlations. The values of $c_n\{4\}$ are obtained as a function of the average number of charged particles per event, $\langle N_{ch} \rangle$, using the recently proposed two-subevent and three-subevent cumulant methods, and compared with results obtained with the standard cumulant method. The standard method is found to be strongly biased by short-range correlations, which originate mostly from jets with a positive contribution to $c_n\{4\}$. The three-subevent method, on the other hand, is found to be least sensitive to short-range correlations. The three-subevent method gives a negative $c_2\{4\}$, and therefore a well-defined $v_2\{4\}$, nearly independent of $\langle N_{ch} \rangle$, which implies that the long-range multi-particle azimuthal correlations persist to events with low multiplicity. Furthermore, $v_2\{4\}$ is found to be smaller than the $v_2\{2\}$ measured using the two-particle correlation method, as expected for long-range collective behavior. Finally, the measured values of $v_2\{4\}$ and $v_2\{2\}$ are used to estimate the number of sources relevant for the initial eccentricity in the collision geometry. The results based on the subevent cumulant technique provide direct evidence, in small collision systems, for a long-range collectivity involving many particles distributed across a broad rapidity interval.

1 Introduction

The study of azimuthal correlations in high-energy nuclear collisions at the Relativistic Heavy Ion Collider (RHIC) and the Large Hadron Collider (LHC) has been important for understanding the multi-parton dynamics of QCD in the strongly coupled non-perturbative regime. One striking observation is the long-range “ridge” [1–5] in two-particle angular correlations (2PC): an apparent collimated emission of particle pairs with small relative azimuthal angle ($\Delta\phi$) and large separation in pseudorapidity ($\Delta\eta$). The ridge signature from 2PC is characterized by a Fourier decomposition of the correlation function $C(\Delta\phi) \sim 1 + 2 \sum_n v_n^2 \cos(n\Delta\phi)$, where v_n denotes the single-particle anisotropy harmonic coefficients. The second-order coefficient v_2 is observed to be the largest, followed by v_3 [3, 4]. These coefficients carry information about the collective behavior of the produced system. The ridge was first discovered in nucleus–nucleus (A+A) collisions [1–6], but was later observed in small systems such as proton–nucleus (p +A) collisions [7–11], light-ion–nucleus collisions [12], and more recently in proton–proton (pp) collisions [13–16]. The ridge in large systems, such as central or mid-central A+A collisions, is commonly interpreted as the result of collective hydrodynamic expansion of hot and dense nuclear matter created in the overlap region of the colliding nuclei. Since the formation of an extended region of nuclear matter is not expected in small collision systems such as p +A and pp , the origin of the ridge there could be different from that formed in large collision systems. There remains considerable debate in the theoretical community as to whether the ridge in small systems is of hydrodynamic origin, like it is in A+A collisions [17], or stems from other effects such as initial-state gluon saturation [18].

An important question about the ridge is whether it involves all particles in the event (collective flow) or if it arises merely from correlations among a few particles, due to resonance decays, jets, or multi-jet production (non-flow). In small systems the contributions from non-flow sources, in particular from jets and dijets, are large. The extraction of a ridge signal using the 2PC method requires a large $\Delta\eta$ gap and careful removal of the significant contribution from dijet production [8–10, 14, 15, 19]. Since collective flow is intrinsically a multi-particle phenomenon, it can be probed more directly using cumulants based on multi-particle correlation techniques [20]. Azimuthal correlations involving four, six, and eight particles have been measured in p +Pb, d+Au and pp collisions, and a significant v_2 signal has been obtained [11, 19, 21, 22]. One weakness of the standard multi-particle cumulant method is that it does not suppress adequately the non-flow correlations in small systems, which lead to a sign-change of $c_2\{4\}$ at smaller values of the charged particle multiplicity, N_{ch} [11, 16, 19, 21]. Furthermore, the magnitude of $c_2\{4\}$ and the N_{ch} value at which the sign change occurs are found to depend sensitively on the exact definition of N_{ch} used to categorize the events. These observations suggest that the standard cumulant method, on which several previous measurements in small systems are based, is strongly contaminated by non-flow correlations [11, 19, 21, 22], especially in pp collisions and low N_{ch} region.

Recently an improved cumulant method based on the correlation between particles from different subevents separated in η has been proposed to further reduce the non-flow correlations [23]. The effectiveness of this method for suppressing non-flow correlations has been validated using the PYTHIA8 event generator [24], which contains only non-flow correlations.

This paper presents measurements of $c_2\{4\}$ and $c_3\{4\}$ in pp collisions at $\sqrt{s} = 5.02$ and 13 TeV, as well as p +Pb collisions at $\sqrt{s_{\text{NN}}} = 5.02$ TeV. They are obtained using two- and three-subevent cumulant methods and are compared with the standard cumulant method. The $c_2\{4\}$ cumulant is converted to the corresponding v_2 coefficient and compared with the results obtained using the two-particle correlation method in Refs. [10, 15] to assess the nature of the event-by-event fluctuation of the collective flow in these collisions.

The paper is organized as follows. Section 2 describes the framework for the standard, two-subevent and three-subevent four-particle cumulant methods used in this analysis. Details of the detector, trigger, datasets, as well as event and track selections are provided in Sections 3 to 5. The correlation analysis and systematic uncertainties are described in Sections 6 and 7, respectively. The measured cumulants from the three datasets are provided in Section 8. A summary is given in Section 9.

2 Four-particle cumulants

The multi-particle cumulant method [20] is used to extract the amplitude of long-range azimuthal correlations of particles produced in high-energy collisions. This method has the advantage of suppressing correlations from jets and dijets, instead of relying on an explicit procedure to correct v_n harmonics for dijet contributions in the 2PC approach, as done in Refs. [10, 14]. The framework for the standard cumulant is described in Refs. [25, 26], which was recently extended to the case of subevent cumulants in Ref. [23]. This paper presents measurements of four-particle cumulants obtained with the standard, two-subevent and three-subevent methods. The following discussion first describes the standard cumulant method, then describes the two- and three-subevent methods focusing on the differences from the standard method.

The cumulant methods involve the calculation of $2k$ -particle azimuthal correlations $\langle\{2k\}_n\rangle$, and $2k$ -particle cumulants, $c_n\{2k\}$, for the n^{th} -order flow harmonics. The two- or four-particle azimuthal correlations in one event are evaluated as [23, 25, 26]:

$$\langle\{2\}_n\rangle = \langle e^{in(\phi_1 - \phi_2)} \rangle = \frac{q_n^2 - \tau_1}{1 - \tau_1}, \quad (1)$$

$$\langle\{4\}_n\rangle = \langle e^{in(\phi_1 + \phi_2 - \phi_3 - \phi_4)} \rangle = \frac{q_n^4 - 2\tau_1(\text{Re}[q_{2n;2}q_n^{*2}] + 2q_n^2) + 8\tau_2\text{Re}[q_{n;3}q_n^*] + \tau_1^2(2 + q_{2n;2}^2) - 6\tau_3}{1 - 6\tau_1 + 8\tau_2 + 3\tau_1^2 - 6\tau_3}, \quad (2)$$

where “ $\langle \rangle$ ” denotes a single-event average over all pairs or quadruplets, respectively. The averages from Eqs. (1) and (2) are expanded into per-particle normalized flow vectors $\mathbf{q}_{n;l}$ and factors τ_l with $l = 1, 2, \dots$:

$$\mathbf{q}_{n;l} \equiv \frac{\sum_j w_j^l e^{in\phi_j}}{\sum_j w_j^l}, \quad q_{n;l} \equiv |\mathbf{q}_{n;l}|, \quad q_n \equiv q_{n;1}, \quad \tau_l \equiv \frac{\sum_j w_j^{l+1}}{(\sum_j w_j)^{l+1}}, \quad (3)$$

where the sum runs over all M particles in the event and w_j is a weight assigned to the j^{th} particle. This weight is constructed to correct for both detector non-uniformity and tracking inefficiency as explained in Section 6. For unit weight $w_j = 1$, then $\mathbf{q}_{mn;m} = \mathbf{q}_{mn}$, and $\tau_l = 1/M^l$.

The two- and four-particle cumulants are obtained from the azimuthal correlations as:

$$c_n\{2\} = \langle\langle\{2\}_n\rangle\rangle, \quad (4)$$

$$c_n\{4\} = \langle\langle\{4\}_n\rangle\rangle - 2\langle\langle\{2\}_n\rangle\rangle^2, \quad (5)$$

where “ $\langle\langle \rangle\rangle$ ” represents a weighted average of $\langle\{2k\}_n\rangle$ over an event ensemble. In the absence of non-flow correlations, $c_n\{2k\}$ reflects the moments of the distribution of the flow coefficient v_n :

$$c_n\{2\}_{\text{flow}} = \langle v_n^2 \rangle, \quad c_n\{4\}_{\text{flow}} = \langle v_n^4 \rangle - 2\langle v_n^2 \rangle^2. \quad (6)$$

If harmonic coefficients do not fluctuate event by event, Eq. (6) gives $c_n\{2\}_{\text{flow}} = v_n^2$, $c_n\{4\}_{\text{flow}} = -v_n^4$, and $c_n\{4\}_{\text{flow}}$ is expected to be negative. Therefore, the flow coefficients from two- and four-particle cumulants are defined as:

$$v_n\{2\} = \sqrt{c_n\{2\}}, \quad v_n\{4\} = \sqrt[4]{-c_n\{4\}}. \quad (7)$$

In the standard cumulant method described so far, all $2k$ -particle multiplets involved in $\langle\{2k\}_n\rangle$ are selected using the entire detector acceptance. To further suppress the non-flow correlations that typically involve particles emitted within a localized region in η , the particles can be grouped into several subevents, each covering a non-overlapping η interval [23]. The multi-particle correlations are then constructed by correlating particles between different subevents, further reducing non-flow correlations. This analysis uses the subevent cumulant methods based on two and three subevents as described in the following.

In the two-subevent cumulant method, the entire event is divided into two subevents, labeled as a and b , for example according to $-\eta_{\text{max}} < \eta_a < 0$ and $0 < \eta_b < \eta_{\text{max}}$, where $\eta_{\text{max}} = 2.5$ is the maximum η used in the analysis and corresponds to the ATLAS detector acceptance for charged particles. The per-event two- and four-particle azimuthal correlations are then evaluated as:

$$\langle\{2\}_n\rangle_{a|b} = \left\langle e^{in(\phi_1^a - \phi_2^b)} \right\rangle = \text{Re}[\mathbf{q}_{n,a} \mathbf{q}_{n,b}^*], \quad (8)$$

$$\langle\{4\}_n\rangle_{2a|2b} = \left\langle e^{in(\phi_1^a + \phi_2^a - \phi_3^b - \phi_4^b)} \right\rangle = \frac{(\mathbf{q}_n^2 - \tau_1 \mathbf{q}_{2n})_a (\mathbf{q}_n^2 - \tau_1 \mathbf{q}_{2n})_b^*}{(1 - \tau_1)_a (1 - \tau_1)_b}, \quad (9)$$

where the superscript or subscript a (b) indicates particles chosen from the subevent a (b). Here the four-particle cumulant is defined as:

$$c_n^{2a|2b}\{4\} = \langle\{4\}_n\rangle_{2a|2b} - 2 \langle\{2\}_n\rangle_{a|b}^2. \quad (10)$$

The two-subevent method should suppress correlations within a single jet (intra-jet correlations), since each jet usually emits particles into only one subevent.

In the three-subevent cumulant method, the event is divided into three subevents a , b and c each covering a unique η range, for example $-\eta_{\text{max}} < \eta_a < -\eta_{\text{max}}/3$, $|\eta_b| < \eta_{\text{max}}/3$ and $\eta_{\text{max}}/3 < \eta_c < \eta_{\text{max}}$. The four-particle azimuthal correlations and cumulants are then evaluated as:

$$\langle\{4\}_n\rangle_{2a|b,c} = \left\langle e^{in(\phi_1^a + \phi_2^a - \phi_3^b - \phi_4^c)} \right\rangle = \frac{(\mathbf{q}_n^2 - \tau_1 \mathbf{q}_{2n})_a \mathbf{q}_{n,b}^* \mathbf{q}_{n,c}^*}{(1 - \tau_1)_a}, \quad (11)$$

$$c_n^{2a|b,c}\{4\} \equiv \langle\{4\}_n\rangle_{2a|b,c} - 2 \langle\{2\}_n\rangle_{a|b} \langle\{2\}_n\rangle_{a|c}, \quad (12)$$

where $\langle\{2\}_n\rangle_{a|b}$ and $\langle\{2\}_n\rangle_{a|c}$ are two-particle correlators defined as in Eq. (8). Since the two jets in a dijet event usually produce particles in at most two subevents, the three-subevent method further suppresses non-flow contributions from inter-jet correlations associated with dijets. To enhance the statistical precision, the η range for subevent a is also interchanged with that for subevent b or c , and the resulting three $c_n^{2a|b,c}\{4\}$ values are averaged to obtain the final result.

3 Detector and trigger

The ATLAS detector [27] provides nearly full solid-angle coverage around the collision point with tracking detectors, calorimeters, and muon chambers, and is well suited for measurement of multi-particle correlations over a large pseudorapidity range¹. The measurements were performed primarily using the inner detector (ID), minimum-bias trigger scintillators (MBTS) and the zero-degree calorimeters (ZDC). The ID detects charged particles within $|\eta| < 2.5$ using a combination of silicon pixel detector, a silicon microstrip detector (SCT), and a straw-tube transition radiation tracker, all immersed in a 2 T axial magnetic field [28]. An additional pixel layer, the “insertable B-layer” (IBL) [29] installed between Run 1 (2010–2013) and Run 2 (2015–2018), is available for the Run-2 datasets. The MBTS, rebuilt before Run 2, detects charged particles within $2.1 \lesssim |\eta| \lesssim 3.9$ using two hodoscopes of counters positioned at $z = \pm 3.6$ m. The ZDC are positioned at ± 140 m from the collision point, and detect neutral particles, primarily neutrons and photons, with $|\eta| > 8.3$.

The ATLAS trigger system [30] consists of a Level-1 (L1) trigger implemented using a combination of dedicated electronics and programmable logic, and a high-level trigger (HLT) implemented in processors. The HLT reconstructs charged-particle tracks using methods similar to those applied in the offline analysis, allowing high-multiplicity track (HMT) triggers that select events based on the number of tracks with $p_T > 0.4$ GeV associated with the vertex with the largest number of tracks. The different HMT triggers also apply additional requirements on either the transverse energy (E_T) in the calorimeters or on the number of hits in the MBTS at L1, and on the number of charged-particle tracks reconstructed by the HLT. The pp and p +Pb data were collected using a combination of the minimum-bias and HMT triggers. More details of the triggers used for the pp and p +Pb data can be found in Refs. [15, 31] and Refs. [10, 32], respectively.

4 Datasets and Monte Carlo simulations

This analysis uses integrated luminosities of 28 nb^{-1} of p +Pb data recorded at $\sqrt{s_{\text{NN}}} = 5.02$ TeV, 0.17 pb^{-1} of pp data recorded at $\sqrt{s} = 5.02$ TeV, and 0.9 pb^{-1} of pp data recorded at $\sqrt{s} = 13$ TeV, all taken by the ATLAS experiment at the LHC. The p +Pb data were mainly collected in 2013, but also include 0.3 nb^{-1} data collected in November 2016 which increases the number of events at moderate multiplicity (see Section 5). During both p +Pb runs, the LHC was configured with a 4 TeV proton beam and a 1.57 TeV per-nucleon Pb beam that together produced collisions at $\sqrt{s_{\text{NN}}} = 5.02$ TeV, with a rapidity shift of 0.465 of the nucleon–nucleon center-of-mass frame towards the proton beam direction relative to the ATLAS rest frame. The direction of the Pb beam is always defined to have negative pseudorapidity. The 5.02 TeV pp data were collected in November 2015. The 13 TeV pp data were collected during several special low-luminosity runs of the LHC in 2015 and 2016.

Monte Carlo (MC) simulated event samples are used to determine the track reconstruction efficiency (Section 5). The 13 TeV and 5.02 TeV pp data were simulated by the PYTHIA8 MC event generator [24] using the A2 set of tuned parameters with MSTW2008LO parton distribution functions [33]. The HIJING

¹ ATLAS typically uses a right-handed coordinate system with its origin at the nominal interaction point (IP) in the center of the detector and the z -axis along the beam pipe. The x -axis points from the IP to the center of the LHC ring, and the y -axis points upward. Cylindrical coordinates (r, ϕ) are used in the transverse plane, ϕ being the azimuthal angle around the beam pipe. By default, the pseudorapidity is defined in terms of the polar angle θ as $\eta = -\ln \tan(\theta/2)$. However, for asymmetric p +Pb or Pb+ p collisions, the $-z$ direction is always defined as the direction of the Pb beam.

event generator [34] was used to produce p+Pb collisions with the same energy and the same boost of the center-of-mass system as in the data. The detector response was simulated using GEANT4 [35, 36] with detector conditions matching those during the data-taking. The simulated events and data events are reconstructed with the same algorithms, including those for track reconstruction.

5 Event and track selection

The offline event selection for the p+Pb and pp data requires at least one reconstructed vertex with its longitudinal position satisfying $|z_{\text{vtx}}| < 100$ mm. The vertex is required to have at least two associated tracks with $p_T > 0.4$ GeV. The mean collision rate per bunch crossing μ was approximately 0.03 for the 2013 p+Pb data, 0.001–0.006 for the 2016 p+Pb data, 0.02–1.5 for 5.02 TeV pp data and 0.002–0.8 for the 13 TeV pp data. In order to suppress additional interactions in the same bunch crossing (referred to as pileup) in pp collisions, events containing additional vertices with at least four associated tracks are rejected. In p+Pb collisions, events with more than one good vertex, defined as any vertex for which the scalar sum of the p_T of the associated tracks is greater than 5 GeV, are rejected. The remaining pileup events are further suppressed by using the signal in the ZDC on the Pb-fragmentation side. This signal is calibrated to the number of detected neutrons (N_n) by using the location of the peak corresponding to a single neutron. The distribution of N_n in events with pileup is broader than that for the events without pileup. Hence a simple requirement on the ZDC signal distribution is used to further suppress events with pileup, while retaining more than 98% of the events without pileup. The impact of residual pileup, at a level of $\lesssim 10^{-3}$, is studied by comparing the results obtained from data with different μ values.

Charged-particle tracks and collision vertices are reconstructed using the same algorithms and methods applied in previous minimum-bias pp and p+Pb measurements [10, 14, 31]. For the 2013 p+Pb analysis, tracks are required to have a p_T -dependent minimum number of hits in the SCT. The transverse (d_0) and longitudinal ($z_0 \sin \theta$) impact parameters of the track relative to the primary vertex are both required to be less than 1.5 mm. A more detailed description of the track selection for the 2013 p+Pb data can be found in Ref. [10].

For all the data taken since the start of Run 2, the track selection criteria make use of the IBL, as described in Refs. [14, 31]. Furthermore, the requirements of $|d_0^{\text{BL}}| < 1.5$ mm and $|z_0 \sin \theta| < 1.5$ mm are applied, where d_0^{BL} is the transverse impact parameter of the track relative to the beam line (BL).

The cumulants are calculated using tracks passing the above selection requirements, and having $|\eta| < 2.5$ and $0.3 < p_T < 3$ GeV or $0.5 < p_T < 5$ GeV. These two p_T ranges are chosen because they were often used in previous ridge measurements at the LHC [11, 14–16, 19]. However, to count the number of reconstructed charged particles for event-class definition (denoted by $N_{\text{ch}}^{\text{rec}}$), tracks with $p_T > 0.4$ GeV and $|\eta| < 2.5$ are used for compatibility with the requirements in the HLT selections described above. Due to different trigger requirements, most of the p+Pb events with $N_{\text{ch}}^{\text{rec}} > 150$ are provided by the 2013 dataset, while the 2016 dataset provides most of the events at lower $N_{\text{ch}}^{\text{rec}}$.

The efficiency of the combined track reconstruction and selection requirements in data is estimated using the MC samples reconstructed with the same tracking algorithms and the same track selection requirements. Efficiencies, $\epsilon(\eta, p_T)$, are evaluated as a function of track η , p_T and the number of reconstructed charged-particle tracks, but averaged over the full range in azimuth. For all collision systems, the efficiency increases by about 4% as p_T increases from 0.3 GeV to 0.6 GeV. Above 0.6 GeV, the efficiency is independent of p_T and reaches 86% (72%) at $\eta \approx 0$ ($|\eta| > 2$) for pp collisions and 83% (70%) for

p +Pb collisions, respectively. The efficiency is independent of the event multiplicity for $N_{\text{ch}}^{\text{rec}} > 40$. For lower-multiplicity events the efficiency is smaller by up to a few percent due to broader d_0^{BL} and $z_0 \sin \theta$ distributions.

The rate of falsely reconstructed charged-particle tracks is also estimated and found to be negligibly small in all datasets. This rate decreases with increasing p_{T} , and even at the lowest transverse momenta of 0.2 GeV it is below 1% of the total number of tracks. Therefore, there is no correction for the presence of these tracks in the analysis.

In the simulated events, the reconstruction efficiency reduces the measured charged-particle multiplicity relative to the generated multiplicity for primary charged particles. The multiplicity correction factor b is used to correct $N_{\text{ch}}^{\text{rec}}$ to obtain the efficiency-corrected number of charged particles per event, $\langle N_{\text{ch}} \rangle = b \langle N_{\text{ch}}^{\text{rec}} \rangle$. The value of the correction factor is found to be independent of $N_{\text{ch}}^{\text{rec}}$ in the range used in this analysis. Its value and the associated uncertainties are $b = 1.29 \pm 0.05$ for the 2013 p +Pb collisions and $b = 1.18 \pm 0.05$ for Run-2 p +Pb and pp collisions [37]. Both $c_n\{4\}$ and $v_n\{4\}$ are then studied as a function of $\langle N_{\text{ch}} \rangle$.

6 Data analysis

The multi-particle cumulants are calculated in three steps using charged particles with $|\eta| < 2.5$. In the first step, the multi-particle correlators $\langle \{2k\}_n \rangle$ from Eqs. (1), (2), (8), (9) and (11) are calculated for each event from particles in one of two p_{T} ranges, $0.3 < p_{\text{T}} < 3$ GeV and $0.5 < p_{\text{T}} < 5$ GeV.

In the second step, the correlators $\langle \{2k\}_n \rangle$ are averaged over events with the same $N_{\text{ch}}^{\text{sel}}$, the number of reconstructed charged particles in a given p_{T} range, to obtain $\langle \langle \{2k\}_n \rangle \rangle$ and $c_n\{2k\}$ from Eqs. (4), (10) and (12). In a previous study [16], it was observed that the $c_n\{2k\}$ values varied with the exact definition of $N_{\text{ch}}^{\text{sel}}$. This is because different definitions of $N_{\text{ch}}^{\text{sel}}$ lead to different multiplicity fluctuations and therefore different non-flow correlations associated with these multiplicity fluctuations. The observed dependence of $c_n\{2k\}$ on the definition of $N_{\text{ch}}^{\text{sel}}$ has been attributed to the change in the non-flow correlations when $N_{\text{ch}}^{\text{sel}}$ is changed [16].

In order to further test the sensitivity of $c_n\{2k\}$ to the exact definition of $N_{\text{ch}}^{\text{sel}}$, four different p_{T} requirements are used to define $N_{\text{ch}}^{\text{sel}}$ as follows: when $\langle \{2k\}_n \rangle$ is calculated in the range $0.3 < p_{\text{T}} < 3$ GeV, $N_{\text{ch}}^{\text{sel}}$ is evaluated in four different track p_{T} ranges: $0.3 < p_{\text{T}} < 3$ GeV, $p_{\text{T}} > 0.2$ GeV, $p_{\text{T}} > 0.4$ GeV and $p_{\text{T}} > 0.6$ GeV. When $\langle \{2k\}_n \rangle$ is calculated in $0.5 < p_{\text{T}} < 5$ GeV, $N_{\text{ch}}^{\text{sel}}$ is evaluated in four different track p_{T} ranges: $0.5 < p_{\text{T}} < 5$ GeV, $p_{\text{T}} > 0.2$ GeV, $p_{\text{T}} > 0.4$ GeV and $p_{\text{T}} > 0.6$ GeV. In each case, the $c_n\{2k\}$ value is first calculated for events with the same $N_{\text{ch}}^{\text{sel}}$; the $c_n\{2k\}$ values are then combined in the broader $N_{\text{ch}}^{\text{sel}}$ range of the event ensemble to obtain statistically significant results.

In the third step, the $c_n\{2k\}$ and $v_n\{2k\}$ values obtained for a given $N_{\text{ch}}^{\text{sel}}$ are mapped to a given $\langle N_{\text{ch}}^{\text{rec}} \rangle$, the average number of reconstructed charged particles with $p_{\text{T}} > 0.4$ GeV. The mapping procedure is necessary so that $c_n\{2k\}$ obtained for different $N_{\text{ch}}^{\text{sel}}$ can be compared using a common x -axis defined by $\langle N_{\text{ch}}^{\text{rec}} \rangle$. The $\langle N_{\text{ch}}^{\text{rec}} \rangle$ value is then converted to $\langle N_{\text{ch}} \rangle$, the efficiency-corrected average number of charged particles with $p_{\text{T}} > 0.4$ GeV, as discussed in Section 5.

In order to account for detector inefficiencies and non-uniformity, particle weights used in Eq. (3) are defined as:

$$w_i(\phi, \eta, p_{\text{T}}) = d(\phi, \eta) / \epsilon(\eta, p_{\text{T}}) . \quad (13)$$

The additional weight factor $d(\phi, \eta)$ accounts for non-uniformities in the azimuthal acceptance of the detector as a function of η . All reconstructed charged particles with $p_T > 0.2$ GeV are entered into a two-dimensional histogram $N(\phi, \eta)$, and the weight factor is then obtained as $d(\phi, \eta) \equiv \langle N(\eta) \rangle / N(\phi, \eta)$, where $\langle N(\eta) \rangle$ is the track density averaged over ϕ in the given η bin. This procedure removes most ϕ -dependent non-uniformity from track reconstruction for any azimuthal correlation analysis [16].

7 Systematic uncertainties

The main sources of systematic uncertainty are related to the detector azimuthal non-uniformity, track selection, track reconstruction efficiency, trigger efficiency and pileup. Most of the systematic uncertainties enter the analysis through the particle weights, Eq. (13). Since $c_2\{4\}$ often changes sign in the low $\langle N_{\text{ch}} \rangle$ region, the absolute uncertainties (instead of relative uncertainties) in $c_2\{4\}$ are determined for each source. The uncertainties are typically of the order of 10^{-6} , which translates into an absolute uncertainty of $\sqrt[4]{10^{-6}} = 0.032$ for zero flow signal.

The effect of detector azimuthal non-uniformity is accounted for using the weight factor $d(\phi, \eta)$. The impact of the reweighting procedure is studied by fixing the weight to unity and repeating the analysis. The results are mostly consistent with the nominal results within statistical uncertainties. As a cross-check, the multi-particle correlations are calculated using a mixed-event procedure, where each particle in a $2k$ -multiplet is selected from a different event with similar $N_{\text{ch}}^{\text{rec}}$ ($|\Delta N_{\text{ch}}^{\text{rec}}| < 10$) and similar z_{vtx} ($|\Delta z_{\text{vtx}}| < 10$ mm). The particle weights defined in Eq. (13) are applied for each particle forming the mixed event. The $c_2\{4\}$ signal obtained from the mixed events is less than 0.2×10^{-6} in all datasets.

The systematic uncertainty associated with the track selection is estimated by tightening the $|d_0|$ and $|z_0 \sin \theta|$ requirements. For each variation, the tracking efficiency is re-evaluated and the analysis is repeated. The maximum differences from the nominal results are observed to be less than 0.3×10^{-6} , 0.2×10^{-6} and 0.1×10^{-6} in 5.02 TeV pp , 13 TeV pp and $p+\text{Pb}$ collisions, respectively.

Previous measurements indicate that the azimuthal correlations (both the flow and non-flow components) have a strong dependence on p_T , but a relatively weak dependence on η [10, 15]. Therefore, p_T -dependent systematic effects in the track reconstruction efficiency could affect $c_n\{2k\}$ and $v_n\{2k\}$ values. The uncertainty in the track reconstruction efficiency is mainly due to differences in the detector conditions and material description between the simulation and the data. The efficiency uncertainty varies between 1% and 4%, depending on track η and p_T [15, 16]. Its impact on multi-particle cumulants is evaluated by repeating the analysis with the tracking efficiency varied up and down by its corresponding uncertainty as a function of p_T . For the standard cumulant method, which is more sensitive to jets and dijets, the evaluated uncertainty amounts to $(0.1\text{--}1.5) \times 10^{-6}$ in pp collisions and less than 0.3×10^{-6} in $p+\text{Pb}$ collisions for $\langle N_{\text{ch}} \rangle > 50$. For the two- and three-subevent methods, the evaluated uncertainty is typically less than 0.3×10^{-6} for most of the $\langle N_{\text{ch}} \rangle$ ranges.

Most events used in the analysis are collected with the HMT triggers with several $N_{\text{ch}}^{\text{rec}}$ thresholds. In order to estimate the possible bias due to trigger inefficiency as a function of $\langle N_{\text{ch}} \rangle$, the offline $N_{\text{ch}}^{\text{rec}}$ requirements are changed such that the HMT trigger efficiency is at least 50% or 80%. The results are obtained independently for each variation. These results are found to be consistent with each other for the two- and three-subevent methods, and show a small difference for the standard cumulant method in the

low $\langle N_{\text{ch}} \rangle$ region. The nominal analysis is performed using the 50% efficiency selection and the differences between the nominal results and those from the 80% efficiency selection are used as a systematic uncertainty. The change amounts to $(0.1-0.7)\times 10^{-6}$.

In this analysis, a pileup rejection criterion is applied to reject events containing additional vertices. In order to check the impact of residual pileup, the analysis is repeated without the pileup rejection criterion, and no difference is observed. For the 5.02 and 13 TeV pp datasets, which have relatively high pileup, the data is divided into two samples based on the μ value: $\mu > 0.4$ and $\mu < 0.4$, and the results are compared. The average μ values differ by a factor of two between the two samples, and the difference in $c_2\{4\}$ is found to be less than 0.5×10^{-6} .

To check the impact of dijet events, where both jets have pseudorapidities close to the boundaries of relevant subevent regions, the three-subevent cumulants are calculated by requiring a $\Delta\eta = 0.5$ gap between the adjacent regions. The results are found to be consistent with the nominal result.

The systematic uncertainties from different sources are added in quadrature to determine the total systematic uncertainty. The uncertainty is $(0.1-1)\times 10^{-6}$ for two- and three-subevent methods in the region $\langle N_{\text{ch}} \rangle > 50$, where there is a negative $c_2\{4\}$ signal. The total systematic uncertainty for the standard method is typically about a factor of two larger.

The systematic uncertainty studies described above are also carried out for $c_3\{4\}$, and the absolute uncertainties are found to be smaller than those for $c_2\{4\}$, presumably because $c_3\{4\}$ is less sensitive to the influence from dijets.

8 Results

8.1 Dependence on the event-class definition

This section presents the sensitivity of $c_2\{4\}$ to $N_{\text{ch}}^{\text{sel}}$, which defines the event class used to calculate $\langle\langle\{2\}_n\rangle\rangle$ and $\langle\langle\{4\}_n\rangle\rangle$ in Eqs. (10)–(12). The discussion is based on results obtained from the 13 TeV pp data, but the observations for the 5.02 TeV pp and $p+\text{Pb}$ data are qualitatively similar.

Figure 1 shows the $c_2\{4\}$ values obtained using the standard method for four event-class definitions based on $N_{\text{ch}}^{\text{sel}}$. The $c_2\{4\}$ values changes dramatically as the event-class definition is varied, which, as points out in Ref. [23], reflects different amount of non-flow fluctuations associated with different $N_{\text{ch}}^{\text{sel}}$. The $c_2\{4\}$ values for $0.3 < p_{\text{T}} < 3$ GeV become negative when the reference $N_{\text{ch}}^{\text{sel}}$ is obtained for $p_{\text{T}} > 0.4$ GeV or higher, but the four cases do not converge to the same $c_2\{4\}$ values. On the other hand, $c_2\{4\}$ values for $0.5 < p_{\text{T}} < 5$ GeV are always positive, independent of the definition of $N_{\text{ch}}^{\text{sel}}$. These behaviors suggest that the $c_2\{4\}$ values from the standard method are strongly influenced by non-flow effects in all $\langle N_{\text{ch}} \rangle$ and p_{T} ranges. Therefore the previously observed negative $c_2\{4\}$ in pp collisions for $0.3 < p_{\text{T}} < 3$ GeV and $N_{\text{ch}}^{\text{sel}}$ with $p_{\text{T}} > 0.4$ GeV [19] may be dominated by non-flow correlations instead of long-range collective flow.

Figure 2 shows that the $c_2\{4\}$ values calculated using the two-subevent method are closer to each other among different event-class definitions. The $c_2\{4\}$ values decrease gradually with $\langle N_{\text{ch}} \rangle$ and become negative for $\langle N_{\text{ch}} \rangle > 70$ when $c_2\{4\}$ is calculated in the range $0.3 < p_{\text{T}} < 3$ GeV range and for $\langle N_{\text{ch}} \rangle > 150$ when $c_2\{4\}$ is calculated in the range $0.5 < p_{\text{T}} < 5$ GeV. Therefore, the $c_2\{4\}$ values from the two-subevent method are more sensitive to long-range ridge correlations, but nevertheless may still be affected by non-flow effects, especially in the low $\langle N_{\text{ch}} \rangle$ region and higher p_{T} .

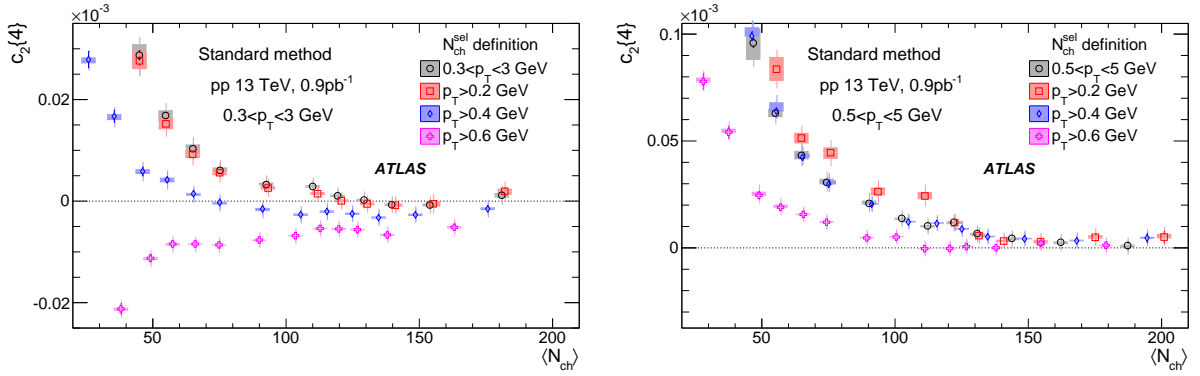


Figure 1: The $c_2\{4\}$ values calculated for charged particles with $0.3 < p_T < 3$ GeV (left panel) and $0.5 < p_T < 5$ GeV (right panel) with the standard cumulant method from the 13 TeV pp data. The event averaging is performed for $N_{\text{ch}}^{\text{sel}}$ calculated for various p_T selections as indicated in the figure, which is then mapped to $\langle N_{\text{ch}} \rangle$, the average number of charged particles with $p_T > 0.4$ GeV. The error bars and shaded boxes represent the statistical and systematic uncertainties, respectively.

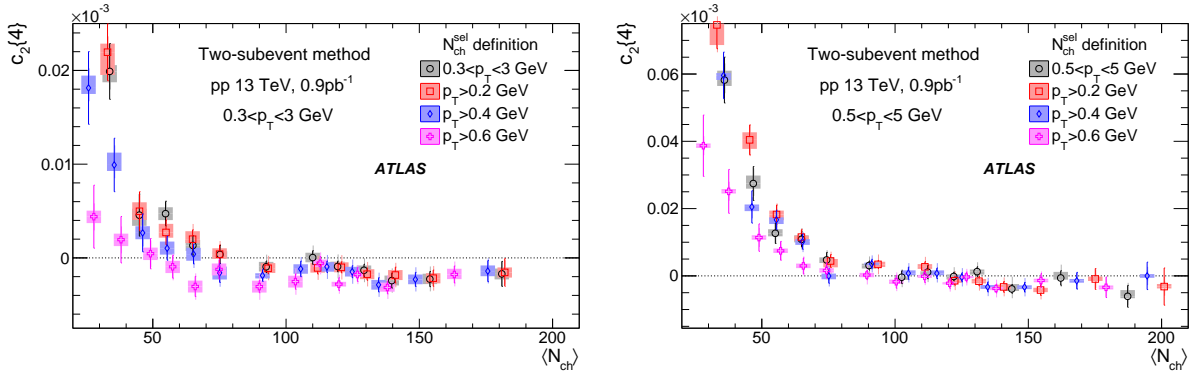


Figure 2: The $c_2\{4\}$ values calculated for charged particles with $0.3 < p_T < 3$ GeV (left panel) and $0.5 < p_T < 5$ GeV (right panel) with the two-subevent cumulant method from the 13 TeV pp data. The event averaging is performed for $N_{\text{ch}}^{\text{sel}}$ calculated for various p_T selections as indicated in the figure, which is then mapped to $\langle N_{\text{ch}} \rangle$, the average number of charged particles with $p_T > 0.4$ GeV. The error bars and shaded boxes represent the statistical and systematic uncertainties, respectively.

Figure 3 shows the results from the three-subevent method. For most of the $\langle N_{\text{ch}} \rangle$ range, the $c_2\{4\}$ values are negative, i.e., having the sign expected for long-range ridge correlations. The $c_2\{4\}$ values show some sensitivity to the definition of the reference $N_{\text{ch}}^{\text{sel}}$ but they are close to each other for all definitions in the region $\langle N_{\text{ch}} \rangle > 100$. This suggests that the residual non-flow effects may still be important at small $\langle N_{\text{ch}} \rangle$, but are negligible at $\langle N_{\text{ch}} \rangle > 100$. It is also observed that the $c_2\{4\}$ values for $0.5 < p_T < 5$ GeV are more negative than those for $0.3 < p_T < 3$ GeV, which is consistent with the observation that the v_2 value associated with the long-range collectivity increases with p_T [10, 15].

Given the relatively small dependence of $c_2\{4\}$ on the reference $N_{\text{ch}}^{\text{sel}}$ in the three-subevent method, the remaining discussion focuses on cases where the reference $N_{\text{ch}}^{\text{sel}}$ is calculated in the same p_T ranges as those used for calculating $c_2\{4\}$, i.e. $0.3 < p_T < 3$ GeV and $0.5 < p_T < 5$ GeV.

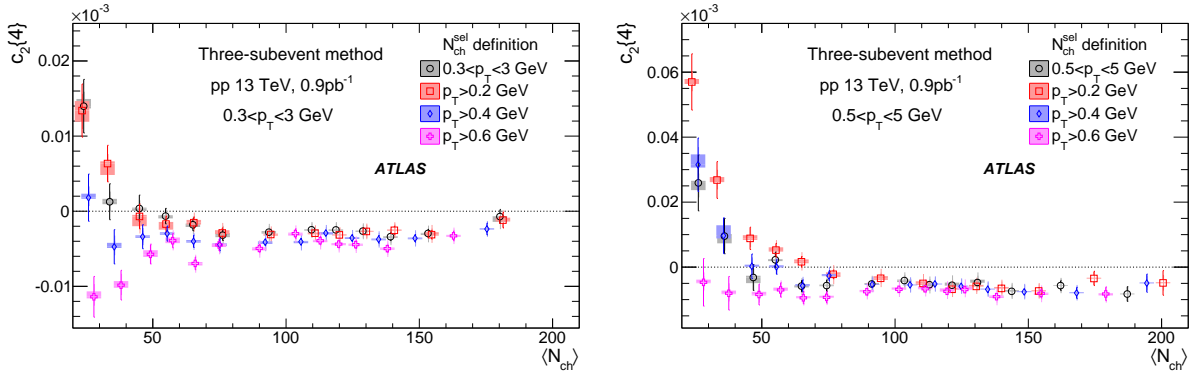


Figure 3: The $c_2\{4\}$ values calculated for charged particles with $0.3 < p_T < 3$ GeV (left panel) and $0.5 < p_T < 5$ GeV (right panel) with the three-subevent cumulant method from the 13 TeV pp data. The event averaging is performed for $N_{\text{ch}}^{\text{sel}}$ calculated for various p_T selections as indicated in the figure, which is then mapped to $\langle N_{\text{ch}} \rangle$, the average number of charged particles with $p_T > 0.4$ GeV. The error bars and shaded boxes represent the statistical and systematic uncertainties, respectively.

8.2 Comparison between different cumulant methods

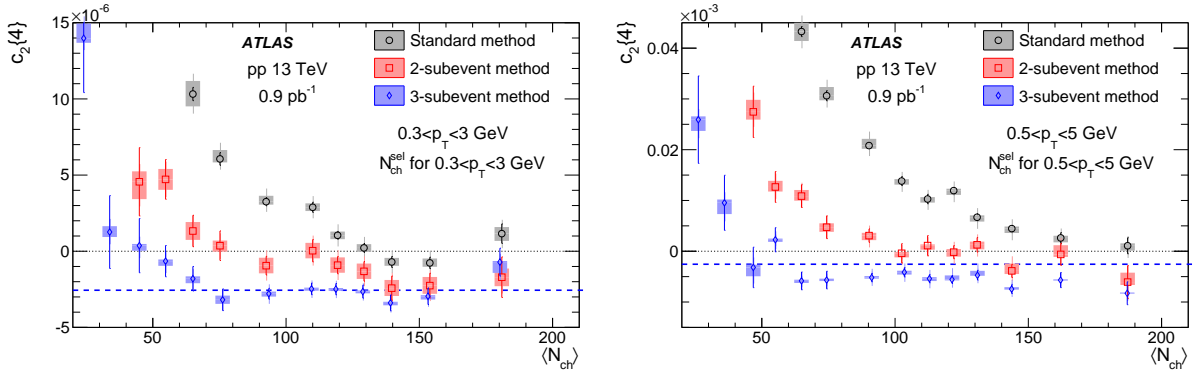


Figure 4: The $c_2\{4\}$ values calculated for charged particles with $0.3 < p_T < 3$ GeV (left panel) and $0.5 < p_T < 5$ GeV (right panel) compared for the three cumulant methods from the 13 TeV pp data. The event averaging is performed for $N_{\text{ch}}^{\text{sel}}$ calculated for the same p_T range, which is then mapped to $\langle N_{\text{ch}} \rangle$, the average number of charged particles with $p_T > 0.4$ GeV. The dashed line indicates the $c_2\{4\}$ value corresponding to a 4% v_2 signal. The error bars and shaded boxes represent the statistical and systematic uncertainties, respectively.

Figures 4–6 show direct comparisons of the results for the standard, two-subevent, and three-subevent methods for pp collisions at $\sqrt{s} = 13$ TeV, pp at $\sqrt{s} = 5.02$ TeV and $p+\text{Pb}$ collisions at $\sqrt{s_{\text{NN}}} = 5.02$ TeV, respectively. The results from 5.02 TeV pp collisions are qualitatively similar to those from the 13 TeV pp collisions, i.e. the $c_2\{4\}$ values are smallest for the three-subevent method and largest for the standard method. The same hierarchy between the three methods is also observed in $p+\text{Pb}$ collisions, but only for the $\langle N_{\text{ch}} \rangle < 100$ region, suggesting that non-flow effects in $p+\text{Pb}$ collisions are much smaller than those in pp collisions at comparable $\langle N_{\text{ch}} \rangle$. In $p+\text{Pb}$ collisions, all three methods give consistent results for $\langle N_{\text{ch}} \rangle > 100$. Furthermore, the three-subevent method gives negative $c_2\{4\}$ values in most of the measured $\langle N_{\text{ch}} \rangle$ range.

The comparison of the $c_2\{4\}$ values between the three datasets, for the standard and the three-subevent

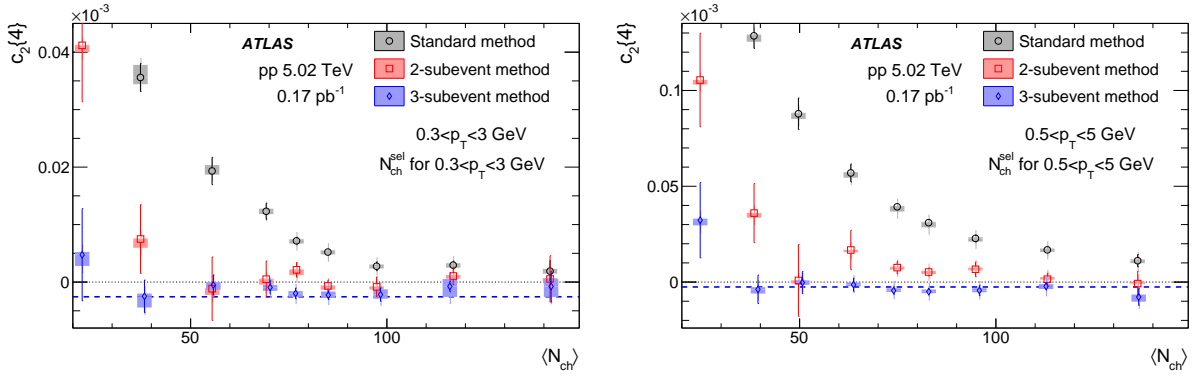


Figure 5: The $c_2\{4\}$ values calculated for charged particles with $0.3 < p_T < 3$ GeV (left panel) and $0.5 < p_T < 5$ GeV (right panel) compared for the three cumulant methods from the 5.02 TeV pp data. The event averaging is performed for $N_{\text{ch}}^{\text{sel}}$ calculated for the same p_T range, which is then mapped to $\langle N_{\text{ch}} \rangle$, the average number of charged particles with $p_T > 0.4$ GeV. The dashed line indicates the $c_2\{4\}$ value corresponding to a 4% v_2 signal. The error bars and shaded boxes represent the statistical and systematic uncertainties, respectively.

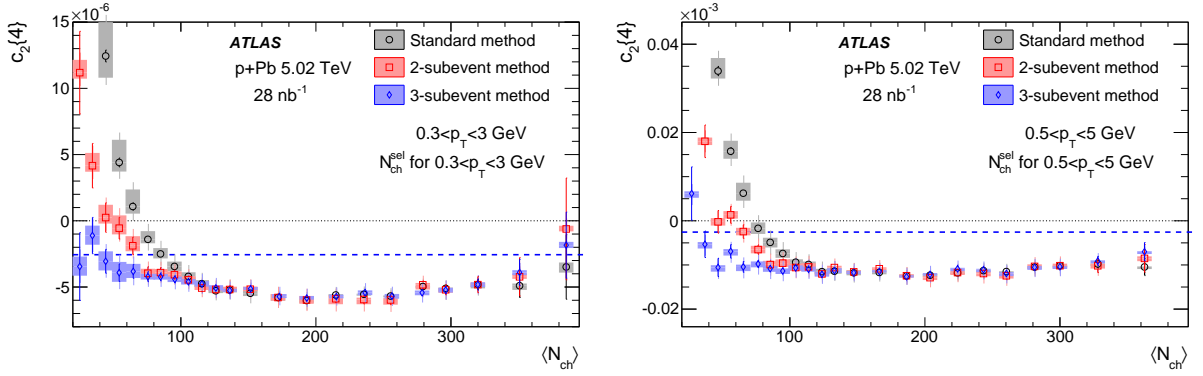


Figure 6: The $c_2\{4\}$ values calculated for charged particles with $0.3 < p_T < 3$ GeV (left panel) and $0.5 < p_T < 5$ GeV (right panel) compared for the three cumulant methods from the 5.02 TeV $p+\text{Pb}$ data. The event averaging is performed for $N_{\text{ch}}^{\text{sel}}$ calculated for the same p_T range, which is then mapped to $\langle N_{\text{ch}} \rangle$, the average number of charged particles with $p_T > 0.4$ GeV. The dashed line indicates the $c_2\{4\}$ value corresponding to a 4% v_2 signal. The error bars and shaded boxes represent the statistical and systematic uncertainties, respectively.

methods, is shown in Figures 7 and 8. The large positive $c_2\{4\}$ values observed in the small $\langle N_{\text{ch}} \rangle$ region in the standard method are likely due to non-flow correlations, since this trend is absent when using the three-subevent cumulant method. In $p+\text{Pb}$ collisions, the absolute value of $c_2\{4\}$ seems to become smaller for $\langle N_{\text{ch}} \rangle > 200$.

The same analysis is performed for the third-order harmonics. Figures 9 and 10 compare the $c_3\{4\}$ values between the three datasets for the standard cumulant method and the three-subevent method. The $c_3\{4\}$ values from the three-subevent method are close to zero in all three systems. For the standard method, the positive $c_3\{4\}$ values in the small $\langle N_{\text{ch}} \rangle$ region indicate the influence of non-flow correlations, but the influence is not as strong as that for $c_2\{4\}$.

Figure 11 shows the $c_3\{4\}$ values from $p+\text{Pb}$ collisions in the two p_T ranges, obtained with the three-subevent method; they are zoomed-in version of the $p+\text{Pb}$ data shown in Figures 8 and 9. Within their large statistical and systematic uncertainties, the values of $c_3\{4\}$ are systematically below zero, especially for $0.5 < p_T < 5$ GeV, where the $c_3\{4\}$ values are comparable to -0.16×10^{-6} , corresponding to a v_3 value

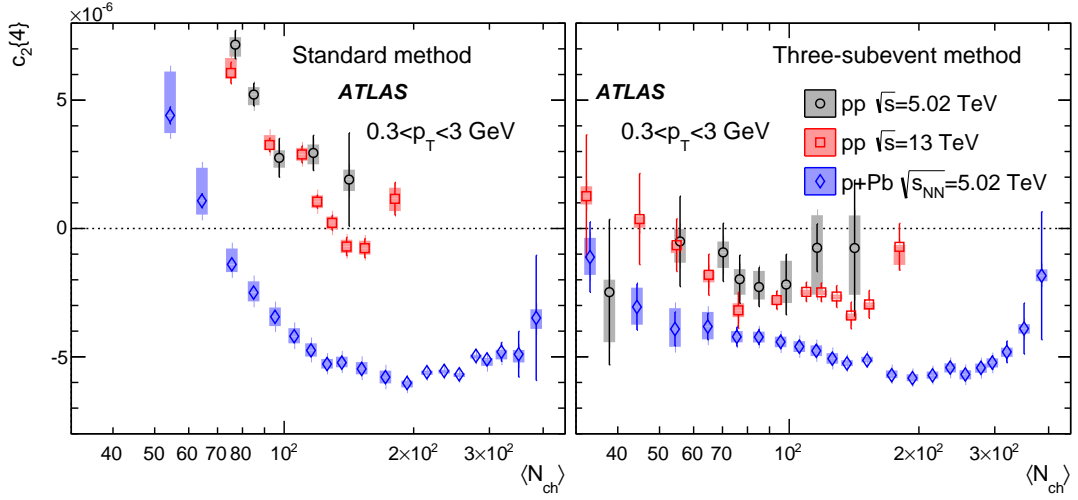


Figure 7: The $c_2\{4\}$ values calculated for charged particles with $0.3 < p_T < 3$ GeV using the standard cumulants (left panel) and the three-subevent method (right panel) compared between 5.02 TeV pp , 13 TeV pp and 5.02 TeV $p+Pb$. The event averaging is performed for N_{ch}^{sel} calculated for the same p_T range, which is then mapped to $\langle N_{ch} \rangle$, the average number of charged particles with $p_T > 0.4$ GeV. The error bars and shaded boxes represent the statistical and systematic uncertainties, respectively.

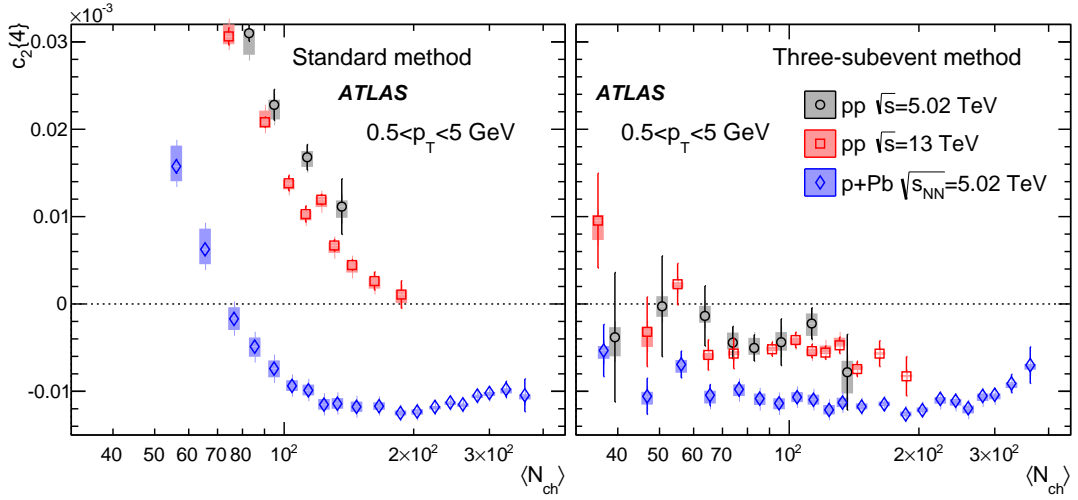


Figure 8: The $c_2\{4\}$ values calculated for charged particles with $0.5 < p_T < 5$ GeV using the standard cumulants (left panel) and the three-subevent method (right panel) compared between 5.02 TeV pp , 13 TeV pp and 5.02 TeV $p+Pb$. The event averaging is performed for N_{ch}^{sel} calculated for the same p_T range, which is then mapped to $\langle N_{ch} \rangle$, the average number of charged particles with $p_T > 0.4$ GeV. The error bars and shaded boxes represent the statistical and systematic uncertainties, respectively.

of 2% as indicated in the figure. The negative $c_3\{4\}$ values from the three-subevent method support the existence of long-range multi-particle triangular flow in $p+Pb$ collisions.

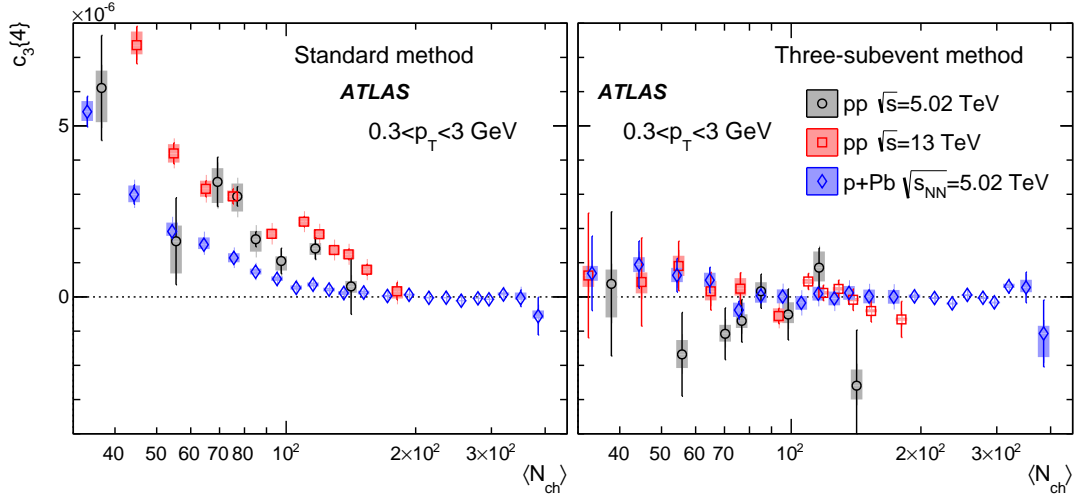


Figure 9: The $c_3\{4\}$ values calculated for charged particles with $0.3 < p_T < 3$ GeV using the standard cumulants (left panel) and the three-subevent method (right panel) compared between 5.02 TeV pp , 13 TeV pp and 5.02 TeV $p+Pb$. The event averaging is performed for N_{ch}^{sel} calculated for the same p_T range, which is then mapped to $\langle N_{ch} \rangle$, the average number of charged particles with $p_T > 0.4$ GeV. The error bars and shaded boxes represent the statistical and systematic uncertainties, respectively.

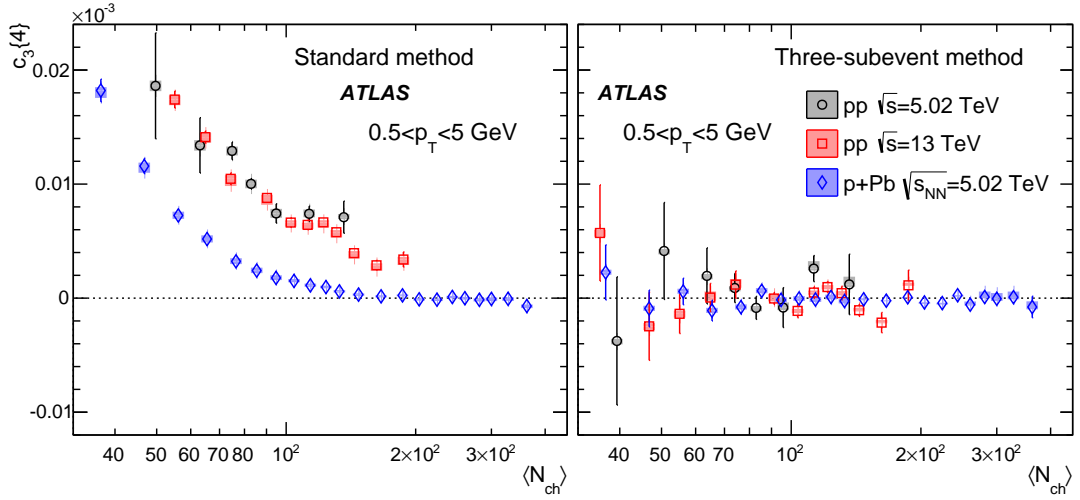


Figure 10: The $c_3\{4\}$ values calculated for charged particles with $0.5 < p_T < 5$ GeV using the standard cumulants (left panel) and the three-subevent method (right panel) compared between 5.02 TeV pp , 13 TeV pp and 5.02 TeV $p+Pb$. The event averaging is performed for N_{ch}^{sel} calculated for the same p_T range, which is then mapped to $\langle N_{ch} \rangle$, the average number of charged particles with $p_T > 0.4$ GeV. The error bars and shaded boxes represent the statistical and systematic uncertainties, respectively.

8.3 Three-subevent flow harmonic $v_2\{4\}$

The harmonic flow coefficients $v_2\{4\}$ can be obtained from the measured values of $c_2\{4\}$ according to Eq. (7). Figure 12 shows the $v_2\{4\}$ values for charged particles with $0.3 < p_T < 3$ GeV calculated using

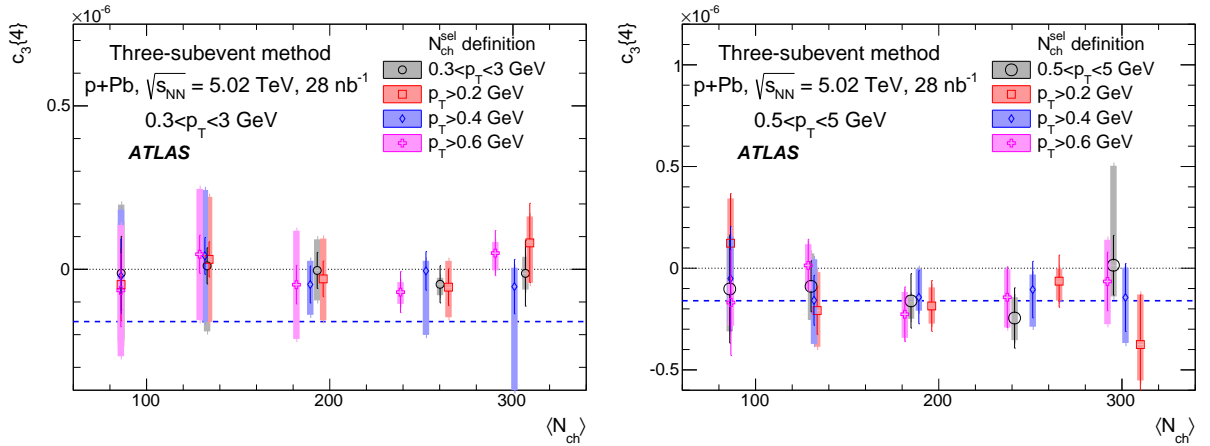


Figure 11: The $c_3\{4\}$ values calculated for charged particles with $0.3 < p_T < 3$ GeV (left panel) or $0.5 < p_T < 5$ GeV (right panel) with the three-subevent cumulant method for the $p+\text{Pb}$ data. The event averaging is performed for $N_{\text{ch}}^{\text{sel}}$ calculated for various p_T selections as indicated in the figure, which is then mapped to $\langle N_{\text{ch}} \rangle$, the average number of charged particles with $p_T > 0.4$ GeV. The dashed line indicates the $c_3\{4\}$ value corresponding to a 2% v_3 signal. The error bars and shaded boxes represent the statistical and systematic uncertainties, respectively.

the three-subevent method in the three datasets. Results for the higher p_T range ($0.5 < p_T < 5$ GeV) are presented in Figure 13. The value of $v_2\{4\}$ is measured down to $\langle N_{\text{ch}} \rangle \approx 50$ in pp collisions and down to $\langle N_{\text{ch}} \rangle \approx 20\text{--}40$ in $p+\text{Pb}$ collisions. The $v_2\{4\}$ values are observed to be approximately independent of $\langle N_{\text{ch}} \rangle$ in the measured range in the three datasets: $50 < \langle N_{\text{ch}} \rangle < 150$ for 5.02 TeV pp , $50 < \langle N_{\text{ch}} \rangle < 200$ for 13 TeV pp , and $20 < \langle N_{\text{ch}} \rangle < 380$ for 5.02 TeV $p+\text{Pb}$, respectively. Moreover, the $p+\text{Pb}$ data suggest the value of $v_2\{4\}$ is lower for $\langle N_{\text{ch}} \rangle > 200$, as expected from the similar behavior of $|c_2\{4\}|$ in Figures 7 and 8 at large $\langle N_{\text{ch}} \rangle$.

The values of $v_2\{4\}$ presented in Figures 12 and 13 are also compared to the values of $v_2\{2\}$ obtained from the 2PC measurements [10, 15] where the non-flow effects are estimated using low-multiplicity events ($\langle N_{\text{ch}} \rangle < 20$) and then subtracted. The subtraction was performed either by a “template fit”, which includes the pedestal level from the $\langle N_{\text{ch}} \rangle < 20$ events, or by a “peripheral subtraction”, which sets the pedestal level by a zero-yield at minimum (ZYAM) procedure [6]. The “peripheral subtraction” explicitly assumes that the most peripheral events do not contain any long-range correlations [15], and so v_2 is forced to be zero at the corresponding $\langle N_{\text{ch}} \rangle$ value, which biases v_2 to a lower value in other multiplicity ranges.

8.4 Dependence on the number of sources in the initial state

Figures 12 and 13 show that the $v_2\{4\}$ values are smaller than the $v_2\{2\}$ values extracted using the template-fit method in both the pp and $p+\text{Pb}$ collisions. In various hydrodynamic models for small collision systems [38, 39], this difference can be interpreted as the influence of event-by-event flow fluctuations associated with the initial state, which is closely related to the effective number of sources N_s for particle production in the transverse density distribution of the initial state [39]:

$$\frac{v_2\{4\}}{v_2\{2\}} = \left[\frac{4}{(3 + N_s)} \right]^{1/4} \quad \text{or} \quad N_s = \frac{4v_2\{2\}^4}{v_2\{4\}^4} - 3. \quad (14)$$

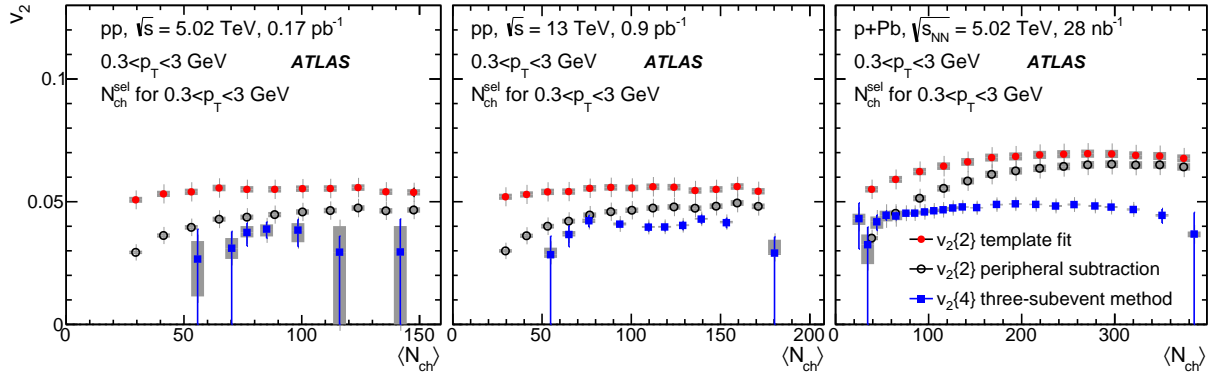


Figure 12: The $v_2\{4\}$ values calculated for charged particles with $0.3 < p_T < 3$ GeV using the three-subevent method in 5.02 TeV pp (left panel), 13 TeV pp (middle panel) and 5.02 TeV $p+Pb$ collisions (right panel). They are compared to v_2 obtained from the 2PC analyses [10, 15] where the non-flow effects are removed by a template fit procedure (solid circles) or with a fit after subtraction with a ZYAM assumption (peripheral subtraction, open circles). The error bars and shaded boxes represent the statistical and systematic uncertainties, respectively.

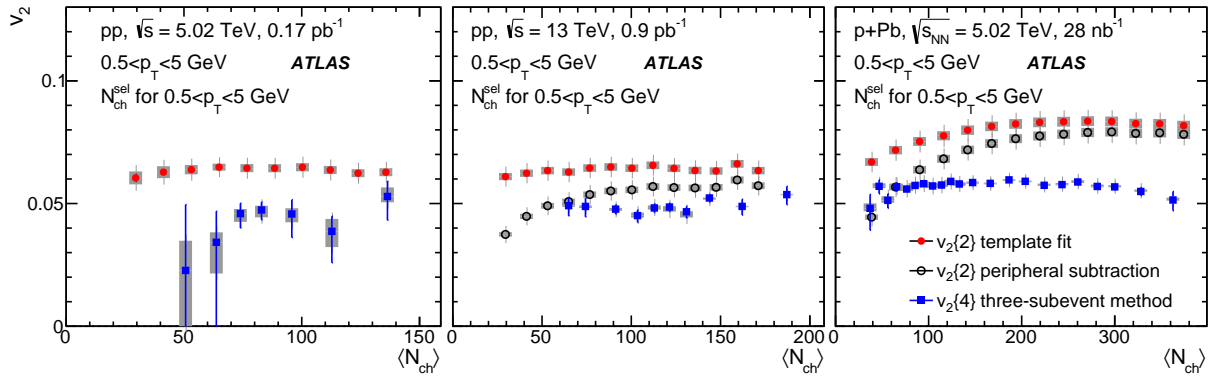


Figure 13: The $v_2\{4\}$ values calculated for charged particles with $0.5 < p_T < 5$ GeV using the three-subevent method in 5.02 TeV pp (left panel), 13 TeV pp (middle panel) and 5.02 TeV $p+Pb$ collisions (right panel). They are compared to v_2 obtained from the 2PC analyses [10, 15] where the non-flow effects are removed by a template fit procedure (solid circles) or with a fit after subtraction with a ZYAM assumption (peripheral subtraction, open circles). The error bars and shaded boxes represent the statistical and systematic uncertainties, respectively.

Figure 14 shows the extracted values of N_s as a function of $\langle N_{ch} \rangle$ in 13 TeV pp and 5.02 $p+Pb$ collisions, estimated using charged particles with $0.3 < p_T < 3$ GeV and $0.5 < p_T < 5$ GeV. It is observed that the N_s value increases with $\langle N_{ch} \rangle$ in $p+Pb$ collisions, reaching $N_s \sim 20$ in the highest multiplicity class, and it is consistent between the two p_T ranges.

In the model framework in Refs. [38, 39], the values of $|c_2\{4\}|$ and $v_2\{4\}$ are expected to decrease for large N_s , which is compatible with the presented results. The slight decreases of $|c_2\{4\}|$ shown in Figures 7 and 8 for $p+Pb$ collisions are compatible with the model predictions. The results for 13 TeV pp collisions cover a limited $\langle N_{ch} \rangle$ range compared to $p+Pb$, but agree with $p+Pb$ collisions in this range.

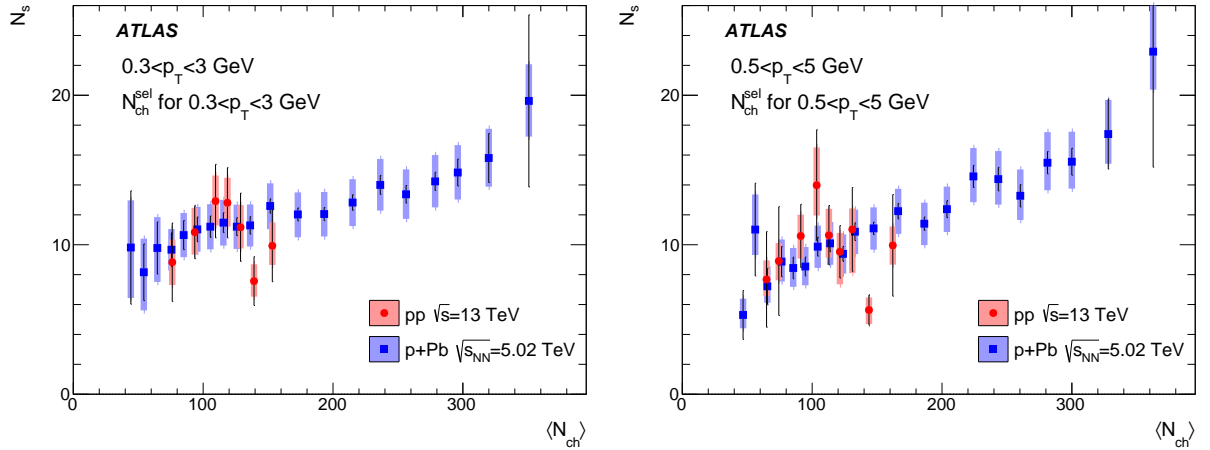


Figure 14: The number of sources inferred from $v_2\{2\}$ and $v_2\{4\}$ measurements via the model framework in Refs. [38,39] and Eq. (14) in 13 TeV pp and 5.02 TeV p +Pb collisions, for charged particles with $0.3 < p_T < 3$ GeV (left panel) and $0.5 < p_T < 5$ GeV (right panel). The error bars and shaded boxes represent the statistical and systematic uncertainties, respectively.

9 Summary

Measurements of the four-particle cumulants $c_n\{4\}$ and harmonic flow coefficients $v_n\{4\}$ for $n = 2$ and 3 are presented using 0.17 pb^{-1} of pp data at $\sqrt{s} = 5.02$ TeV, 0.9 pb^{-1} of pp data at $\sqrt{s} = 13$ TeV and 28 nb^{-1} p +Pb of data at $\sqrt{s_{NN}} = 5.02$ TeV. These measurements were performed with the ATLAS detector at the LHC. The $c_2\{4\}$ values are calculated using the standard cumulant method and the recently proposed two-subevent and three-subevent methods. They are all presented as a function of the average number of charged particles with $p_T > 0.4$ GeV, $\langle N_{ch} \rangle$. It is found that the $c_2\{4\}$ value from the standard method is sensitive to the choice of particles used to form the event classes used for averaging. This suggests that the previous $c_2\{4\}$ measurement in pp collisions [16, 19], based on the standard method, may be dominated by non-flow correlations instead of a long-range collective flow correlation. In general, it is easy to obtain incorrect results from the standard cumulant method, depending on the nature of the non-flow fluctuations associated with the event class chosen for the analysis.

On the other hand, the sensitivity of $c_2\{4\}$ on event class definition is greatly reduced in the two-subevent method and is almost fully removed in the three-subevent method, demonstrating that the three-subevent method is more robust against non-flow effects. Similarly, the values of $c_3\{4\}$ are found to differ in the three datasets using the standard method, but are consistent with each other and much closer to zero using the three-subevent method. This gives confidence that non-flow correlations make a much smaller contribution to the three-subevent results, and that this method is more appropriate for studying long-range collective behaviour than the standard cumulant method.

The three-subevent method provides a measurement of $c_2\{4\}$ that is negative in all three datasets over a broad range of $\langle N_{ch} \rangle$. The magnitude of $c_2\{4\}$ increases with p_T and is nearly independent of $\langle N_{ch} \rangle$ but in p +Pb collisions the values become smaller at high multiplicities. These results provide direct evidence for the presence of long-range multi-particle azimuthal correlations in broad $\langle N_{ch} \rangle$ ranges in pp and p +Pb collisions, and these long-range multi-particle correlations persist even in events with rather low multiplicity of $\langle N_{ch} \rangle \sim 40$. The $c_3\{4\}$ values are consistent with zero in pp collisions, but are

systematically below zero in p +Pb collisions, compatible with the presence of significant long-range multi-particle triangular flow in p +Pb collisions.

The single-particle harmonic coefficient $v_2\{4\} = (-c_2\{4\})^{1/4}$ is calculated and compared with $v_2\{2\}$ obtained previously using the two-particle correlation method, where the non-flow contributions were estimated and subtracted. The magnitude of $v_2\{4\}$ is smaller than that for $v_2\{2\}$, as expected for a long-range final-state hydrodynamic collective effect. The ratio of $v_2\{4\}$ to $v_2\{2\}$ is used, in a model-dependent framework, to infer the number of particle-emitting sources in the initial-state geometric configuration. The number of sources extracted within this framework is found to increase with $\langle N_{\text{ch}} \rangle$ in p +Pb collisions.

The subevent cumulant technique and the new results provide direct evidence that the ridge is indeed a long-range collective phenomenon involving many particles distributed across a broad rapidity interval. The results of $v_2\{4\}$ and its dependence on p_T and $\langle N_{\text{ch}} \rangle$, largely free from non-flow effects, can be used to understand the space-time dynamics and the properties of the medium created in small collision systems.

Acknowledgments

We thank CERN for the very successful operation of the LHC, as well as the support staff from our institutions without whom ATLAS could not be operated efficiently.

We acknowledge the support of ANPCyT, Argentina; YerPhI, Armenia; ARC, Australia; BMWFW and FWF, Austria; ANAS, Azerbaijan; SSTC, Belarus; CNPq and FAPESP, Brazil; NSERC, NRC and CFI, Canada; CERN; CONICYT, Chile; CAS, MOST and NSFC, China; COLCIENCIAS, Colombia; MSMT CR, MPO CR and VSC CR, Czech Republic; DNRF and DNSRC, Denmark; IN2P3-CNRS, CEA-DSM/IRFU, France; SRNSF, Georgia; BMBF, HGF, and MPG, Germany; GSRT, Greece; RGC, Hong Kong SAR, China; ISF, I-CORE and Benoziyo Center, Israel; INFN, Italy; MEXT and JSPS, Japan; CNRST, Morocco; NWO, Netherlands; RCN, Norway; MNiSW and NCN, Poland; FCT, Portugal; MNE/IFA, Romania; MES of Russia and NRC KI, Russian Federation; JINR; MESTD, Serbia; MSSR, Slovakia; ARRS and MIZŠ, Slovenia; DST/NRF, South Africa; MINECO, Spain; SRC and Wallenberg Foundation, Sweden; SERI, SNSF and Cantons of Bern and Geneva, Switzerland; MOST, Taiwan; TAEK, Turkey; STFC, United Kingdom; DOE and NSF, United States of America. In addition, individual groups and members have received support from BCKDF, the Canada Council, CANARIE, CRC, Compute Canada, FQRNT, and the Ontario Innovation Trust, Canada; EPLANET, ERC, ERDF, FP7, Horizon 2020 and Marie Skłodowska-Curie Actions, European Union; Investissements d’Avenir Labex and IDEX, ANR, Région Auvergne and Fondation Partager le Savoir, France; DFG and AvH Foundation, Germany; Herakleitos, Thales and Aristeia programmes co-financed by EU-ESF and the Greek NSRF; BSF, GIF and Minerva, Israel; BRF, Norway; CERCA Programme Generalitat de Catalunya, Generalitat Valenciana, Spain; the Royal Society and Leverhulme Trust, United Kingdom.

The crucial computing support from all WLCG partners is acknowledged gratefully, in particular from CERN, the ATLAS Tier-1 facilities at TRIUMF (Canada), NDGF (Denmark, Norway, Sweden), CC-IN2P3 (France), KIT/GridKA (Germany), INFN-CNAF (Italy), NL-T1 (Netherlands), PIC (Spain), ASGC (Taiwan), RAL (UK) and BNL (USA), the Tier-2 facilities worldwide and large non-WLCG resource providers. Major contributors of computing resources are listed in Ref. [40].

References

- [1] STAR Collaboration, B. I. Abelev et al., *Long range rapidity correlations and jet production in high energy nuclear collisions*, *Phys. Rev. C* **80** (2009) 064912, [arXiv:0909.0191 \[nucl-ex\]](#).
- [2] PHOBOS Collaboration, B. Alver et al., *High transverse momentum triggered correlations over a large pseudorapidity acceptance in Au+Au collisions at $s(NN)^{1/2} = 200$ GeV*, *Phys. Rev. Lett.* **104** (2010) 062301, [arXiv:0903.2811 \[nucl-ex\]](#).
- [3] ALICE Collaboration, K. Aamodt et al., *Higher harmonic anisotropic flow measurements of charged particles in Pb-Pb collisions at $\sqrt{s_{NN}} = 2.76$ TeV*, *Phys. Rev. Lett.* **107** (2011) 032301, [arXiv:1105.3865 \[nucl-ex\]](#).
- [4] ATLAS Collaboration, *Measurement of the azimuthal anisotropy for charged particle production in $\sqrt{s_{NN}} = 2.76$ TeV lead-lead collisions with the ATLAS detector*, *Phys. Rev. C* **86** (2012) 014907, [arXiv:1203.3087 \[hep-ex\]](#).
- [5] CMS Collaboration, *Measurement of higher-order harmonic azimuthal anisotropy in PbPb collisions at $\sqrt{s_{NN}} = 2.76$ TeV*, *Phys. Rev. C* **89** (2014) 044906, [arXiv:1310.8651 \[nucl-ex\]](#).
- [6] PHENIX Collaboration, A. Adare et al., *Dihadron azimuthal correlations in Au+Au collisions at $s(NN)^{1/2} = 200$ -GeV*, *Phys. Rev. C* **78** (2008) 014901, [arXiv:0801.4545 \[nucl-ex\]](#).
- [7] CMS Collaboration, *Observation of long-range near-side angular correlations in proton-lead collisions at the LHC*, *Phys. Lett. B* **718** (2013) 795, [arXiv:1210.5482 \[nucl-ex\]](#).
- [8] ALICE Collaboration, B. Abelev et al., *Long-range angular correlations on the near and away side in p-Pb collisions at $\sqrt{s_{NN}} = 5.02$ TeV*, *Phys. Lett. B* **719** (2013) 29, [arXiv:1212.2001 \[nucl-ex\]](#).
- [9] ATLAS Collaboration, *Observation of Associated Near-side and Away-side Long-range Correlations in $\sqrt{s_{NN}}=5.02$ TeV Proton-lead Collisions with the ATLAS Detector*, *Phys. Rev. Lett.* **110** (2013) 182302, [arXiv:1212.5198 \[hep-ex\]](#).
- [10] ATLAS Collaboration, *Measurement of long-range pseudorapidity correlations and azimuthal harmonics in $\sqrt{s_{NN}} = 5.02$ TeV proton-lead collisions with the ATLAS detector*, *Phys. Rev. C* **90** (2014) 044906, [arXiv:1409.1792 \[hep-ex\]](#).
- [11] CMS Collaboration, *Evidence for Collective Multiparticle Correlations in p-Pb Collisions*, *Phys. Rev. Lett.* **115** (2015) 012301, [arXiv:1502.05382 \[nucl-ex\]](#).
- [12] PHENIX Collaboration, A. Adare et al., *Quadrupole Anisotropy in Dihadron Azimuthal Correlations in Central d+Au Collisions at $\sqrt{s_{NN}}=200$ GeV*, *Phys. Rev. Lett.* **111** (2013) 212301, [arXiv:1303.1794 \[nucl-ex\]](#).
- [13] CMS Collaboration, *Observation of Long-Range Near-Side Angular Correlations in Proton-Proton Collisions at the LHC*, *JHEP* **09** (2010) 091, [arXiv:1009.4122 \[hep-ex\]](#).
- [14] ATLAS Collaboration, *Observation of Long-Range Elliptic Azimuthal Anisotropies in $\sqrt{s} = 13$ and 2.76 TeV pp Collisions with the ATLAS Detector*, *Phys. Rev. Lett.* **116** (2016) 172301, [arXiv:1509.04776 \[hep-ex\]](#).

- [15] ATLAS Collaboration, *Measurements of long-range azimuthal anisotropies and associated Fourier coefficients for pp collisions at $\sqrt{s} = 5.02$ and 13 TeV and p+Pb collisions at $\sqrt{s_{NN}} = 5.02$ TeV with the ATLAS detector*, *Phys. Rev. C* **96** (2017) 024908, [arXiv:1609.06213 \[nucl-ex\]](#).
- [16] ATLAS Collaboration, *Measurement of multi-particle azimuthal correlations in pp, p+Pb and low-multiplicity Pb+Pb collisions with the ATLAS detector*, *Eur. Phys. J. C* **77** (2017) 428, [arXiv:1705.04176 \[hep-ex\]](#).
- [17] P. Bozek and W. Broniowski, *Collective dynamics in high-energy proton-nucleus collisions*, *Phys. Rev. C* **88** (2013) 014903, [arXiv:1304.3044 \[nucl-th\]](#).
- [18] K. Dusling and R. Venugopalan, *Comparison of the color glass condensate to dihadron correlations in proton-proton and proton-nucleus collisions*, *Phys. Rev. D* **87** (2013) 094034, [arXiv:1302.7018 \[hep-ph\]](#).
- [19] CMS Collaboration, *Evidence for collectivity in pp collisions at the LHC*, *Phys. Lett. B* **765** (2017) 193, [arXiv:1606.06198 \[nucl-ex\]](#).
- [20] N. Borghini, P. M. Dinh, and J.-Y. Ollitrault, *A New method for measuring azimuthal distributions in nucleus-nucleus collisions*, *Phys. Rev. C* **63** (2001) 054906, [arXiv:nucl-th/0007063 \[nucl-th\]](#).
- [21] ATLAS Collaboration, *Measurement with the ATLAS detector of multi-particle azimuthal correlations in p+Pb collisions at $\sqrt{s_{NN}} = 5.02$ TeV*, *Phys. Lett. B* **725** (2013) 60, [arXiv:1303.2084 \[hep-ex\]](#).
- [22] PHENIX Collaboration, C. Aidala et al., *Measurements of multiparticle correlations in d+Au collisions at 200, 62.4, 39, and 19.6 GeV and p+Au collisions at 200 GeV and implications for collective behavior*, [arXiv:1707.06108 \[nucl-ex\]](#).
- [23] J. Jia, M. Zhou, and A. Trzupek, *Revealing long-range multi-particle collectivity in small collision systems via subevent cumulants*, *Phys. Rev. C* **96** (2017) 034906, [arXiv:1701.03830 \[nucl-th\]](#).
- [24] T. Sjöstrand, S. Mrenna, and P. Z. Skands, *A Brief Introduction to PYTHIA 8.1*, *Comput. Phys. Commun.* **178** (2008) 852, [arXiv:0710.3820 \[hep-ph\]](#).
- [25] A. Bilandzic, R. Snellings, and S. Voloshin, *Flow analysis with cumulants: Direct calculations*, *Phys. Rev. C* **83** (2011) 044913, [arXiv:1010.0233 \[nucl-ex\]](#).
- [26] A. Bilandzic, C. H. Christensen, K. Gulbrandsen, A. Hansen, and Y. Zhou, *Generic framework for anisotropic flow analyses with multiparticle azimuthal correlations*, *Phys. Rev. C* **89** (2014) 064904, [arXiv:1312.3572 \[nucl-ex\]](#).
- [27] ATLAS Collaboration, *The ATLAS Experiment at the CERN Large Hadron Collider*, *JINST* **3** (2008) S08003.
- [28] ATLAS Collaboration, *The ATLAS Inner Detector commissioning and calibration*, *Eur. Phys. J. C* **70** (2010) 787, [arXiv:1004.5293 \[physics.ins-det\]](#).
- [29] ATLAS Collaboration, *ATLAS Insertable B-Layer Technical Design Report*, Atlas-tdr-19, 2010, <https://cds.cern.ch/record/1291633>, *ATLAS Insertable B-Layer Technical Design Report Addendum*, ATLAS-TDR-19-ADD-1, 2012, URL: <https://cds.cern.ch/record/1451888>.

- [30] ATLAS Collaboration, *Performance of the ATLAS Trigger System in 2010*, *Eur. Phys. J. C* **72** (2012) 1849, [arXiv:1110.1530 \[hep-ex\]](#).
- [31] ATLAS Collaboration, *Charged-particle distributions in $\sqrt{s}=13$ TeV pp interactions measured with the ATLAS detector at the LHC*, *Phys. Lett. B* **758** (2016) 67, [arXiv:1602.01633 \[hep-ex\]](#).
- [32] ATLAS Collaboration, *Performance of the ATLAS Minimum Bias and Forward Detector Triggers in pPb collisions*, ATLAS-CONF-2013-104, <https://cds.cern.ch/record/1624013>.
- [33] ATLAS Collaboration, *ATLAS tunes of PYTHIA 6 and Pythia 8 for MC11*, ATLAS-PHYS-PUB-2011-009, <https://cds.cern.ch/record/1363300>.
- [34] M. Gyulassy and X.-N. Wang, *HIJING 1.0: A Monte Carlo program for parton and particle production in high-energy hadronic and nuclear collisions*, *Comput. Phys. Commun.* **83** (1994) 307, [arXiv:nucl-th/9502021](#).
- [35] GEANT4 Collaboration, S. Agostinelli et al., *GEANT4: A Simulation toolkit*, *Nucl. Instrum. Meth. A* **506** (2003) 250.
- [36] ATLAS Collaboration, *The ATLAS Simulation Infrastructure*, *Eur. Phys. J. C* **70** (2010) 823, [arXiv:1005.4568 \[physics.ins-det\]](#).
- [37] ATLAS Collaboration, *Measurement of forward-backward multiplicity correlations in lead-lead, proton-lead and proton-proton collisions with the ATLAS detector*, *Phys. Rev. C* **95** (2017) 064914, [arXiv:1606.08170 \[hep-ex\]](#).
- [38] A. Bzdak, P. Bozek, and L. McLerran, *Fluctuation induced equality of multi-particle eccentricities for four or more particles*, *Nucl. Phys. A* **927** (2014) 15, [arXiv:1311.7325 \[hep-ph\]](#).
- [39] L. Yan and J.-Y. Ollitrault, *Universal fluctuation-driven eccentricities in proton-proton, proton-nucleus and nucleus-nucleus collisions*, *Phys. Rev. Lett.* **112** (2014) 082301, [arXiv:1312.6555 \[nucl-th\]](#).
- [40] ATLAS Collaboration, *ATLAS Computing Acknowledgements 2016–2017*, ATL-GEN-PUB-2016-002, <https://cds.cern.ch/record/2202407>.

The ATLAS Collaboration

M. Aaboud^{137d}, G. Aad⁸⁸, B. Abbott¹¹⁵, O. Abidinov^{12,*}, B. Abeloos¹¹⁹, S.H. Abidi¹⁶¹, O.S. AbouZeid¹³⁹, N.L. Abraham¹⁵¹, H. Abramowicz¹⁵⁵, H. Abreu¹⁵⁴, R. Abreu¹¹⁸, Y. Abulaiti^{148a,148b}, B.S. Acharya^{167a,167b,a}, S. Adachi¹⁵⁷, L. Adamczyk^{41a}, J. Adelman¹¹⁰, M. Adersberger¹⁰², T. Adye¹³³, A.A. Affolder¹³⁹, Y. Afik¹⁵⁴, T. Agatonovic-Jovin¹⁴, C. Agheorghiesei^{28c}, J.A. Aguilar-Saavedra^{128a,128f}, S.P. Ahlen²⁴, F. Ahmadov^{68,b}, G. Aielli^{135a,135b}, S. Akatsuka⁷¹, H. Akerstedt^{148a,148b}, T.P.A. Åkesson⁸⁴, E. Akilli⁵², A.V. Akimov⁹⁸, G.L. Alberghi^{22a,22b}, J. Albert¹⁷², P. Albicocco⁵⁰, M.J. Alconada Verzini⁷⁴, S.C. Alderweireldt¹⁰⁸, M. Aleksa³², I.N. Aleksandrov⁶⁸, C. Alexa^{28b}, G. Alexander¹⁵⁵, T. Alexopoulos¹⁰, M. Alhroob¹¹⁵, B. Ali¹³⁰, M. Aliev^{76a,76b}, G. Alimonti^{94a}, J. Alison³³, S.P. Alkire³⁸, B.M.M. Allbrooke¹⁵¹, B.W. Allen¹¹⁸, P.P. Allport¹⁹, A. Aloisio^{106a,106b}, A. Alonso³⁹, F. Alonso⁷⁴, C. Alpigiani¹⁴⁰, A.A. Alshehri⁵⁶, M.I. Alstary⁸⁸, B. Alvarez Gonzalez³², D. Álvarez Piqueras¹⁷⁰, M.G. Alvigi^{106a,106b}, B.T. Amadio¹⁶, Y. Amaral Coutinho^{26a}, C. Amelung²⁵, D. Amidei⁹², S.P. Amor Dos Santos^{128a,128c}, S. Amoroso³², G. Amundsen²⁵, C. Anastopoulos¹⁴¹, L.S. Ancu⁵², N. Andari¹⁹, T. Andeen¹¹, C.F. Anders^{60b}, J.K. Anders⁷⁷, K.J. Anderson³³, A. Andreazza^{94a,94b}, V. Andrei^{60a}, S. Angelidakis³⁷, I. Angelozzi¹⁰⁹, A. Angerami³⁸, A.V. Anisenkov^{111,c}, N. Anjos¹³, A. Annovi^{126a,126b}, C. Antel^{60a}, M. Antonelli⁵⁰, A. Antonov^{100,*}, D.J. Antrim¹⁶⁶, F. Anulli^{134a}, M. Aoki⁶⁹, L. Aperio Bella³², G. Arabidze⁹³, Y. Arai⁶⁹, J.P. Araque^{128a}, V. Araujo Ferraz^{26a}, A.T.H. Arce⁴⁸, R.E. Ardell⁸⁰, F.A. Arduh⁷⁴, J-F. Arguin⁹⁷, S. Argyropoulos⁶⁶, M. Arik^{20a}, A.J. Armbruster³², L.J. Armitage⁷⁹, O. Arnaez¹⁶¹, H. Arnold⁵¹, M. Arratia³⁰, O. Arslan²³, A. Artamonov^{99,*}, G. Artoni¹²², S. Artz⁸⁶, S. Asai¹⁵⁷, N. Asbah⁴⁵, A. Ashkenazi¹⁵⁵, L. Asquith¹⁵¹, K. Assamagan²⁷, R. Astalos^{146a}, M. Atkinson¹⁶⁹, N.B. Atlay¹⁴³, K. Augsten¹³⁰, G. Avolio³², B. Axen¹⁶, M.K. Ayoub^{35a}, G. Azuelos^{97,d}, A.E. Baas^{60a}, M.J. Baca¹⁹, H. Bachacou¹³⁸, K. Bachas^{76a,76b}, M. Backes¹²², P. Bagnaia^{134a,134b}, M. Bahmani⁴², H. Bahrasemani¹⁴⁴, J.T. Baines¹³³, M. Bajic³⁹, O.K. Baker¹⁷⁹, P.J. Bakker¹⁰⁹, E.M. Baldin^{111,c}, P. Balek¹⁷⁵, F. Balli¹³⁸, W.K. Balunas¹²⁴, E. Banas⁴², A. Bandyopadhyay²³, Sw. Banerjee^{176,e}, A.A.E. Bannoura¹⁷⁸, L. Barak¹⁵⁵, E.L. Barberio⁹¹, D. Barberis^{53a,53b}, M. Barbero⁸⁸, T. Barillari¹⁰³, M-S Barisits³², J.T. Barkeloo¹¹⁸, T. Barklow¹⁴⁵, N. Barlow³⁰, S.L. Barnes^{36c}, B.M. Barnett¹³³, R.M. Barnett¹⁶, Z. Barnovska-Blenessy^{36a}, A. Baroncelli^{136a}, G. Barone²⁵, A.J. Barr¹²², L. Barranco Navarro¹⁷⁰, F. Barreiro⁸⁵, J. Barreiro Guimarães da Costa^{35a}, R. Bartoldus¹⁴⁵, A.E. Barton⁷⁵, P. Bartos^{146a}, A. Basalae¹²⁵, A. Bassalat^{119,f}, R.L. Bates⁵⁶, S.J. Batista¹⁶¹, J.R. Batley³⁰, M. Battaglia¹³⁹, M. Bauce^{134a,134b}, F. Bauer¹³⁸, H.S. Bawa^{145,g}, J.B. Beacham¹¹³, M.D. Beattie⁷⁵, T. Beau⁸³, P.H. Beauchemin¹⁶⁵, P. Bechtel²³, H.P. Beck^{18,h}, H.C. Beck⁵⁷, K. Becker¹²², M. Becker⁸⁶, C. Becot¹¹², A.J. Beddall^{20e}, A. Beddall^{20b}, V.A. Bednyakov⁶⁸, M. Bedognetti¹⁰⁹, C.P. Bee¹⁵⁰, T.A. Beermann³², M. Begalli^{26a}, M. Begel²⁷, J.K. Behr⁴⁵, A.S. Bell⁸¹, G. Bella¹⁵⁵, L. Bellagamba^{22a}, A. Bellerive³¹, M. Bellomo¹⁵⁴, K. Belotskiy¹⁰⁰, O. Beltramello³², N.L. Belyaev¹⁰⁰, O. Benary^{155,*}, D. Bencheikroun^{137a}, M. Bender¹⁰², N. Benekos¹⁰, Y. Benhammou¹⁵⁵, E. Benhar Noccioli¹⁷⁹, J. Benitez⁶⁶, D.P. Benjamin⁴⁸, M. Benoit⁵², J.R. Bensinger²⁵, S. Bentvelsen¹⁰⁹, L. Beresford¹²², M. Beretta⁵⁰, D. Berge¹⁰⁹, E. Bergeas Kuutmann¹⁶⁸, N. Berger⁵, J. Beringer¹⁶, S. Berlendis⁵⁸, N.R. Bernard⁸⁹, G. Bernardi⁸³, C. Bernius¹⁴⁵, F.U. Bernlochner²³, T. Berry⁸⁰, P. Berta⁸⁶, C. Bertella^{35a}, G. Bertoli^{148a,148b}, I.A. Bertram⁷⁵, C. Bertsche⁴⁵, D. Bertsche¹¹⁵, G.J. Besjes³⁹, O. Bessidskaia Bylund^{148a,148b}, M. Bessner⁴⁵, N. Besson¹³⁸, A. Bethani⁸⁷, S. Bethke¹⁰³, A. Betti²³, A.J. Bevan⁷⁹, J. Beyer¹⁰³, R.M. Bianchi¹²⁷, O. Biebel¹⁰², D. Biedermann¹⁷, R. Bielski⁸⁷, K. Bierwagen⁸⁶, N.V. Biesuz^{126a,126b}, M. Biglietti^{136a}, T.R.V. Billoud⁹⁷, H. Bilokon⁵⁰, M. Bindi⁵⁷, A. Bingul^{20b}, C. Bini^{134a,134b}, S. Biondi^{22a,22b}, T. Bisanz⁵⁷, C. Bittrich⁴⁷, D.M. Bjergaard⁴⁸, J.E. Black¹⁴⁵, K.M. Black²⁴, R.E. Blair⁶, T. Blazek^{146a}, I. Bloch⁴⁵, C. Blocker²⁵, A. Blue⁵⁶, U. Blumenschein⁷⁹, S. Blunier^{34a}, G.J. Bobbink¹⁰⁹,

V.S. Bobrovnikov^{111,c}, S.S. Bocchetta⁸⁴, A. Bocci⁴⁸, C. Bock¹⁰², M. Boehler⁵¹, D. Boerner¹⁷⁸, D. Bogavac¹⁰², A.G. Bogdanchikov¹¹¹, C. Bohm^{148a}, V. Boisvert⁸⁰, P. Bokan^{168,i}, T. Bold^{41a}, A.S. Boldyrev¹⁰¹, A.E. Bolz^{60b}, M. Bomben⁸³, M. Bona⁷⁹, M. Boonekamp¹³⁸, A. Borisov¹³², G. Borisso⁷⁵, J. Bortfeldt³², D. Bortoletto¹²², V. Bortolotto^{62a}, D. Boscherini^{22a}, M. Bosman¹³, J.D. Bossio Sola²⁹, J. Boudreau¹²⁷, E.V. Bouhova-Thacker⁷⁵, D. Boumediene³⁷, C. Bourdarios¹¹⁹, S.K. Boutle⁵⁶, A. Boveia¹¹³, J. Boyd³², I.R. Boyko⁶⁸, A.J. Bozson⁸⁰, J. Bracinik¹⁹, A. Brandt⁸, G. Brandt⁵⁷, O. Brandt^{60a}, F. Braren⁴⁵, U. Bratzler¹⁵⁸, B. Brau⁸⁹, J.E. Brau¹¹⁸, W.D. Breaden Madden⁵⁶, K. Brendlinger⁴⁵, A.J. Brennan⁹¹, L. Brenner¹⁰⁹, R. Brenner¹⁶⁸, S. Bressler¹⁷⁵, D.L. Briglin¹⁹, T.M. Bristow⁴⁹, D. Britton⁵⁶, D. Britzger⁴⁵, F.M. Brochu³⁰, I. Brock²³, R. Brock⁹³, G. Brooijmans³⁸, T. Brooks⁸⁰, W.K. Brooks^{34b}, J. Brosamer¹⁶, E. Brost¹¹⁰, J.H. Broughton¹⁹, P.A. Bruckman de Renstrom⁴², D. Bruncko^{146b}, A. Bruni^{22a}, G. Bruni^{22a}, L.S. Bruni¹⁰⁹, S. Bruno^{135a,135b}, B.H. Brunt³⁰, M. Bruschi^{22a}, N. Brusino¹²⁷, P. Bryant³³, L. Bryngemark⁴⁵, T. Buanes¹⁵, Q. Buat¹⁴⁴, P. Buchholz¹⁴³, A.G. Buckley⁵⁶, I.A. Budagov⁶⁸, F. Buehrer⁵¹, M.K. Bugge¹²¹, O. Bulekov¹⁰⁰, D. Bullock⁸, T.J. Burch¹¹⁰, S. Burdin⁷⁷, C.D. Burgard¹⁰⁹, A.M. Burger⁵, B. Burghgrave¹¹⁰, K. Burka⁴², S. Burke¹³³, I. Burmeister⁴⁶, J.T.P. Burr¹²², D. Büscher⁵¹, V. Büscher⁸⁶, P. Bussey⁵⁶, J.M. Butler²⁴, C.M. Buttar⁵⁶, J.M. Butterworth⁸¹, P. Butti³², W. Buttinger²⁷, A. Buzatu¹⁵³, A.R. Buzykaev^{111,c}, S. Cabrera Urbán¹⁷⁰, D. Caforio¹³⁰, H. Cai¹⁶⁹, V.M. Cairo^{40a,40b}, O. Cakir^{4a}, N. Calace⁵², P. Calafiura¹⁶, A. Calandri⁸⁸, G. Calderini⁸³, P. Calfayan⁶⁴, G. Callea^{40a,40b}, L.P. Caloba^{26a}, S. Calvente Lopez⁸⁵, D. Calvet³⁷, S. Calvet³⁷, T.P. Calvet⁸⁸, R. Camacho Toro³³, S. Camarda³², P. Camarri^{135a,135b}, D. Cameron¹²¹, R. Caminal Armadans¹⁶⁹, C. Camincher⁵⁸, S. Campana³², M. Campanelli⁸¹, A. Camplani^{94a,94b}, A. Campoverde¹⁴³, V. Canale^{106a,106b}, M. Cano Bret^{36c}, J. Cantero¹¹⁶, T. Cao¹⁵⁵, M.D.M. Capeans Garrido³², I. Caprini^{28b}, M. Caprini^{28b}, M. Capua^{40a,40b}, R.M. Carbone³⁸, R. Cardarelli^{135a}, F. Cardillo⁵¹, I. Carli¹³¹, T. Carli³², G. Carlino^{106a}, B.T. Carlson¹²⁷, L. Carminati^{94a,94b}, R.M.D. Carney^{148a,148b}, S. Caron¹⁰⁸, E. Carquin^{34b}, S. Carrá^{94a,94b}, G.D. Carrillo-Montoya³², D. Casadei¹⁹, M.P. Casado^{13,j}, M. Casolino¹³, D.W. Casper¹⁶⁶, R. Castelijm¹⁰⁹, V. Castillo Gimenez¹⁷⁰, N.F. Castro^{128a,k}, A. Catinaccio³², J.R. Catmore¹²¹, A. Cattai³², J. Caudron²³, V. Cavaliere¹⁶⁹, E. Cavallaro¹³, D. Cavalli^{94a}, M. Cavalli-Sforza¹³, V. Cavasinni^{126a,126b}, E. Celebi^{20d}, F. Ceradini^{136a,136b}, L. Cerda Alberich¹⁷⁰, A.S. Cerqueira^{26b}, A. Cerri¹⁵¹, L. Cerrito^{135a,135b}, F. Cerutti¹⁶, A. Cervelli^{22a,22b}, S.A. Cetin^{20d}, A. Chafaq^{137a}, D. Chakraborty¹¹⁰, S.K. Chan⁵⁹, W.S. Chan¹⁰⁹, Y.L. Chan^{62a}, P. Chang¹⁶⁹, J.D. Chapman³⁰, D.G. Charlton¹⁹, C.C. Chau³¹, C.A. Chavez Barajas¹⁵¹, S. Che¹¹³, S. Cheatham^{167a,167c}, A. Chegwiddden⁹³, S. Chekanov⁶, S.V. Chekulaev^{163a}, G.A. Chelkov^{68,l}, M.A. Chelstowska³², C. Chen^{36a}, C. Chen⁶⁷, H. Chen²⁷, J. Chen^{36a}, S. Chen^{35b}, S. Chen¹⁵⁷, X. Chen^{35c,m}, Y. Chen⁷⁰, H.C. Cheng⁹², H.J. Cheng^{35a}, A. Cheplakov⁶⁸, E. Cheremushkina¹³², R. Cherkaoui El Moursli^{137e}, E. Cheu⁷, K. Cheung⁶³, L. Chevalier¹³⁸, V. Chiarella⁵⁰, G. Chiarelli^{126a,126b}, G. Chiodini^{76a}, A.S. Chisholm³², A. Chitan^{28b}, Y.H. Chiu¹⁷², M.V. Chizhov⁶⁸, K. Choi⁶⁴, A.R. Chomont³⁷, S. Chouridou¹⁵⁶, Y.S. Chow^{62a}, V. Christodoulou⁸¹, M.C. Chu^{62a}, J. Chudoba¹²⁹, A.J. Chuinard⁹⁰, J.J. Chwastowski⁴², L. Chytka¹¹⁷, A.K. Ciftci^{4a}, D. Cinca⁴⁶, V. Cindro⁷⁸, I.A. Cioara²³, A. Ciocio¹⁶, F. Ciroto^{106a,106b}, Z.H. Citron¹⁷⁵, M. Citterio^{94a}, M. Ciubancan^{28b}, A. Clark⁵², B.L. Clark⁵⁹, M.R. Clark³⁸, P.J. Clark⁴⁹, R.N. Clarke¹⁶, C. Clement^{148a,148b}, Y. Coadou⁸⁸, M. Cobal^{167a,167c}, A. Coccaro⁵², J. Cochran⁶⁷, L. Colasurdo¹⁰⁸, B. Cole³⁸, A.P. Colijn¹⁰⁹, J. Collot⁵⁸, T. Colombo¹⁶⁶, P. Conde Muiño^{128a,128b}, E. Coniavitis⁵¹, S.H. Connell^{147b}, I.A. Connelly⁸⁷, S. Constantinescu^{28b}, G. Conti³², F. Conventi^{106a,n}, M. Cooke¹⁶, A.M. Cooper-Sarkar¹²², F. Cormier¹⁷¹, K.J.R. Cormier¹⁶¹, M. Corradi^{134a,134b}, F. Corriveau^{90,o}, A. Cortes-Gonzalez³², G. Costa^{94a}, M.J. Costa¹⁷⁰, D. Costanzo¹⁴¹, G. Cottin³⁰, G. Cowan⁸⁰, B.E. Cox⁸⁷, K. Cranmer¹¹², S.J. Crawley⁵⁶, R.A. Creager¹²⁴, G. Cree³¹, S. Crépe-Renaudin⁵⁸, F. Crescioli⁸³, W.A. Cribbs^{148a,148b}, M. Cristinziani²³, V. Croft¹¹², G. Crosetti^{40a,40b}, A. Cueto⁸⁵, T. Cuhadar Donszelmann¹⁴¹, A.R. Cukierman¹⁴⁵, J. Cummings¹⁷⁹, M. Curatolo⁵⁰, J. Cúth⁸⁶,

S. Czekierda⁴², P. Czodrowski³², G. D'amen^{22a,22b}, S. D'Auria⁵⁶, L. D'eraimo⁸³, M. D'Onofrio⁷⁷,
 M.J. Da Cunha Sargedas De Sousa^{128a,128b}, C. Da Via⁸⁷, W. Dabrowski^{41a}, T. Dado^{146a}, T. Dai⁹²,
 O. Dale¹⁵, F. Dallaire⁹⁷, C. Dallapiccola⁸⁹, M. Dam³⁹, J.R. Dandoy¹²⁴, M.F. Daneri²⁹, N.P. Dang¹⁷⁶,
 A.C. Daniells¹⁹, N.S. Dann⁸⁷, M. Danning¹⁷¹, M. Dano Hoffmann¹³⁸, V. Dao¹⁵⁰, G. Darbo^{53a},
 S. Darmora⁸, J. Dassoulas³, A. Dattagupta¹¹⁸, T. Daubney⁴⁵, W. Davey²³, C. David⁴⁵, T. Davidek¹³¹,
 D.R. Davis⁴⁸, P. Davison⁸¹, E. Dawe⁹¹, I. Dawson¹⁴¹, K. De⁸, R. de Asmundis^{106a}, A. De Benedetti¹¹⁵,
 S. De Castro^{22a,22b}, S. De Cecco⁸³, N. De Groot¹⁰⁸, P. de Jong¹⁰⁹, H. De la Torre⁹³, F. De Lorenzi⁶⁷,
 A. De Maria⁵⁷, D. De Pedis^{134a}, A. De Salvo^{134a}, U. De Sanctis^{135a,135b}, A. De Santo¹⁵¹,
 K. De Vasconcelos Corga⁸⁸, J.B. De Vivie De Regie¹¹⁹, R. Debbe²⁷, C. Debenedetti¹³⁹,
 D.V. Dedovich⁶⁸, N. Dehghanian³, I. Deigaard¹⁰⁹, M. Del Gaudio^{40a,40b}, J. Del Peso⁸⁵, D. Delgove¹¹⁹,
 F. Deliot¹³⁸, C.M. Delitzsch⁷, A. Dell'Acqua³², L. Dell'Asta²⁴, M. Dell'Orso^{126a,126b},
 M. Della Pietra^{106a,106b}, D. della Volpe⁵², M. Delmastro⁵, C. Delporte¹¹⁹, P.A. Delsart⁵⁸,
 D.A. DeMarco¹⁶¹, S. Demers¹⁷⁹, M. Demichev⁶⁸, A. Demilly⁸³, S.P. Denisov¹³², D. Denysiuk¹³⁸,
 D. Derendarz⁴², J.E. Derkaoui^{137d}, F. Derue⁸³, P. Dervan⁷⁷, K. Desch²³, C. Deterre⁴⁵, K. Dette¹⁶¹,
 M.R. Devesa²⁹, P.O. Deviveiros³², A. Dewhurst¹³³, S. Dhaliwal²⁵, F.A. Di Bello⁵²,
 A. Di Ciaccio^{135a,135b}, L. Di Ciaccio⁵, W.K. Di Clemente¹²⁴, C. Di Donato^{106a,106b}, A. Di Girolamo³²,
 B. Di Girolamo³², B. Di Micco^{136a,136b}, R. Di Nardo³², K.F. Di Petrillo⁵⁹, A. Di Simone⁵¹,
 R. Di Sipio¹⁶¹, D. Di Valentino³¹, C. Diaconu⁸⁸, M. Diamond¹⁶¹, F.A. Dias³⁹, M.A. Diaz^{34a},
 E.B. Diehl⁹², J. Dietrich¹⁷, S. Díez Cornell⁴⁵, A. Dimitrievska¹⁴, J. Dingfelder²³, P. Dita^{28b}, S. Dita^{28b},
 F. Dittus³², F. Djama⁸⁸, T. Djobava^{54b}, J.I. Djuvsland^{160a}, M.A.B. do Vale^{26c}, D. Dobos³², M. Dobre^{28b},
 D. Dodsworth²⁵, C. Doglioni⁸⁴, J. Dolejsi¹³¹, Z. Dolezal¹³¹, M. Donadelli^{26d}, S. Donati^{126a,126b},
 P. Dondero^{123a,123b}, J. Donini³⁷, J. Dopke¹³³, A. Doria^{106a}, M.T. Dova⁷⁴, A.T. Doyle⁵⁶, E. Drechsler⁵⁷,
 M. Dris¹⁰, Y. Du^{36b}, J. Duarte-Campderros¹⁵⁵, F. Dubinin⁹⁸, A. Dubreuil⁵², E. Duchovni¹⁷⁵,
 G. Duceck¹⁰², A. Ducourthial⁸³, O.A. Ducu^{97.p}, D. Duda¹⁰⁹, A. Dudarev³², A.Chr. Dudder⁸⁶,
 E.M. Duffield¹⁶, L. Dufflot¹¹⁹, M. Dührssen³², C. Dulsen¹⁷⁸, M. Dumancic¹⁷⁵, A.E. Dumitriu^{28b},
 A.K. Duncan⁵⁶, M. Dunford^{60a}, A. Duperrin⁸⁸, H. Duran Yildiz^{4a}, M. Düren⁵⁵, A. Durglishvili^{54b},
 D. Duschinger⁴⁷, B. Dutta⁴⁵, D. Duvnjak¹, M. Dyndal⁴⁵, B.S. Dziedzic⁴², C. Eckardt⁴⁵, K.M. Ecker¹⁰³,
 R.C. Edgar⁹², T. Eifert³², G. Eigen¹⁵, K. Einsweiler¹⁶, T. Ekelof¹⁶⁸, M. El Kacimi^{137c}, R. El Kosseifi⁸⁸,
 V. Ellajosyula⁸⁸, M. Ellert¹⁶⁸, S. Elles⁵, F. Ellinghaus¹⁷⁸, A.A. Elliot¹⁷², N. Ellis³², J. Elmsheuser²⁷,
 M. Elsing³², D. Emelianov¹³³, Y. Enari¹⁵⁷, J.S. Ennis¹⁷³, M.B. Epland⁴⁸, J. Erdmann⁴⁶, A. Ereditato¹⁸,
 M. Ernst²⁷, S. Errede¹⁶⁹, M. Escalier¹¹⁹, C. Escobar¹⁷⁰, B. Esposito⁵⁰, O. Estrada Pastor¹⁷⁰,
 A.I. Etienne¹³⁸, E. Etzion¹⁵⁵, H. Evans⁶⁴, A. Ezhilov¹²⁵, M. Ezzi^{137e}, F. Fabbri^{22a,22b}, L. Fabbri^{22a,22b},
 V. Fabiani¹⁰⁸, G. Facini⁸¹, R.M. Fakhruddinov¹³², S. Falciano^{134a}, R.J. Falla⁸¹, J. Faltova³², Y. Fang^{35a},
 M. Fanti^{94a,94b}, A. Farbin⁸, A. Farilla^{136a}, C. Farina¹²⁷, E.M. Farina^{123a,123b}, T. Faroque⁹³, S. Farrell¹⁶,
 S.M. Farrington¹⁷³, P. Farthouat³², F. Fassi^{137e}, P. Fassnacht³², D. Fassouliotis⁹, M. Faucci Giannelli⁴⁹,
 A. Favareto^{53a,53b}, W.J. Fawcett¹²², L. Fayard¹¹⁹, O.L. Fedin^{125.q}, W. Fedorko¹⁷¹, S. Feigl¹²¹,
 L. Felgioni⁸⁸, C. Feng^{36b}, E.J. Feng³², M.J. Fenton⁵⁶, A.B. Fenyuk¹³², L. Feremenga⁸,
 P. Fernandez Martinez¹⁷⁰, J. Ferrando⁴⁵, A. Ferrari¹⁶⁸, P. Ferrari¹⁰⁹, R. Ferrari^{123a},
 D.E. Ferreira de Lima^{60b}, A. Ferrer¹⁷⁰, D. Ferrere⁵², C. Ferretti⁹², F. Fiedler⁸⁶, A. Filipčić⁷⁸,
 M. Filipuzzi⁴⁵, F. Filthaut¹⁰⁸, M. Fincke-Keeler¹⁷², K.D. Finelli²⁴, M.C.N. Fiolhais^{128a,128c,r},
 L. Fiorini¹⁷⁰, A. Fischer², C. Fischer¹³, J. Fischer¹⁷⁸, W.C. Fisher⁹³, N. Flaschel⁴⁵, I. Fleck¹⁴³,
 P. Fleischmann⁹², R.R.M. Fletcher¹²⁴, T. Flick¹⁷⁸, B.M. Flierl¹⁰², L.R. Flores Castillo^{62a},
 M.J. Flowerdew¹⁰³, G.T. Forcolin⁸⁷, A. Formica¹³⁸, F.A. Förster¹³, A. Forti⁸⁷, A.G. Foster¹⁹,
 D. Fournier¹¹⁹, H. Fox⁷⁵, S. Fracchia¹⁴¹, P. Francavilla⁸³, M. Franchini^{22a,22b}, S. Franchino^{60a},
 D. Francis³², L. Franconi¹²¹, M. Franklin⁵⁹, M. Frate¹⁶⁶, M. Fraternali^{123a,123b}, D. Freeborn⁸¹,
 S.M. Fressard-Batraneanu³², B. Freund⁹⁷, D. Froidevaux³², J.A. Frost¹²², C. Fukunaga¹⁵⁸,
 T. Fusayasu¹⁰⁴, J. Fuster¹⁷⁰, O. Gabizon¹⁵⁴, A. Gabrielli^{22a,22b}, A. Gabrielli¹⁶, G.P. Gach^{41a},

S. Gadatsch³², S. Gadomski⁸⁰, G. Gagliardi^{53a,53b}, L.G. Gagnon⁹⁷, C. Galea¹⁰⁸, B. Galhardo^{128a,128c},
 E.J. Gallas¹²², B.J. Gallop¹³³, P. Gallus¹³⁰, G. Galster³⁹, K.K. Gan¹¹³, S. Ganguly³⁷, Y. Gao⁷⁷,
 Y.S. Gao^{145,g}, F.M. Garay Walls^{34a}, C. García¹⁷⁰, J.E. García Navarro¹⁷⁰, J.A. García Pascual^{35a},
 M. Garcia-Sciveres¹⁶, R.W. Gardner³³, N. Garelli¹⁴⁵, V. Garonne¹²¹, A. Gascon Bravo⁴⁵,
 K. Gasnikova⁴⁵, C. Gatti⁵⁰, A. Gaudiello^{53a,53b}, G. Gaudio^{123a}, I.L. Gavrilenko⁹⁸, C. Gay¹⁷¹,
 G. Gaycken²³, E.N. Gazis¹⁰, C.N.P. Gee¹³³, J. Geisen⁵⁷, M. Geisen⁸⁶, M.P. Geisler^{60a},
 K. Gellerstedt^{148a,148b}, C. Gemme^{53a}, M.H. Genest⁵⁸, C. Geng⁹², S. Gentile^{134a,134b}, C. Gentsos¹⁵⁶,
 S. George⁸⁰, D. Gerbaudo¹³, G. Geßner⁴⁶, S. Ghasemi¹⁴³, M. Ghneimat²³, B. Giacobbe^{22a},
 S. Giagu^{134a,134b}, N. Giangiacomi^{22a,22b}, P. Giannetti^{126a,126b}, S.M. Gibson⁸⁰, M. Gignac¹⁷¹,
 M. Gilchriese¹⁶, D. Gillberg³¹, G. Gilles¹⁷⁸, D.M. Gingrich^{3,d}, M.P. Giordani^{167a,167c}, F.M. Giorgi^{22a},
 P.F. Giraud¹³⁸, P. Giromini⁵⁹, G. Giugliarelli^{167a,167c}, D. Giugni^{94a}, F. Giuli¹²², C. Giuliani¹⁰³,
 M. Giuliani^{60b}, B.K. Gjølsten¹²¹, S. Gkaitatzis¹⁵⁶, I. Gkialas^{9,s}, E.L. Gkoukousis¹³, P. Gkoutoumis¹⁰,
 L.K. Gladilin¹⁰¹, C. Glasman⁸⁵, J. Glatzer¹³, P.C.F. Glaysher⁴⁵, A. Glazov⁴⁵, M. Goblirsch-Kolb²⁵,
 J. Godlewski⁴², S. Goldfarb⁹¹, T. Golling⁵², D. Golubkov¹³², A. Gomes^{128a,128b,128d}, R. Gonçalves^{128a},
 R. Goncalves Gama^{26a}, J. Goncalves Pinto Firmino Da Costa¹³⁸, G. Gonella⁵¹, L. Gonella¹⁹,
 A. Gongadze⁶⁸, J.L. Gonski⁵⁹, S. González de la Hoz¹⁷⁰, S. Gonzalez-Sevilla⁵², L. Goossens³²,
 P.A. Gorbounov⁹⁹, H.A. Gordon²⁷, I. Gorelov¹⁰⁷, B. Gorini³², E. Gorini^{76a,76b}, A. Gorišek⁷⁸,
 A.T. Goshaw⁴⁸, C. Gössling⁴⁶, M.I. Gostkin⁶⁸, C.A. Gottardo²³, C.R. Goudet¹¹⁹, D. Goujdami^{137c},
 A.G. Goussiou¹⁴⁰, N. Govender^{147b,t}, E. Gozani¹⁵⁴, I. Grabowska-Bold^{41a}, P.O.J. Gradin¹⁶⁸,
 J. Gramling¹⁶⁶, E. Gramstad¹²¹, S. Grancagnolo¹⁷, V. Gratchev¹²⁵, P.M. Gravila^{28f}, C. Gray⁵⁶,
 H.M. Gray¹⁶, Z.D. Greenwood^{82,u}, C. Grefe²³, K. Gregersen⁸¹, I.M. Gregor⁴⁵, P. Grenier¹⁴⁵,
 K. Grevtsov⁵, J. Griffiths⁸, A.A. Grillo¹³⁹, K. Grimm⁷⁵, S. Grinstein^{13,v}, Ph. Gris³⁷, J.-F. Grivaz¹¹⁹,
 S. Groh⁸⁶, E. Gross¹⁷⁵, J. Grosse-Knetter⁵⁷, G.C. Grossi⁸², Z.J. Grout⁸¹, A. Grummer¹⁰⁷, L. Guan⁹²,
 W. Guan¹⁷⁶, J. Guenther³², F. Guescini^{163a}, D. Guest¹⁶⁶, O. Gueta¹⁵⁵, B. Gui¹¹³, E. Guido^{53a,53b},
 T. Guillemin⁵, S. Guindon³², U. Gul⁵⁶, C. Gumpert³², J. Guo^{36c}, W. Guo⁹², Y. Guo^{36a,w}, R. Gupta⁴³,
 S. Gurbuz^{20a}, G. Gustavino¹¹⁵, B.J. Gutelman¹⁵⁴, P. Gutierrez¹¹⁵, N.G. Gutierrez Ortiz⁸¹,
 C. Gutsche⁸¹, C. Guyot¹³⁸, M.P. Guzik^{41a}, C. Gwenlan¹²², C.B. Gwilliam⁷⁷, A. Haas¹¹², C. Haber¹⁶,
 H.K. Hadavand⁸, N. Haddad^{137e}, A. Hadeef⁸⁸, S. Hageböck²³, M. Hagihara¹⁶⁴, H. Hakobyan^{180,*},
 M. Haleem⁴⁵, J. Haley¹¹⁶, G. Halladjian⁹³, G.D. Hallewell⁸⁸, K. Hamacher¹⁷⁸, P. Hamal¹¹⁷,
 K. Hamano¹⁷², A. Hamilton^{147a}, G.N. Hamity¹⁴¹, P.G. Hamnett⁴⁵, L. Han^{36a}, S. Han^{35a},
 K. Hanagaki^{69,x}, K. Hanawa¹⁵⁷, M. Hance¹³⁹, D.M. Handl¹⁰², B. Haney¹²⁴, P. Hanke^{60a}, J.B. Hansen³⁹,
 J.D. Hansen³⁹, M.C. Hansen²³, P.H. Hansen³⁹, K. Hara¹⁶⁴, A.S. Hard¹⁷⁶, T. Harenberg¹⁷⁸, F. Hariri¹¹⁹,
 S. Harkusha⁹⁵, P.F. Harrison¹⁷³, N.M. Hartmann¹⁰², Y. Hasegawa¹⁴², A. Hasib⁴⁹, S. Hassani¹³⁸,
 S. Haug¹⁸, R. Hauser⁹³, L. Hauswald⁴⁷, L.B. Havener³⁸, M. Havranek¹³⁰, C.M. Hawkes¹⁹,
 R.J. Hawkings³², D. Hayakawa¹⁵⁹, D. Hayden⁹³, C.P. Hays¹²², J.M. Hays⁷⁹, H.S. Hayward⁷⁷,
 S.J. Haywood¹³³, S.J. Head¹⁹, T. Heck⁸⁶, V. Hedberg⁸⁴, L. Heelan⁸, S. Heer²³, K.K. Heidegger⁵¹,
 S. Heim⁴⁵, T. Heim¹⁶, B. Heinemann^{45,y}, J.J. Heinrich¹⁰², L. Heinrich¹¹², C. Heinz⁵⁵, J. Hejbal¹²⁹,
 L. Helary³², A. Held¹⁷¹, S. Hellman^{148a,148b}, C. Helsen³², R.C.W. Henderson⁷⁵, Y. Heng¹⁷⁶,
 S. Henkelmann¹⁷¹, A.M. Henriques Correia³², S. Henrot-Versille¹¹⁹, G.H. Herbert¹⁷, H. Herde²⁵,
 V. Herget¹⁷⁷, Y. Hernández Jiménez^{147c}, H. Herr⁸⁶, G. Herten⁵¹, R. Hertenberger¹⁰², L. Hervas³²,
 T.C. Herwig¹²⁴, G.G. Hesketh⁸¹, N.P. Hessey^{163a}, J.W. Hetherly⁴³, S. Higashino⁶⁹,
 E. Higón-Rodríguez¹⁷⁰, K. Hildebrand³³, E. Hill¹⁷², J.C. Hill³⁰, K.H. Hiller⁴⁵, S.J. Hillier¹⁹, M. Hils⁴⁷,
 I. Hinchliffe¹⁶, M. Hirose⁵¹, D. Hirschbuehl¹⁷⁸, B. Hiti⁷⁸, O. Hladik¹²⁹, D.R. Hlaluku^{147c}, X. Hoad⁴⁹,
 J. Hobbs¹⁵⁰, N. Hod^{163a}, M.C. Hodgkinson¹⁴¹, P. Hodgson¹⁴¹, A. Hoecker³², M.R. Hoferkamp¹⁰⁷,
 F. Hoenig¹⁰², D. Hohn²³, T.R. Holmes³³, M. Homann⁴⁶, S. Honda¹⁶⁴, T. Honda⁶⁹, T.M. Hong¹²⁷,
 B.H. Hooberman¹⁶⁹, W.H. Hopkins¹¹⁸, Y. Horii¹⁰⁵, A.J. Horton¹⁴⁴, J.-Y. Hostachy⁵⁸, A. Hostiuc¹⁴⁰,
 S. Hou¹⁵³, A. Hoummada^{137a}, J. Howarth⁸⁷, J. Hoya⁷⁴, M. Hrabovsky¹¹⁷, J. Hrdinka³², I. Hristova¹⁷,

J. Hrivnac¹¹⁹, T. Hryn'ova⁵, A. Hrynevich⁹⁶, P.J. Hsu⁶³, S.-C. Hsu¹⁴⁰, Q. Hu²⁷, S. Hu^{36c}, Y. Huang^{35a}, Z. Hubacek¹³⁰, F. Hubaut⁸⁸, F. Huegging²³, T.B. Huffman¹²², E.W. Hughes³⁸, M. Huhtinen³², R.F.H. Hunter³¹, P. Huo¹⁵⁰, N. Huseynov^{68,b}, J. Huston⁹³, J. Huth⁵⁹, R. Hyneman⁹², G. Iacobucci⁵², G. Iakovidis²⁷, I. Ibragimov¹⁴³, L. Iconomidou-Fayard¹¹⁹, Z. Idrissi^{137e}, P. Iengo³², O. Igonkina^{109,z}, T. Iizawa¹⁷⁴, Y. Ikegami⁶⁹, M. Ikeno⁶⁹, Y. Ilchenko^{11,aa}, D. Iliadis¹⁵⁶, N. Ilic¹⁴⁵, F. Iltzsche⁴⁷, G. Introzzi^{123a,123b}, P. Ioannou^{9,*}, M. Iodice^{136a}, K. Iordanidou³⁸, V. Ippolito⁵⁹, M.F. Isacson¹⁶⁸, N. Ishijima¹²⁰, M. Ishino¹⁵⁷, M. Ishitsuka¹⁵⁹, C. Issever¹²², S. Istin^{20a}, F. Ito¹⁶⁴, J.M. Iturbe Ponce^{62a}, R. Iuppa^{162a,162b}, H. Iwasaki⁶⁹, J.M. Izen⁴⁴, V. Izzo^{106a}, S. Jabbar³, P. Jackson¹, R.M. Jacobs²³, V. Jain², K.B. Jakobi⁸⁶, K. Jakobs⁵¹, S. Jakobsen⁶⁵, T. Jakoubek¹²⁹, D.O. Jamin¹¹⁶, D.K. Jana⁸², R. Jansky⁵², J. Janssen²³, M. Janus⁵⁷, P.A. Janus^{41a}, G. Jarlskog⁸⁴, N. Javadov^{68,b}, T. Javůrek⁵¹, M. Javurkova⁵¹, F. Jeanneau¹³⁸, L. Jeanty¹⁶, J. Jejelava^{54a,ab}, A. Jelinskas¹⁷³, P. Jenni^{51,ac}, C. Jeske¹⁷³, S. Jézéquel⁵, H. Ji¹⁷⁶, J. Jia¹⁵⁰, H. Jiang⁶⁷, Y. Jiang^{36a}, Z. Jiang¹⁴⁵, S. Jiggins⁸¹, J. Jimenez Pena¹⁷⁰, S. Jin^{35b}, A. Jinaru^{28b}, O. Jinnouchi¹⁵⁹, H. Jivan^{147c}, P. Johansson¹⁴¹, K.A. Johns⁷, C.A. Johnson⁶⁴, W.J. Johnson¹⁴⁰, K. Jon-And^{148a,148b}, R.W.L. Jones⁷⁵, S.D. Jones¹⁵¹, S. Jones⁷, T.J. Jones⁷⁷, J. Jongmanns^{60a}, P.M. Jorge^{128a,128b}, J. Jovicevic^{163a}, X. Ju¹⁷⁶, A. Juste Rozas^{13,v}, M.K. Köhler¹⁷⁵, A. Kaczmarska⁴², M. Kado¹¹⁹, H. Kagan¹¹³, M. Kagan¹⁴⁵, S.J. Kahn⁸⁸, T. Kaji¹⁷⁴, E. Kajomovitz¹⁵⁴, C.W. Kalderon⁸⁴, A. Kaluza⁸⁶, S. Kama⁴³, A. Kamenshchikov¹³², N. Kanaya¹⁵⁷, L. Kanjir⁷⁸, V.A. Kantserov¹⁰⁰, J. Kanzaki⁶⁹, B. Kaplan¹¹², L.S. Kaplan¹⁷⁶, D. Kar^{147c}, K. Karakostas¹⁰, N. Karastathis¹⁰, M.J. Kareem^{163b}, E. Karentzos¹⁰, S.N. Karpov⁶⁸, Z.M. Karpova⁶⁸, K. Karthik¹¹², V. Kartvelishvili⁷⁵, A.N. Karyukhin¹³², K. Kasahara¹⁶⁴, L. Kashif¹⁷⁶, R.D. Kass¹¹³, A. Kastanas¹⁴⁹, Y. Kataoka¹⁵⁷, C. Kato¹⁵⁷, A. Katre⁵², J. Katzy⁴⁵, K. Kawade⁷⁰, K. Kawagoe⁷³, T. Kawamoto¹⁵⁷, G. Kawamura⁵⁷, E.F. Kay⁷⁷, V.F. Kazanin^{111,c}, R. Keeler¹⁷², R. Kehoe⁴³, J.S. Keller³¹, E. Kellermann⁸⁴, J.J. Kempster⁸⁰, J. Kendrick¹⁹, H. Keoshkerian¹⁶¹, O. Kepka¹²⁹, B.P. Kerševan⁷⁸, S. Kersten¹⁷⁸, R.A. Keyes⁹⁰, M. Khader¹⁶⁹, F. Khalil-zada¹², A. Khanov¹¹⁶, A.G. Kharlamov^{111,c}, T. Kharlamova^{111,c}, A. Khodinov¹⁶⁰, T.J. Khoo⁵², V. Khovanskiy^{99,*}, E. Khramov⁶⁸, J. Khubua^{54b,ad}, S. Kido⁷⁰, C.R. Kilby⁸⁰, H.Y. Kim⁸, S.H. Kim¹⁶⁴, Y.K. Kim³³, N. Kimura¹⁵⁶, O.M. Kind¹⁷, B.T. King⁷⁷, D. Kirchmeier⁴⁷, J. Kirk¹³³, A.E. Kiryunin¹⁰³, T. Kishimoto¹⁵⁷, D. Kisielewska^{41a}, V. Kitali⁴⁵, O. Kiverny⁵, E. Kladiva^{146b}, T. Klapdor-Kleingrothaus⁵¹, M.H. Klein⁹², M. Klein⁷⁷, U. Klein⁷⁷, K. Kleinknecht⁸⁶, P. Klimek¹¹⁰, A. Klimentov²⁷, R. Klingenberg^{46,*}, T. Klingl²³, T. Klioutchnikova³², F.F. Klitzner¹⁰², E.-E. Kluge^{60a}, P. Kluit¹⁰⁹, S. Kluth¹⁰³, E. Kneringer⁶⁵, E.B.F.G. Knoops⁸⁸, A. Knue¹⁰³, A. Kobayashi¹⁵⁷, D. Kobayashi⁷³, T. Kobayashi¹⁵⁷, M. Kobel⁴⁷, M. Kocian¹⁴⁵, P. Kodys¹³¹, T. Koffas³¹, E. Koffeman¹⁰⁹, N.M. Köhler¹⁰³, T. Koi¹⁴⁵, M. Kolb^{60b}, I. Koletsou⁵, A.A. Komar^{98,*}, T. Kondo⁶⁹, N. Kondrashova^{36c}, K. Köneke⁵¹, A.C. König¹⁰⁸, T. Kono^{69,ae}, R. Konoplich^{112,af}, N. Konstantinidis⁸¹, B. Konya⁸⁴, R. Kopeliansky⁶⁴, S. Koperny^{41a}, A.K. Kopp⁵¹, K. Korcyl⁴², K. Kordas¹⁵⁶, A. Korn⁸¹, A.A. Korol^{111,c}, I. Korolkov¹³, E.V. Korolkova¹⁴¹, O. Kortner¹⁰³, S. Kortner¹⁰³, T. Kosek¹³¹, V.V. Kostyukhin²³, A. Kotwal⁴⁸, A. Koulouris¹⁰, A. Kourkouveli-Charalampidi^{123a,123b}, C. Kourkouvelis⁹, E. Kourlitis¹⁴¹, V. Kouskoura²⁷, A.B. Kowalewska⁴², R. Kowalewski¹⁷², T.Z. Kowalski^{41a}, C. Kozakai¹⁵⁷, W. Kozanecki¹³⁸, A.S. Kozhin¹³², V.A. Kramarenko¹⁰¹, G. Kramberger⁷⁸, D. Krasnopevtsev¹⁰⁰, M.W. Krasny⁸³, A. Krasznahorkay³², D. Krauss¹⁰³, J.A. Kremer^{41a}, J. Kretschmar⁷⁷, K. Kreutzfeldt⁵⁵, P. Krieger¹⁶¹, K. Krizka¹⁶, K. Kroeninger⁴⁶, H. Kroha¹⁰³, J. Kroll¹²⁹, J. Kroll¹²⁴, J. Kroseberg²³, J. Krstic¹⁴, U. Kruchonak⁶⁸, H. Krüger²³, N. Krumnack⁶⁷, M.C. Kruse⁴⁸, T. Kubota⁹¹, H. Kucuk⁸¹, S. Kudah^{4b}, J.T. Kuechler¹⁷⁸, S. Kuehn³², A. Kugel^{60a}, F. Kuger¹⁷⁷, T. Kuhl⁴⁵, V. Kukhtin⁶⁸, R. Kukla⁸⁸, Y. Kulchitsky⁹⁵, S. Kuleshov^{34b}, Y.P. Kulinich¹⁶⁹, M. Kuna^{134a,134b}, T. Kunigo⁷¹, A. Kupco¹²⁹, T. Kupfer⁴⁶, O. Kuprash¹⁵⁵, H. Kurashige⁷⁰, L.L. Kurchaninov^{163a}, Y.A. Kurochkin⁹⁵, M.G. Kurth^{35a}, E.S. Kuwertz¹⁷², M. Kuze¹⁵⁹, J. Kvita¹¹⁷, T. Kwan¹⁷², D. Kyriazopoulos¹⁴¹, A. La Rosa¹⁰³, J.L. La Rosa Navarro^{26d}, L. La Rotonda^{40a,40b}, F. La Ruffa^{40a,40b}, C. Lacasta¹⁷⁰, F. Lacava^{134a,134b}, J. Lacey⁴⁵, D.P.J. Lack⁸⁷,

H. Lacker¹⁷, D. Lacour⁸³, E. Ladygin⁶⁸, R. Lafaye⁵, B. Laforge⁸³, T. Lagouri¹⁷⁹, S. Lai⁵⁷,
 S. Lammers⁶⁴, W. Lampl⁷, E. Lançon²⁷, U. Landgraf⁵¹, M.P.J. Landon⁷⁹, M.C. Lanfermann⁵²,
 V.S. Lang⁴⁵, J.C. Lange¹³, R.J. Langenberg³², A.J. Lankford¹⁶⁶, F. Lanni²⁷, K. Lantzscht²³, A. Lanza^{123a},
 A. Lapertosa^{53a,53b}, S. Laplace⁸³, J.F. Laporte¹³⁸, T. Lari^{94a}, F. Lasagni Manghi^{22a,22b}, M. Lassnig³²,
 T.S. Lau^{62a}, P. Laurelli⁵⁰, W. Lavrijsen¹⁶, A.T. Law¹³⁹, P. Laycock⁷⁷, T. Lazovich⁵⁹, M. Lazzaroni^{94a,94b},
 B. Le⁹¹, O. Le Dortz⁸³, E. Le Guirriec⁸⁸, E.P. Le Quilleuc¹³⁸, M. LeBlanc¹⁷², T. LeCompte⁶,
 F. Ledroit-Guillon⁵⁸, C.A. Lee²⁷, G.R. Lee^{34a}, S.C. Lee¹⁵³, L. Lee⁵⁹, B. Lefebvre⁹⁰, G. Lefebvre⁸³,
 M. Lefebvre¹⁷², F. Legger¹⁰², C. Leggett¹⁶, G. Lehmann Miotto³², X. Lei⁷, W.A. Leight⁴⁵,
 M.A.L. Leite^{26d}, R. Leitner¹³¹, D. Lellouch¹⁷⁵, B. Lemmer⁵⁷, K.J.C. Leney⁸¹, T. Lenz²³, B. Lenzi³²,
 R. Leone⁷, S. Leone^{126a,126b}, C. Leonidopoulos⁴⁹, G. Lerner¹⁵¹, C. Leroy⁹⁷, R. Les¹⁶¹, A.A.J. Lesage¹³⁸,
 C.G. Lester³⁰, M. Levchenko¹²⁵, J. Levêque⁵, D. Levin⁹², L.J. Levinson¹⁷⁵, M. Levy¹⁹, D. Lewis⁷⁹,
 B. Li^{36a,w}, Changqiao Li^{36a}, H. Li¹⁵⁰, L. Li^{36c}, Q. Li^{35a}, Q. Li^{36a}, S. Li⁴⁸, X. Li^{36c}, Y. Li¹⁴³, Z. Liang^{35a},
 B. Liberti^{135a}, A. Liblong¹⁶¹, K. Lie^{62c}, J. Liebal²³, W. Liebig¹⁵, A. Limosani¹⁵², K. Lin⁹³, S.C. Lin¹⁸²,
 T.H. Lin⁸⁶, R.A. Linck⁶⁴, B.E. Lindquist¹⁵⁰, A.E. Lioni⁵², E. Lipeles¹²⁴, A. Lipniacka¹⁵, M. Lisovyi^{60b},
 T.M. Liss^{169,ag}, A. Lister¹⁷¹, A.M. Litke¹³⁹, B. Liu⁶⁷, H. Liu⁹², H. Liu²⁷, J.K.K. Liu¹²², J. Liu^{36b},
 J.B. Liu^{36a}, K. Liu⁸⁸, L. Liu¹⁶⁹, M. Liu^{36a}, Y.L. Liu^{36a}, Y. Liu^{36a}, M. Livan^{123a,123b}, A. Lleres⁵⁸,
 J. Llorente Merino^{35a}, S.L. Lloyd⁷⁹, C.Y. Lo^{62b}, F. Lo Sterzo⁴³, E.M. Lobodzinska⁴⁵, P. Loch⁷,
 F.K. Loebinger⁸⁷, A. Loesle⁵¹, K.M. Loew²⁵, T. Lohse¹⁷, K. Lohwasser¹⁴¹, M. Lokajicek¹²⁹,
 B.A. Long²⁴, J.D. Long¹⁶⁹, R.E. Long⁷⁵, L. Longo^{76a,76b}, K.A. Looper¹¹³, J.A. Lopez^{34b}, I. Lopez Paz¹³,
 A. Lopez Solis⁸³, J. Lorenz¹⁰², N. Lorenzo Martinez⁵, M. Losada²¹, P.J. Lösel¹⁰², X. Lou^{35a},
 A. Lounis¹¹⁹, J. Love⁶, P.A. Love⁷⁵, H. Lu^{62a}, N. Lu⁹², Y.J. Lu⁶³, H.J. Lubatti¹⁴⁰, C. Luci^{134a,134b},
 A. Lucotte⁵⁸, C. Luedtke⁵¹, F. Luehring⁶⁴, W. Lukas⁶⁵, L. Luminari^{134a}, O. Lundberg^{148a,148b},
 B. Lund-Jensen¹⁴⁹, M.S. Lutz⁸⁹, P.M. Luzi⁸³, D. Lynn²⁷, R. Lysak¹²⁹, E. Lytken⁸⁴, F. Lyu^{35a},
 V. Lyubushkin⁶⁸, H. Ma²⁷, L.L. Ma^{36b}, Y. Ma^{36b}, G. Maccarrone⁵⁰, A. Macchiolo¹⁰³,
 C.M. Macdonald¹⁴¹, B. Maček⁷⁸, J. Machado Miguens^{124,128b}, D. Madaffari¹⁷⁰, R. Madar³⁷,
 W.F. Mader⁴⁷, A. Madsen⁴⁵, N. Madysa⁴⁷, J. Maeda⁷⁰, S. Maeland¹⁵, T. Maeno²⁷, A.S. Maevskiy¹⁰¹,
 V. Magerl⁵¹, C. Maiani¹¹⁹, C. Maidantchik^{26a}, T. Maier¹⁰², A. Maio^{128a,128b,128d}, O. Majersky^{146a},
 S. Majewski¹¹⁸, Y. Makida⁶⁹, N. Makovec¹¹⁹, B. Malaescu⁸³, Pa. Malecki⁴², V.P. Maleev¹²⁵, F. Malek⁵⁸,
 U. Mallik⁶⁶, D. Malon⁶, C. Malone³⁰, S. Maltezos¹⁰, S. Malyukov³², J. Mamuzic¹⁷⁰, G. Mancini⁵⁰,
 I. Mandić⁷⁸, J. Maneira^{128a,128b}, L. Manhaes de Andrade Filho^{26b}, J. Manjarres Ramos⁴⁷,
 K.H. Mankinen⁸⁴, A. Mann¹⁰², A. Manousos³², B. Mansoulie¹³⁸, J.D. Mansour^{35a}, R. Mantifel⁹⁰,
 M. Mantoani⁵⁷, S. Manzoni^{94a,94b}, L. Mapelli³², G. Marceca²⁹, L. March⁵², L. Marchese¹²²,
 G. Marchiori⁸³, M. Marcisovsky¹²⁹, C.A. Marin Tobon³², M. Marjanovic³⁷, D.E. Marley⁹²,
 F. Marroquim^{26a}, S.P. Marsden⁸⁷, Z. Marshall¹⁶, M.U.F. Martensson¹⁶⁸, S. Marti-Garcia¹⁷⁰,
 C.B. Martin¹¹³, T.A. Martin¹⁷³, V.J. Martin⁴⁹, B. Martin dit Latour¹⁵, M. Martinez^{13,v},
 V.I. Martinez Outschoorn¹⁶⁹, S. Martin-Haugh¹³³, V.S. Martoiu^{28b}, A.C. Martyniuk⁸¹, A. Marzin³²,
 L. Masetti⁸⁶, T. Mashimo¹⁵⁷, R. Mashinistov⁹⁸, J. Masik⁸⁷, A.L. Maslennikov^{111,c}, L.H. Mason⁹¹,
 L. Massa^{135a,135b}, P. Mastrandrea⁵, A. Mastroberardino^{40a,40b}, T. Masubuchi¹⁵⁷, P. Mättig¹⁷⁸,
 J. Maurer^{28b}, S.J. Maxfield⁷⁷, D.A. Maximov^{111,c}, R. Mazini¹⁵³, I. Maznas¹⁵⁶, S.M. Mazza^{94a,94b},
 N.C. Mc Fadden¹⁰⁷, G. Mc Goldrick¹⁶¹, S.P. Mc Kee⁹², A. McCarn⁹², R.L. McCarthy¹⁵⁰,
 T.G. McCarthy¹⁰³, L.I. McClymont⁸¹, E.F. McDonald⁹¹, J.A. Mcfayden³², G. Mchedlidze⁵⁷,
 S.J. McMahon¹³³, P.C. McNamara⁹¹, C.J. McNicol¹⁷³, R.A. McPherson^{172,o}, S. Meehan¹⁴⁰,
 T.J. Megy⁵¹, S. Mehlhase¹⁰², A. Mehta⁷⁷, T. Meideck⁵⁸, K. Meier^{60a}, B. Meirose⁴⁴, D. Melini^{170,ah},
 B.R. Mellado Garcia^{147c}, J.D. Mellenthin⁵⁷, M. Melo^{146a}, F. Meloni¹⁸, A. Melzer²³, S.B. Menary⁸⁷,
 L. Meng⁷⁷, X.T. Meng⁹², A. Mengarelli^{22a,22b}, S. Menke¹⁰³, E. Meoni^{40a,40b}, S. Mergelmeyer¹⁷,
 C. Merlassino¹⁸, P. Mermod⁵², L. Merola^{106a,106b}, C. Meroni^{94a}, F.S. Merritt³³, A. Messina^{134a,134b},
 J. Metcalfe⁶, A.S. Mete¹⁶⁶, C. Meyer¹²⁴, J-P. Meyer¹³⁸, J. Meyer¹⁰⁹, H. Meyer Zu Theenhausen^{60a},

F. Miano¹⁵¹, R.P. Middleton¹³³, S. Miglioranzi^{53a,53b}, L. Mijović⁴⁹, G. Mikenberg¹⁷⁵,
M. Mikestikova¹²⁹, M. Mikuž⁷⁸, M. Milesi⁹¹, A. Milic¹⁶¹, D.A. Millar⁷⁹, D.W. Miller³³, C. Mills⁴⁹,
A. Milov¹⁷⁵, D.A. Milstead^{148a,148b}, A.A. Minaenko¹³², Y. Minami¹⁵⁷, I.A. Minashvili^{54b},
A.I. Mincer¹¹², B. Mindur^{41a}, M. Mineev⁶⁸, Y. Minegishi¹⁵⁷, Y. Ming¹⁷⁶, L.M. Mir¹³, A. Mirto^{76a,76b},
K.P. Mistry¹²⁴, T. Mitani¹⁷⁴, J. Mitrevski¹⁰², V.A. Mitsou¹⁷⁰, A. Miucci¹⁸, P.S. Miyagawa¹⁴¹,
A. Mizukami⁶⁹, J.U. Mjörnmark⁸⁴, T. Mkrtchyan¹⁸⁰, M. Mlynarikova¹³¹, T. Moa^{148a,148b},
K. Mochizuki⁹⁷, P. Mogg⁵¹, S. Mohapatra³⁸, S. Molander^{148a,148b}, R. Moles-Valls²³, M.C. Mondragon⁹³,
K. Mönig⁴⁵, J. Monk³⁹, E. Monnier⁸⁸, A. Montalbano¹⁵⁰, J. Montejo Berlingen³², F. Monticelli⁷⁴,
S. Monzani^{94a,94b}, R.W. Moore³, N. Morange¹¹⁹, D. Moreno²¹, M. Moreno Llácer³², P. Morettini^{53a},
S. Morgenstern³², D. Mori¹⁴⁴, T. Mori¹⁵⁷, M. Morii⁵⁹, M. Morinaga¹⁷⁴, V. Morisbak¹²¹, A.K. Morley³²,
G. Mornacchi³², J.D. Morris⁷⁹, L. Morvaj¹⁵⁰, P. Moschovakos¹⁰, M. Mosidze^{54b}, H.J. Moss¹⁴¹,
J. Moss^{145,ai}, K. Motohashi¹⁵⁹, R. Mount¹⁴⁵, E. Mountricha²⁷, E.J.W. Moyse⁸⁹, S. Muanza⁸⁸,
F. Mueller¹⁰³, J. Mueller¹²⁷, R.S.P. Mueller¹⁰², D. Muenstermann⁷⁵, P. Mullen⁵⁶, G.A. Mullier¹⁸,
F.J. Munoz Sanchez⁸⁷, W.J. Murray^{173,133}, H. Musheghyan³², M. Muškinja⁷⁸, A.G. Myagkov^{132,aj},
M. Myska¹³⁰, B.P. Nachman¹⁶, O. Nackenhorst⁵², K. Nagai¹²², R. Nagai^{69,ae}, K. Nagano⁶⁹,
Y. Nagasaka⁶¹, K. Nagata¹⁶⁴, M. Nagel⁵¹, E. Nagy⁸⁸, A.M. Nairz³², Y. Nakahama¹⁰⁵, K. Nakamura⁶⁹,
T. Nakamura¹⁵⁷, I. Nakano¹¹⁴, R.F. Naranjo Garcia⁴⁵, R. Narayan¹¹, D.I. Narrias Villar^{60a},
I. Naryshkin¹²⁵, T. Naumann⁴⁵, G. Navarro²¹, R. Nayyar⁷, H.A. Neal⁹², P.Yu. Nechaeva⁹⁸, T.J. Neep¹³⁸,
A. Negri^{123a,123b}, M. Negrini^{22a}, S. Nektarijevic¹⁰⁸, C. Nellist⁵⁷, A. Nelson¹⁶⁶, M.E. Nelson¹²²,
S. Nemecek¹²⁹, P. Nemethy¹¹², M. Nessi^{32,ak}, M.S. Neubauer¹⁶⁹, M. Neumann¹⁷⁸, P.R. Newman¹⁹,
T.Y. Ng^{62c}, T. Nguyen Manh⁹⁷, R.B. Nickerson¹²², R. Nicolaidou¹³⁸, J. Nielsen¹³⁹, N. Nikiforou¹¹,
V. Nikolaenko^{132,aj}, I. Nikolic-Audit⁸³, K. Nikolopoulos¹⁹, J.K. Nilsen¹²¹, P. Nilsson²⁷, Y. Ninomiya⁶⁹,
A. Nisati^{134a}, N. Nishu^{36c}, R. Nisius¹⁰³, I. Nitsche⁴⁶, T. Nitta¹⁷⁴, T. Nobe¹⁵⁷, Y. Noguchi⁷¹,
M. Nomachi¹²⁰, I. Nomidis³¹, M.A. Nomura²⁷, T. Nooney⁷⁹, M. Nordberg³², N. Norjoharuddeen¹²²,
O. Novgorodova⁴⁷, M. Nozaki⁶⁹, L. Nozka¹¹⁷, K. Ntekas¹⁶⁶, E. Nurse⁸¹, F. Nuti⁹¹, K. O'connor²⁵,
D.C. O'Neil¹⁴⁴, A.A. O'Rourke⁴⁵, V. O'Shea⁵⁶, F.G. Oakham^{31,d}, H. Oberlack¹⁰³, T. Obermann²³,
J. Ocariz⁸³, A. Ochi⁷⁰, I. Ochoa³⁸, J.P. Ochoa-Ricoux^{34a}, S. Oda⁷³, S. Odaka⁶⁹, A. Oh⁸⁷, S.H. Oh⁴⁸,
C.C. Ohm¹⁴⁹, H. Ohman¹⁶⁸, H. Oide^{53a,53b}, H. Okawa¹⁶⁴, Y. Okumura¹⁵⁷, T. Okuyama⁶⁹, A. Olariu^{28b},
L.F. Oleiro Seabra^{128a}, S.A. Olivares Pino^{34a}, D. Oliveira Damazio²⁷, A. Olszewski⁴², J. Olszowska⁴²,
A. Onofre^{128a,128e}, K. Onogi¹⁰⁵, P.U.E. Onyisi^{11,aa}, H. Oppen¹²¹, M.J. Oreglia³³, Y. Oren¹⁵⁵,
D. Orestano^{136a,136b}, N. Orlando^{62b}, R.S. Orr¹⁶¹, B. Osculati^{53a,53b,*}, R. Ospanov^{36a},
G. Otero y Garzon²⁹, H. Otono⁷³, M. Ouchrif^{137d}, F. Ould-Saada¹²¹, A. Ouraou¹³⁸, K.P. Oussoren¹⁰⁹,
Q. Ouyang^{35a}, M. Owen⁵⁶, R.E. Owen¹⁹, V.E. Ozcan^{20a}, N. Ozturk⁸, K. Pachal¹⁴⁴, A. Pacheco Pages¹³,
L. Pacheco Rodriguez¹³⁸, C. Padilla Aranda¹³, S. Pagan Griso¹⁶, M. Paganini¹⁷⁹, F. Paige²⁷,
G. Palacino⁶⁴, S. Palazzo^{40a,40b}, S. Palestini³², M. Palka^{41b}, D. Pallin³⁷, E.St. Panagiotopoulou¹⁰,
I. Panagoulas¹⁰, C.E. Pandini⁵², J.G. Panduro Vazquez⁸⁰, P. Pani³², S. Panitkin²⁷, D. Pantea^{28b},
L. Paolozzi⁵², Th.D. Papadopoulou¹⁰, K. Papageorgiou^{9,s}, A. Paramonov⁶, D. Paredes Hernandez¹⁷⁹,
A.J. Parker⁷⁵, M.A. Parker³⁰, K.A. Parker⁴⁵, F. Parodi^{53a,53b}, J.A. Parsons³⁸, U. Parzefall⁵¹,
V.R. Pascuzzi¹⁶¹, J.M. Pasner¹³⁹, E. Pasqualucci^{134a}, S. Passaggio^{53a}, Fr. Pastore⁸⁰, S. Patariaia⁸⁶,
J.R. Pater⁸⁷, T. Pauly³², B. Pearson¹⁰³, S. Pedraza Lopez¹⁷⁰, R. Pedro^{128a,128b}, S.V. Peleganchuk^{111,c},
O. Penc¹²⁹, C. Peng^{35a}, H. Peng^{36a}, J. Penwell⁶⁴, B.S. Peralva^{26b}, M.M. Perego¹³⁸, D.V. Perepelitsa²⁷,
F. Peri¹⁷, L. Perini^{94a,94b}, H. Pernegger³², S. Perrella^{106a,106b}, R. Peschke⁴⁵, V.D. Peshekhonov^{68,*},
K. Peters⁴⁵, R.F.Y. Peters⁸⁷, B.A. Petersen³², T.C. Petersen³⁹, E. Petit⁵⁸, A. Petridis¹, C. Petridou¹⁵⁶,
P. Petroff¹¹⁹, E. Petrolo^{134a}, M. Petrov¹²², F. Petrucci^{136a,136b}, N.E. Pettersson⁸⁹, A. Peyaud¹³⁸,
R. Pezoa^{34b}, F.H. Phillips⁹³, P.W. Phillips¹³³, G. Piacquadio¹⁵⁰, E. Pianori¹⁷³, A. Picazio⁸⁹,
M.A. Pickering¹²², R. Piegaia²⁹, J.E. Pilcher³³, A.D. Pilkington⁸⁷, M. Pinamonti^{135a,135b}, J.L. Pinfold³,
H. Pirumov⁴⁵, M. Pitt¹⁷⁵, L. Plazak^{146a}, M.-A. Pleier²⁷, V. Pleskot⁸⁶, E. Plotnikova⁶⁸, D. Pluth⁶⁷,

P. Podberezko¹¹¹, R. Poettgen⁸⁴, R. Poggi^{123a,123b}, L. Poggioli¹¹⁹, I. Pogrebnyak⁹³, D. Pohl²³,
 I. Pokharel⁵⁷, G. Polesello^{123a}, A. Poley⁴⁵, A. Policicchio^{40a,40b}, R. Polifka³², A. Polini^{22a},
 C.S. Pollard⁵⁶, V. Polychronakos²⁷, K. Pommès³², D. Ponomarenko¹⁰⁰, L. Pontecorvo^{134a},
 G.A. Popeneciu^{28d}, D.M. Portillo Quintero⁸³, S. Pospisil¹³⁰, K. Potamianos⁴⁵, I.N. Potrap⁶⁸,
 C.J. Potter³⁰, H. Potti¹¹, T. Poulsen⁸⁴, J. Poveda³², M.E. Pozo Astigarraga³², P. Pralavorio⁸⁸,
 A. Pranko¹⁶, S. Prell⁶⁷, D. Price⁸⁷, M. Primavera^{76a}, S. Prince⁹⁰, N. Proklova¹⁰⁰, K. Prokofiev^{62c},
 F. Prokoshin^{34b}, S. Protopopescu²⁷, J. Proudfoot⁶, M. Przybycien^{41a}, A. Puri¹⁶⁹, P. Puzo¹¹⁹, J. Qian⁹²,
 G. Qin⁵⁶, Y. Qin⁸⁷, A. Quadt⁵⁷, M. Queitsch-Maitland⁴⁵, D. Quilty⁵⁶, S. Raddum¹²¹, V. Radeka²⁷,
 V. Radescu¹²², S.K. Radhakrishnan¹⁵⁰, P. Radloff¹¹⁸, P. Rados⁹¹, F. Ragusa^{94a,94b}, G. Rahal¹⁸¹,
 J.A. Raine⁸⁷, S. Rajagopalan²⁷, C. Rangel-Smith¹⁶⁸, T. Rashid¹¹⁹, S. Raspopov⁵, M.G. Ratti^{94a,94b},
 D.M. Rauch⁴⁵, F. Rauscher¹⁰², S. Rave⁸⁶, I. Ravinovich¹⁷⁵, J.H. Rawling⁸⁷, M. Raymond³²,
 A.L. Read¹²¹, N.P. Readioff⁵⁸, M. Reale^{76a,76b}, D.M. Rebuffi^{123a,123b}, A. Redelbach¹⁷⁷, G. Redlinger²⁷,
 R. Reece¹³⁹, R.G. Reed^{147c}, K. Reeves⁴⁴, L. Rehnisch¹⁷, J. Reichert¹²⁴, A. Reiss⁸⁶, C. Rembser³²,
 H. Ren^{35a}, M. Rescigno^{134a}, S. Resconi^{94a}, E.D. Resseguie¹²⁴, S. Rettie¹⁷¹, E. Reynolds¹⁹,
 O.L. Rezanova^{111,c}, P. Reznicek¹³¹, R. Rezvani⁹⁷, R. Richter¹⁰³, S. Richter⁸¹, E. Richter-Was^{41b},
 O. Ricken²³, M. Ridel⁸³, P. Rieck¹⁰³, C.J. Riegel¹⁷⁸, J. Rieger⁵⁷, O. Rifki¹¹⁵, M. Rijssenbeek¹⁵⁰,
 A. Rimoldi^{123a,123b}, M. Rimoldi¹⁸, L. Rinaldi^{22a}, G. Ripellino¹⁴⁹, B. Ristic³², E. Ritsch³², I. Riu¹³,
 F. Rizatdinova¹¹⁶, E. Rizvi⁷⁹, C. Rizzi¹³, R.T. Roberts⁸⁷, S.H. Robertson^{90,o},
 A. Robichaud-Veronneau⁹⁰, D. Robinson³⁰, J.E.M. Robinson⁴⁵, A. Robson⁵⁶, E. Rocco⁸⁶,
 C. Roda^{126a,126b}, Y. Rodina^{88,al}, S. Rodriguez Bosca¹⁷⁰, A. Rodriguez Perez¹³,
 D. Rodriguez Rodriguez¹⁷⁰, S. Roe³², C.S. Rogan⁵⁹, O. Røhne¹²¹, J. Roloff⁵⁹, A. Romaniouk¹⁰⁰,
 M. Romano^{22a,22b}, S.M. Romano Saez³⁷, E. Romero Adam¹⁷⁰, N. Rompotis⁷⁷, M. Ronzani⁵¹, L. Roos⁸³,
 S. Rosati^{134a}, K. Rosbach⁵¹, P. Rose¹³⁹, N.-A. Rosien⁵⁷, E. Rossi^{106a,106b}, L.P. Rossi^{53a}, J.H.N. Rosten³⁰,
 R. Rosten¹⁴⁰, M. Rotaru^{28b}, J. Rothberg¹⁴⁰, D. Rousseau¹¹⁹, A. Rozanov⁸⁸, Y. Rozen¹⁵⁴, X. Ruan^{147c},
 F. Rubbo¹⁴⁵, E.M. Ruettinger⁴⁵, F. Rühr⁵¹, A. Ruiz-Martinez³¹, Z. Rurikova⁵¹, N.A. Rusakovich⁶⁸,
 H.L. Russell⁹⁰, J.P. Rutherford⁷, N. Ruthmann³², Y.F. Ryabov¹²⁵, M. Rybar¹⁶⁹, G. Rybkin¹¹⁹, S. Ryu⁶,
 A. Ryzhov¹³², G.F. Rzehorz⁵⁷, A.F. Saavedra¹⁵², G. Sabato¹⁰⁹, S. Sacerdoti²⁹, H.F.-W. Sadrozinski¹³⁹,
 R. Sadykov⁶⁸, F. Safai Tehrani^{134a}, P. Saha¹¹⁰, M. Sahinsoy^{60a}, M. Saimpert⁴⁵, M. Saito¹⁵⁷, T. Saito¹⁵⁷,
 H. Sakamoto¹⁵⁷, Y. Sakurai¹⁷⁴, G. Salamanna^{136a,136b}, J.E. Salazar Loyola^{34b}, D. Salek¹⁰⁹,
 P.H. Sales De Bruin¹⁶⁸, D. Salihagic¹⁰³, A. Salnikov¹⁴⁵, J. Salt¹⁷⁰, D. Salvatore^{40a,40b}, F. Salvatore¹⁵¹,
 A. Salvucci^{62a,62b,62c}, A. Salzburger³², D. Sammel⁵¹, D. Sampsonidis¹⁵⁶, D. Sampsonidou¹⁵⁶,
 J. Sánchez¹⁷⁰, V. Sanchez Martinez¹⁷⁰, A. Sanchez Pineda^{167a,167c}, H. Sandaker¹²¹, R.L. Sandbach⁷⁹,
 C.O. Sander⁴⁵, M. Sandhoff¹⁷⁸, C. Sandoval²¹, D.P.C. Sankey¹³³, M. Sannino^{53a,53b}, Y. Sano¹⁰⁵,
 A. Sansoni⁵⁰, C. Santoni³⁷, H. Santos^{128a}, I. Santoyo Castillo¹⁵¹, A. Saponov⁶⁸, J.G. Saraiva^{128a,128d},
 B. Sarrazin²³, O. Sasaki⁶⁹, K. Sato¹⁶⁴, E. Sauvan⁵, G. Savage⁸⁰, P. Savard^{161,d}, N. Savic¹⁰³,
 C. Sawyer¹³³, L. Sawyer^{82,u}, J. Saxon³³, C. Sbarra^{22a}, A. Sbrizzi^{22a,22b}, T. Scanlon⁸¹,
 D.A. Scannicchio¹⁶⁶, J. Schaarschmidt¹⁴⁰, P. Schacht¹⁰³, B.M. Schachtner¹⁰², D. Schaefer³³,
 L. Schaefer¹²⁴, R. Schaefer⁴⁵, J. Schaeffer⁸⁶, S. Schaepe³², S. Schaezel^{60b}, U. Schäfer⁸⁶,
 A.C. Schaffer¹¹⁹, D. Schaile¹⁰², R.D. Schamberger¹⁵⁰, V.A. Schegelsky¹²⁵, D. Scheirich¹³¹,
 M. Schernau¹⁶⁶, C. Schiavi^{53a,53b}, S. Schier¹³⁹, L.K. Schildgen²³, C. Schillo⁵¹, M. Schioppa^{40a,40b},
 S. Schlenker³², K.R. Schmidt-Sommerfeld¹⁰³, K. Schmieden³², C. Schmitt⁸⁶, S. Schmitt⁴⁵,
 S. Schmitz⁸⁶, U. Schnoor⁵¹, L. Schoeffel¹³⁸, A. Schoening^{60b}, B.D. Schoenrock⁹³, E. Schopf²³,
 M. Schott⁸⁶, J.F.P. Schouwenberg¹⁰⁸, J. Schovancova³², S. Schramm⁵², N. Schuh⁸⁶, A. Schulte⁸⁶,
 M.J. Schultens²³, H.-C. Schultz-Coulon^{60a}, H. Schulz¹⁷, M. Schumacher⁵¹, B.A. Schumm¹³⁹,
 Ph. Schune¹³⁸, A. Schwartzman¹⁴⁵, T.A. Schwarz⁹², H. Schweiger⁸⁷, Ph. Schwemling¹³⁸,
 R. Schwienhorst⁹³, J. Schwindling¹³⁸, A. Sciandra²³, G. Sciolla²⁵, M. Scornajenghi^{40a,40b},
 F. Scuri^{126a,126b}, F. Scutti⁹¹, J. Searcy⁹², P. Seema²³, S.C. Seidel¹⁰⁷, A. Seiden¹³⁹, J.M. Seixas^{26a},

G. Sekhniadze^{106a}, K. Sekhon⁹², S.J. Sekula⁴³, N. Semprini-Cesari^{22a,22b}, S. Senkin³⁷, C. Serfon¹²¹, L. Serin¹¹⁹, L. Serkin^{167a,167b}, M. Sessa^{136a,136b}, R. Seuster¹⁷², H. Severini¹¹⁵, T. Sfiligoj⁷⁸, F. Sforza¹⁶⁵, A. Sfyrla⁵², E. Shabalina⁵⁷, N.W. Shaikh^{148a,148b}, L.Y. Shan^{35a}, R. Shang¹⁶⁹, J.T. Shank²⁴, M. Shapiro¹⁶, P.B. Shatalov⁹⁹, K. Shaw^{167a,167b}, S.M. Shaw⁸⁷, A. Shcherbakova^{148a,148b}, C.Y. Shehu¹⁵¹, Y. Shen¹¹⁵, N. Sherafati³¹, P. Sherwood⁸¹, L. Shi^{153,am}, S. Shimizu⁷⁰, C.O. Shimmin¹⁷⁹, M. Shimojima¹⁰⁴, I.P.J. Shipsey¹²², S. Shirabe⁷³, M. Shiyakova^{68,an}, J. Shlomi¹⁷⁵, A. Shmeleva⁹⁸, D. Shoaleh Saadi⁹⁷, M.J. Shochet³³, S. Shojaii^{94a,94b}, D.R. Shope¹¹⁵, S. Shrestha¹¹³, E. Shulga¹⁰⁰, M.A. Shupe⁷, P. Sicho¹²⁹, A.M. Sickles¹⁶⁹, P.E. Sidebo¹⁴⁹, E. Sideras Haddad^{147c}, O. Sidiropoulou¹⁷⁷, A. Sidoti^{22a,22b}, F. Siegert⁴⁷, Dj. Sijacki¹⁴, J. Silva^{128a,128d}, S.B. Silverstein^{148a}, V. Simak¹³⁰, L. Simic⁶⁸, S. Simion¹¹⁹, E. Simioni⁸⁶, B. Simmons⁸¹, M. Simon⁸⁶, P. Sinervo¹⁶¹, N.B. Sinev¹¹⁸, M. Sioli^{22a,22b}, G. Siragusa¹⁷⁷, I. Siral⁹², S.Yu. Sivoklov¹⁰¹, J. Sjölin^{148a,148b}, M.B. Skinner⁷⁵, P. Skubic¹¹⁵, M. Slater¹⁹, T. Slavicek¹³⁰, M. Slawinska⁴², K. Sliwa¹⁶⁵, R. Slovak¹³¹, V. Smakhtin¹⁷⁵, B.H. Smart⁵, J. Smiesko^{146a}, N. Smirnov¹⁰⁰, S.Yu. Smirnov¹⁰⁰, Y. Smirnov¹⁰⁰, L.N. Smirnova^{101,ao}, O. Smirnova⁸⁴, J.W. Smith⁵⁷, M.N.K. Smith³⁸, R.W. Smith³⁸, M. Smizanska⁷⁵, K. Smolek¹³⁰, A.A. Snesarev⁹⁸, I.M. Snyder¹¹⁸, S. Snyder²⁷, R. Sobie^{172,o}, F. Socher⁴⁷, A. Soffer¹⁵⁵, A. Søggaard⁴⁹, D.A. Soh¹⁵³, G. Sokhrannyi⁷⁸, C.A. Solans Sanchez³², M. Solar¹³⁰, E.Yu. Soldatov¹⁰⁰, U. Soldevila¹⁷⁰, A.A. Solodkov¹³², A. Soloshenko⁶⁸, O.V. Solovyanov¹³², V. Solovyev¹²⁵, P. Sommer¹⁴¹, H. Son¹⁶⁵, A. Sopczak¹³⁰, D. Sosa^{60b}, C.L. Sotiropoulou^{126a,126b}, S. Sottocornola^{123a,123b}, R. Soualah^{167a,167c}, A.M. Soukharev^{111,c}, D. South⁴⁵, B.C. Sowden⁸⁰, S. Spagnolo^{76a,76b}, M. Spalla^{126a,126b}, M. Spangenberg¹⁷³, F. Spanò⁸⁰, D. Sperlich¹⁷, F. Spettel¹⁰³, T.M. Spieker^{60a}, R. Spighi^{22a}, G. Spigo³², L.A. Spiller⁹¹, M. Spousta¹³¹, R.D. St. Denis^{56,*}, A. Stabile^{94a}, R. Stamen^{60a}, S. Stamm¹⁷, E. Stanecka⁴², R.W. Stanek⁶, C. Stanescu^{136a}, M.M. Stanitzki⁴⁵, B.S. Stapf¹⁰⁹, S. Stapnes¹²¹, E.A. Starchenko¹³², G.H. Stark³³, J. Stark⁵⁸, S.H. Stark³⁹, P. Staroba¹²⁹, P. Starovoitov^{60a}, S. Stärz³², R. Staszewski⁴², M. Stegler⁴⁵, P. Steinberg²⁷, B. Stelzer¹⁴⁴, H.J. Stelzer³², O. Stelzer-Chilton^{163a}, H. Stenzel⁵⁵, T.J. Stevenson⁷⁹, G.A. Stewart⁵⁶, M.C. Stockton¹¹⁸, M. Stoebe⁹⁰, G. Stoicea^{28b}, P. Stolte⁵⁷, S. Stonjek¹⁰³, A.R. Stradling⁸, A. Straessner⁴⁷, M.E. Stramaglia¹⁸, J. Strandberg¹⁴⁹, S. Strandberg^{148a,148b}, M. Strauss¹¹⁵, P. Striznec^{146b}, R. Ströhmer¹⁷⁷, D.M. Strom¹¹⁸, R. Stroynowski⁴³, A. Strubig⁴⁹, S.A. Stucci²⁷, B. Stugu¹⁵, N.A. Styles⁴⁵, D. Su¹⁴⁵, J. Su¹²⁷, S. Suchek^{60a}, Y. Sugaya¹²⁰, M. Suk¹³⁰, V.V. Sulim⁹⁸, DMS Sultan^{162a,162b}, S. Sultansoy^{4c}, T. Sumida⁷¹, S. Sun⁵⁹, X. Sun³, K. Suruliz¹⁵¹, C.J.E. Suster¹⁵², M.R. Sutton¹⁵¹, S. Suzuki⁶⁹, M. Svatos¹²⁹, M. Swiatlowski³³, S.P. Swift², I. Sykora^{146a}, T. Sykora¹³¹, D. Ta⁵¹, K. Tackmann⁴⁵, J. Taenzer¹⁵⁵, A. Taffard¹⁶⁶, R. Tafirout^{163a}, E. Tahirovic⁷⁹, N. Taiblum¹⁵⁵, H. Takai²⁷, R. Takashima⁷², E.H. Takasugi¹⁰³, K. Takeda⁷⁰, T. Takeshita¹⁴², Y. Takubo⁶⁹, M. Talby⁸⁸, A.A. Talyshev^{111,c}, J. Tanaka¹⁵⁷, M. Tanaka¹⁵⁹, R. Tanaka¹¹⁹, S. Tanaka⁶⁹, R. Tanioka⁷⁰, B.B. Tannenwald¹¹³, S. Tapia Araya^{34b}, S. Tapprogge⁸⁶, S. Tarem¹⁵⁴, G.F. Tartarelli^{94a}, P. Tas¹³¹, M. Tasevsky¹²⁹, T. Tashiro⁷¹, E. Tassi^{40a,40b}, A. Tavares Delgado^{128a,128b}, Y. Tayalati^{137e}, A.C. Taylor¹⁰⁷, A.J. Taylor⁴⁹, G.N. Taylor⁹¹, P.T.E. Taylor⁹¹, W. Taylor^{163b}, P. Teixeira-Dias⁸⁰, D. Temple¹⁴⁴, H. Ten Kate³², P.K. Teng¹⁵³, J.J. Teoh¹²⁰, F. Tepel¹⁷⁸, S. Terada⁶⁹, K. Terashi¹⁵⁷, J. Terron⁸⁵, S. Terzo¹³, M. Testa⁵⁰, R.J. Teuscher^{161,o}, S.J. Thais¹⁷⁹, T. Theveneaux-Pelzer⁸⁸, F. Thiele³⁹, J.P. Thomas¹⁹, J. Thomas-Wilsker⁸⁰, P.D. Thompson¹⁹, A.S. Thompson⁵⁶, L.A. Thomsen¹⁷⁹, E. Thomson¹²⁴, Y. Tian³⁸, M.J. Tibbetts¹⁶, R.E. Ticse Torres⁵⁷, V.O. Tikhomirov^{98,ap}, Yu.A. Tikhonov^{111,c}, S. Timoshenko¹⁰⁰, P. Tipton¹⁷⁹, S. Tisserant⁸⁸, K. Todome¹⁵⁹, S. Todorova-Nova⁵, S. Todt⁴⁷, J. Tojo⁷³, S. Tokár^{146a}, K. Tokushuku⁶⁹, E. Tolley⁵⁹, L. Tomlinson⁸⁷, M. Tomoto¹⁰⁵, L. Tompkins^{145,aa}, K. Toms¹⁰⁷, B. Tong⁵⁹, P. Tornambe⁵¹, E. Torrence¹¹⁸, H. Torres⁴⁷, E. Torró Pastor¹⁴⁰, J. Toth^{88,ar}, F. Touchard⁸⁸, D.R. Tovey¹⁴¹, C.J. Treado¹¹², T. Trefzger¹⁷⁷, F. Tresoldi¹⁵¹, A. Tricoli²⁷, I.M. Trigger^{163a}, S. Trincaz-Duvoid⁸³, M.F. Tripiana¹³, W. Trischuk¹⁶¹, B. Trocmé⁵⁸, A. Trofymov⁴⁵, C. Troncon^{94a}, M. Trotter-McDonald¹⁶, M. Trovatelli¹⁷², L. Truong^{147b}, M. Trzebinski⁴², A. Trzupek⁴², K.W. Tsang^{62a}, J.C.-L. Tseng¹²², P.V. Tsiarshka⁹⁵, G. Tsipolitis¹⁰, N. Tsirintanis⁹, S. Tsiskaridze¹³,

V. Tsiskaridze⁵¹, E.G. Tskhadadze^{54a}, I.I. Tsukerman⁹⁹, V. Tsulaia¹⁶, S. Tsuno⁶⁹, D. Tsybychev¹⁵⁰, Y. Tu^{62b}, A. Tudorache^{28b}, V. Tudorache^{28b}, T.T. Tulbure^{28a}, A.N. Tuna⁵⁹, S. Turchikhin⁶⁸, D. Turgeman¹⁷⁵, I. Turk Cakir^{4b,as}, R. Turra^{94a}, P.M. Tuts³⁸, G. Uccielli^{22a,22b}, I. Ueda⁶⁹, M. Ughetto^{148a,148b}, F. Ukegawa¹⁶⁴, G. Unal³², A. Undrus²⁷, G. Unel¹⁶⁶, F.C. Ungaro⁹¹, Y. Unno⁶⁹, K. Uno¹⁵⁷, C. Unverdorben¹⁰², J. Urban^{146b}, P. Urquijo⁹¹, P. Urrejola⁸⁶, G. Usai⁸, J. Usui⁶⁹, L. Vacavant⁸⁸, V. Vacek¹³⁰, B. Vachon⁹⁰, K.O.H. Vadla¹²¹, A. Vaidya⁸¹, C. Valderanis¹⁰², E. Valdes Santurio^{148a,148b}, M. Valente⁵², S. Valentineti^{22a,22b}, A. Valero¹⁷⁰, L. Valéry¹³, S. Valkar¹³¹, A. Vallier⁵, J.A. Valls Ferrer¹⁷⁰, W. Van Den Wollenberg¹⁰⁹, H. van der Graaf¹⁰⁹, P. van Gemmeren⁶, J. Van Nieuwkoop¹⁴⁴, I. van Vulpen¹⁰⁹, M.C. van Woerden¹⁰⁹, M. Vanadia^{135a,135b}, W. Vandelli³², A. Vaniachine¹⁶⁰, P. Vankov¹⁰⁹, G. Vardanyan¹⁸⁰, R. Vari^{134a}, E.W. Varnes⁷, C. Varni^{53a,53b}, T. Varol⁴³, D. Varouchas¹¹⁹, A. Vartapetian⁸, K.E. Varvell¹⁵², J.G. Vasquez¹⁷⁹, G.A. Vasquez^{34b}, F. Vazeille³⁷, D. Vazquez Furelos¹³, T. Vazquez Schroeder⁹⁰, J. Veatch⁵⁷, V. Veeraraghavan⁷, L.M. Veloce¹⁶¹, F. Veloso^{128a,128c}, S. Veneziano^{134a}, A. Ventura^{76a,76b}, M. Venturi¹⁷², N. Venturi³², A. Venturini²⁵, V. Vercesi^{123a}, M. Verducci^{136a,136b}, W. Verkerke¹⁰⁹, A.T. Vermeulen¹⁰⁹, J.C. Vermeulen¹⁰⁹, M.C. Vetterli^{144,d}, N. Viaux Maira^{34b}, O. Viazlo⁸⁴, I. Vichou^{169,*}, T. Vickey¹⁴¹, O.E. Vickey Boeriu¹⁴¹, G.H.A. Viehhauser¹²², S. Viel¹⁶, L. Vigani¹²², M. Villa^{22a,22b}, M. Villaplana Perez^{94a,94b}, E. Vilucchi⁵⁰, M.G. Vincter³¹, V.B. Vinogradov⁶⁸, A. Vishwakarma⁴⁵, C. Vittori^{22a,22b}, I. Vivarelli¹⁵¹, S. Vlachos¹⁰, M. Vogel¹⁷⁸, P. Vokac¹³⁰, G. Volpi¹³, H. von der Schmitt¹⁰³, E. von Toerne²³, V. Vorobel¹³¹, K. Vorobev¹⁰⁰, M. Vos¹⁷⁰, R. Voss³², J.H. Vosseveld⁷⁷, N. Vranjes¹⁴, M. Vranjes Milosavljevic¹⁴, V. Vrba¹³⁰, M. Vreeswijk¹⁰⁹, R. Vuillermet³², I. Vukotic³³, P. Wagner²³, W. Wagner¹⁷⁸, J. Wagner-Kuhr¹⁰², H. Wahlberg⁷⁴, S. Wahrenmund⁴⁷, J. Walder⁷⁵, R. Walker¹⁰², W. Walkowiak¹⁴³, V. Wallangen^{148a,148b}, C. Wang^{35b}, C. Wang^{36b,at}, F. Wang¹⁷⁶, H. Wang¹⁶, H. Wang³, J. Wang⁴⁵, J. Wang¹⁵², Q. Wang¹¹⁵, R.-J. Wang⁸³, R. Wang⁶, S.M. Wang¹⁵³, T. Wang³⁸, W. Wang^{153,au}, W. Wang^{36a,av}, Z. Wang^{36c}, C. Wanotayaroj⁴⁵, A. Warburton⁹⁰, C.P. Ward³⁰, D.R. Wardrope⁸¹, A. Washbrook⁴⁹, P.M. Watkins¹⁹, A.T. Watson¹⁹, M.F. Watson¹⁹, G. Watts¹⁴⁰, S. Watts⁸⁷, B.M. Waugh⁸¹, A.F. Webb¹¹, S. Webb⁸⁶, M.S. Weber¹⁸, S.M. Weber^{60a}, S.W. Weber¹⁷⁷, S.A. Weber³¹, J.S. Webster⁶, A.R. Weidberg¹²², B. Weinert⁶⁴, J. Weingarten⁵⁷, M. Weirich⁸⁶, C. Weiser⁵¹, H. Weits¹⁰⁹, P.S. Wells³², T. Wenaus²⁷, T. Wengler³², S. Wenig³², N. Wermes²³, M.D. Werner⁶⁷, P. Werner³², M. Wessels^{60a}, T.D. Weston¹⁸, K. Whalen¹¹⁸, N.L. Whallon¹⁴⁰, A.M. Wharton⁷⁵, A.S. White⁹², A. White⁸, M.J. White¹, R. White^{34b}, D. Whiteson¹⁶⁶, B.W. Whitmore⁷⁵, F.J. Wickens¹³³, W. Wiedenmann¹⁷⁶, M. Wielers¹³³, C. Wiglesworth³⁹, L.A.M. Wiik-Fuchs⁵¹, A. Wildauer¹⁰³, F. Wilk⁸⁷, H.G. Wilkens³², H.H. Williams¹²⁴, S. Williams¹⁰⁹, C. Willis⁹³, S. Willocq⁸⁹, J.A. Wilson¹⁹, I. Wingerter-Seez⁵, E. Winkels¹⁵¹, F. Winklmeier¹¹⁸, O.J. Winston¹⁵¹, B.T. Winter²³, M. Wittgen¹⁴⁵, M. Wobisch^{82,u}, A. Wolf⁸⁶, T.M.H. Wolf¹⁰⁹, R. Wolff⁸⁸, M.W. Wolter⁴², H. Wolters^{128a,128c}, V.W.S. Wong¹⁷¹, N.L. Woods¹³⁹, S.D. Worm¹⁹, B.K. Wosiek⁴², J. Wotschack³², K.W. Wozniak⁴², M. Wu³³, S.L. Wu¹⁷⁶, X. Wu⁵², Y. Wu⁹², T.R. Wyatt⁸⁷, B.M. Wynne⁴⁹, S. Xella³⁹, Z. Xi⁹², L. Xia^{35c}, D. Xu^{35a}, L. Xu²⁷, T. Xu¹³⁸, W. Xu⁹², B. Yabsley¹⁵², S. Yacoub^{147a}, D. Yamaguchi¹⁵⁹, Y. Yamaguchi¹⁵⁹, A. Yamamoto⁶⁹, S. Yamamoto¹⁵⁷, T. Yamanaka¹⁵⁷, F. Yamane⁷⁰, M. Yamatani¹⁵⁷, T. Yamazaki¹⁵⁷, Y. Yamazaki⁷⁰, Z. Yan²⁴, H. Yang^{36c}, H. Yang¹⁶, Y. Yang¹⁵³, Z. Yang¹⁵, W.-M. Yao¹⁶, Y.C. Yap⁴⁵, Y. Yasu⁶⁹, E. Yatsenko⁵, K.H. Yau Wong²³, J. Ye⁴³, S. Ye²⁷, I. Yeletsikh⁶⁸, E. Yigitbasi²⁴, E. Yildirim⁸⁶, K. Yorita¹⁷⁴, K. Yoshihara¹²⁴, C. Young¹⁴⁵, C.J.S. Young³², J. Yu⁸, J. Yu⁶⁷, S.P.Y. Yuen²³, I. Yusuff^{30,aw}, B. Zabinski⁴², G. Zacharis¹⁰, R. Zaidan¹³, A.M. Zaitsev^{132,aj}, N. Zakharchuk⁴⁵, J. Zalieckas¹⁵, A. Zaman¹⁵⁰, S. Zambito⁵⁹, D. Zanzi⁹¹, C. Zeitnitz¹⁷⁸, G. Zemaityte¹²², A. Zemla^{41a}, J.C. Zeng¹⁶⁹, Q. Zeng¹⁴⁵, O. Zenin¹³², T. Ženiš^{146a}, D. Zerwas¹¹⁹, D. Zhang^{36b}, D. Zhang⁹², F. Zhang¹⁷⁶, G. Zhang^{36a,av}, H. Zhang¹¹⁹, J. Zhang⁶, L. Zhang⁵¹, L. Zhang^{36a}, M. Zhang¹⁶⁹, P. Zhang^{35b}, R. Zhang²³, R. Zhang^{36a,at}, X. Zhang^{36b}, Y. Zhang^{35a}, Z. Zhang¹¹⁹, X. Zhao⁴³, Y. Zhao^{36b,ax}, Z. Zhao^{36a}, A. Zhemchugov⁶⁸, B. Zhou⁹², C. Zhou¹⁷⁶, L. Zhou⁴³, M. Zhou^{35a}, M. Zhou¹⁵⁰, N. Zhou^{36c},

C.G. Zhu^{36b}, H. Zhu^{35a}, J. Zhu⁹², Y. Zhu^{36a}, X. Zhuang^{35a}, K. Zhukov⁹⁸, A. Zibell¹⁷⁷, D. Zieminska⁶⁴, N.I. Zimine⁶⁸, C. Zimmermann⁸⁶, S. Zimmermann⁵¹, Z. Zinonos¹⁰³, M. Zinser⁸⁶, M. Ziolkowski¹⁴³, L. Živković¹⁴, G. Zobernig¹⁷⁶, A. Zoccoli^{22a,22b}, R. Zou³³, M. zur Nedden¹⁷, L. Zwalinski³².

¹ Department of Physics, University of Adelaide, Adelaide, Australia

² Physics Department, SUNY Albany, Albany NY, United States of America

³ Department of Physics, University of Alberta, Edmonton AB, Canada

⁴ (a) Department of Physics, Ankara University, Ankara; (b) Istanbul Aydin University, Istanbul; (c)

Division of Physics, TOBB University of Economics and Technology, Ankara, Turkey

⁵ LAPP, CNRS/IN2P3 and Université Savoie Mont Blanc, Annecy-le-Vieux, France

⁶ High Energy Physics Division, Argonne National Laboratory, Argonne IL, United States of America

⁷ Department of Physics, University of Arizona, Tucson AZ, United States of America

⁸ Department of Physics, The University of Texas at Arlington, Arlington TX, United States of America

⁹ Physics Department, National and Kapodistrian University of Athens, Athens, Greece

¹⁰ Physics Department, National Technical University of Athens, Zografou, Greece

¹¹ Department of Physics, The University of Texas at Austin, Austin TX, United States of America

¹² Institute of Physics, Azerbaijan Academy of Sciences, Baku, Azerbaijan

¹³ Institut de Física d'Altes Energies (IFAE), The Barcelona Institute of Science and Technology, Barcelona, Spain

¹⁴ Institute of Physics, University of Belgrade, Belgrade, Serbia

¹⁵ Department for Physics and Technology, University of Bergen, Bergen, Norway

¹⁶ Physics Division, Lawrence Berkeley National Laboratory and University of California, Berkeley CA, United States of America

¹⁷ Department of Physics, Humboldt University, Berlin, Germany

¹⁸ Albert Einstein Center for Fundamental Physics and Laboratory for High Energy Physics, University of Bern, Bern, Switzerland

¹⁹ School of Physics and Astronomy, University of Birmingham, Birmingham, United Kingdom

²⁰ (a) Department of Physics, Bogazici University, Istanbul; (b) Department of Physics Engineering, Gaziantep University, Gaziantep; (d) Istanbul Bilgi University, Faculty of Engineering and Natural Sciences, Istanbul; (e) Bahcesehir University, Faculty of Engineering and Natural Sciences, Istanbul, Turkey

²¹ Centro de Investigaciones, Universidad Antonio Narino, Bogota, Colombia

²² (a) INFN Sezione di Bologna; (b) Dipartimento di Fisica e Astronomia, Università di Bologna, Bologna, Italy

²³ Physikalisches Institut, University of Bonn, Bonn, Germany

²⁴ Department of Physics, Boston University, Boston MA, United States of America

²⁵ Department of Physics, Brandeis University, Waltham MA, United States of America

²⁶ (a) Universidade Federal do Rio De Janeiro COPPE/EE/IF, Rio de Janeiro; (b) Electrical Circuits Department, Federal University of Juiz de Fora (UFJF), Juiz de Fora; (c) Federal University of Sao Joao del Rei (UFSJ), Sao Joao del Rei; (d) Instituto de Fisica, Universidade de Sao Paulo, Sao Paulo, Brazil

²⁷ Physics Department, Brookhaven National Laboratory, Upton NY, United States of America

²⁸ (a) Transilvania University of Brasov, Brasov; (b) Horia Hulubei National Institute of Physics and Nuclear Engineering, Bucharest; (c) Department of Physics, Alexandru Ioan Cuza University of Iasi, Iasi; (d) National Institute for Research and Development of Isotopic and Molecular Technologies, Physics Department, Cluj Napoca; (e) University Politehnica Bucharest, Bucharest; (f) West University in Timisoara, Timisoara, Romania

²⁹ Departamento de Física, Universidad de Buenos Aires, Buenos Aires, Argentina

- ³⁰ Cavendish Laboratory, University of Cambridge, Cambridge, United Kingdom
- ³¹ Department of Physics, Carleton University, Ottawa ON, Canada
- ³² CERN, Geneva, Switzerland
- ³³ Enrico Fermi Institute, University of Chicago, Chicago IL, United States of America
- ³⁴ ^(a) Departamento de Física, Pontificia Universidad Católica de Chile, Santiago; ^(b) Departamento de Física, Universidad Técnica Federico Santa María, Valparaíso, Chile
- ³⁵ ^(a) Institute of High Energy Physics, Chinese Academy of Sciences, Beijing; ^(b) Department of Physics, Nanjing University, Jiangsu; ^(c) Physics Department, Tsinghua University, Beijing 100084, China
- ³⁶ ^(a) Department of Modern Physics and State Key Laboratory of Particle Detection and Electronics, University of Science and Technology of China, Anhui; ^(b) School of Physics, Shandong University, Shandong; ^(c) Department of Physics and Astronomy, Key Laboratory for Particle Physics, Astrophysics and Cosmology, Ministry of Education; Shanghai Key Laboratory for Particle Physics and Cosmology, Shanghai Jiao Tong University, Shanghai(also at PKU-CHEP), China
- ³⁷ Université Clermont Auvergne, CNRS/IN2P3, LPC, Clermont-Ferrand, France
- ³⁸ Nevis Laboratory, Columbia University, Irvington NY, United States of America
- ³⁹ Niels Bohr Institute, University of Copenhagen, Kobenhavn, Denmark
- ⁴⁰ ^(a) INFN Gruppo Collegato di Cosenza, Laboratori Nazionali di Frascati; ^(b) Dipartimento di Fisica, Università della Calabria, Rende, Italy
- ⁴¹ ^(a) AGH University of Science and Technology, Faculty of Physics and Applied Computer Science, Krakow; ^(b) Marian Smoluchowski Institute of Physics, Jagiellonian University, Krakow, Poland
- ⁴² Institute of Nuclear Physics Polish Academy of Sciences, Krakow, Poland
- ⁴³ Physics Department, Southern Methodist University, Dallas TX, United States of America
- ⁴⁴ Physics Department, University of Texas at Dallas, Richardson TX, United States of America
- ⁴⁵ DESY, Hamburg and Zeuthen, Germany
- ⁴⁶ Lehrstuhl für Experimentelle Physik IV, Technische Universität Dortmund, Dortmund, Germany
- ⁴⁷ Institut für Kern- und Teilchenphysik, Technische Universität Dresden, Dresden, Germany
- ⁴⁸ Department of Physics, Duke University, Durham NC, United States of America
- ⁴⁹ SUPA - School of Physics and Astronomy, University of Edinburgh, Edinburgh, United Kingdom
- ⁵⁰ INFN e Laboratori Nazionali di Frascati, Frascati, Italy
- ⁵¹ Fakultät für Mathematik und Physik, Albert-Ludwigs-Universität, Freiburg, Germany
- ⁵² Departement de Physique Nucleaire et Corpusculaire, Université de Genève, Geneva, Switzerland
- ⁵³ ^(a) INFN Sezione di Genova; ^(b) Dipartimento di Fisica, Università di Genova, Genova, Italy
- ⁵⁴ ^(a) E. Andronikashvili Institute of Physics, Iv. Javakhishvili Tbilisi State University, Tbilisi; ^(b) High Energy Physics Institute, Tbilisi State University, Tbilisi, Georgia
- ⁵⁵ II Physikalisches Institut, Justus-Liebig-Universität Giessen, Giessen, Germany
- ⁵⁶ SUPA - School of Physics and Astronomy, University of Glasgow, Glasgow, United Kingdom
- ⁵⁷ II Physikalisches Institut, Georg-August-Universität, Göttingen, Germany
- ⁵⁸ Laboratoire de Physique Subatomique et de Cosmologie, Université Grenoble-Alpes, CNRS/IN2P3, Grenoble, France
- ⁵⁹ Laboratory for Particle Physics and Cosmology, Harvard University, Cambridge MA, United States of America
- ⁶⁰ ^(a) Kirchhoff-Institut für Physik, Ruprecht-Karls-Universität Heidelberg, Heidelberg; ^(b) Physikalisches Institut, Ruprecht-Karls-Universität Heidelberg, Heidelberg, Germany
- ⁶¹ Faculty of Applied Information Science, Hiroshima Institute of Technology, Hiroshima, Japan
- ⁶² ^(a) Department of Physics, The Chinese University of Hong Kong, Shatin, N.T., Hong Kong; ^(b) Department of Physics, The University of Hong Kong, Hong Kong; ^(c) Department of Physics and

Institute for Advanced Study, The Hong Kong University of Science and Technology, Clear Water Bay, Kowloon, Hong Kong, China

⁶³ Department of Physics, National Tsing Hua University, Taiwan, Taiwan

⁶⁴ Department of Physics, Indiana University, Bloomington IN, United States of America

⁶⁵ Institut für Astro- und Teilchenphysik, Leopold-Franzens-Universität, Innsbruck, Austria

⁶⁶ University of Iowa, Iowa City IA, United States of America

⁶⁷ Department of Physics and Astronomy, Iowa State University, Ames IA, United States of America

⁶⁸ Joint Institute for Nuclear Research, JINR Dubna, Dubna, Russia

⁶⁹ KEK, High Energy Accelerator Research Organization, Tsukuba, Japan

⁷⁰ Graduate School of Science, Kobe University, Kobe, Japan

⁷¹ Faculty of Science, Kyoto University, Kyoto, Japan

⁷² Kyoto University of Education, Kyoto, Japan

⁷³ Research Center for Advanced Particle Physics and Department of Physics, Kyushu University, Fukuoka, Japan

⁷⁴ Instituto de Física La Plata, Universidad Nacional de La Plata and CONICET, La Plata, Argentina

⁷⁵ Physics Department, Lancaster University, Lancaster, United Kingdom

⁷⁶ ^(a) INFN Sezione di Lecce; ^(b) Dipartimento di Matematica e Fisica, Università del Salento, Lecce, Italy

⁷⁷ Oliver Lodge Laboratory, University of Liverpool, Liverpool, United Kingdom

⁷⁸ Department of Experimental Particle Physics, Jožef Stefan Institute and Department of Physics, University of Ljubljana, Ljubljana, Slovenia

⁷⁹ School of Physics and Astronomy, Queen Mary University of London, London, United Kingdom

⁸⁰ Department of Physics, Royal Holloway University of London, Surrey, United Kingdom

⁸¹ Department of Physics and Astronomy, University College London, London, United Kingdom

⁸² Louisiana Tech University, Ruston LA, United States of America

⁸³ Laboratoire de Physique Nucléaire et de Hautes Energies, UPMC and Université Paris-Diderot and CNRS/IN2P3, Paris, France

⁸⁴ Fysiska institutionen, Lunds universitet, Lund, Sweden

⁸⁵ Departamento de Física Teórica C-15, Universidad Autónoma de Madrid, Madrid, Spain

⁸⁶ Institut für Physik, Universität Mainz, Mainz, Germany

⁸⁷ School of Physics and Astronomy, University of Manchester, Manchester, United Kingdom

⁸⁸ CPPM, Aix-Marseille Université and CNRS/IN2P3, Marseille, France

⁸⁹ Department of Physics, University of Massachusetts, Amherst MA, United States of America

⁹⁰ Department of Physics, McGill University, Montreal QC, Canada

⁹¹ School of Physics, University of Melbourne, Victoria, Australia

⁹² Department of Physics, The University of Michigan, Ann Arbor MI, United States of America

⁹³ Department of Physics and Astronomy, Michigan State University, East Lansing MI, United States of America

⁹⁴ ^(a) INFN Sezione di Milano; ^(b) Dipartimento di Fisica, Università di Milano, Milano, Italy

⁹⁵ B.I. Stepanov Institute of Physics, National Academy of Sciences of Belarus, Minsk, Republic of Belarus

⁹⁶ Research Institute for Nuclear Problems of Byelorussian State University, Minsk, Republic of Belarus

⁹⁷ Group of Particle Physics, University of Montreal, Montreal QC, Canada

⁹⁸ P.N. Lebedev Physical Institute of the Russian Academy of Sciences, Moscow, Russia

⁹⁹ Institute for Theoretical and Experimental Physics (ITEP), Moscow, Russia

¹⁰⁰ National Research Nuclear University MEPhI, Moscow, Russia

¹⁰¹ D.V. Skobeltsyn Institute of Nuclear Physics, M.V. Lomonosov Moscow State University, Moscow,

Russia

- ¹⁰² Fakultät für Physik, Ludwig-Maximilians-Universität München, München, Germany
- ¹⁰³ Max-Planck-Institut für Physik (Werner-Heisenberg-Institut), München, Germany
- ¹⁰⁴ Nagasaki Institute of Applied Science, Nagasaki, Japan
- ¹⁰⁵ Graduate School of Science and Kobayashi-Maskawa Institute, Nagoya University, Nagoya, Japan
- ¹⁰⁶ ^(a) INFN Sezione di Napoli; ^(b) Dipartimento di Fisica, Università di Napoli, Napoli, Italy
- ¹⁰⁷ Department of Physics and Astronomy, University of New Mexico, Albuquerque NM, United States of America
- ¹⁰⁸ Institute for Mathematics, Astrophysics and Particle Physics, Radboud University Nijmegen/Nikhef, Nijmegen, Netherlands
- ¹⁰⁹ Nikhef National Institute for Subatomic Physics and University of Amsterdam, Amsterdam, Netherlands
- ¹¹⁰ Department of Physics, Northern Illinois University, DeKalb IL, United States of America
- ¹¹¹ Budker Institute of Nuclear Physics, SB RAS, Novosibirsk, Russia
- ¹¹² Department of Physics, New York University, New York NY, United States of America
- ¹¹³ Ohio State University, Columbus OH, United States of America
- ¹¹⁴ Faculty of Science, Okayama University, Okayama, Japan
- ¹¹⁵ Homer L. Dodge Department of Physics and Astronomy, University of Oklahoma, Norman OK, United States of America
- ¹¹⁶ Department of Physics, Oklahoma State University, Stillwater OK, United States of America
- ¹¹⁷ Palacký University, RCPTM, Olomouc, Czech Republic
- ¹¹⁸ Center for High Energy Physics, University of Oregon, Eugene OR, United States of America
- ¹¹⁹ LAL, Univ. Paris-Sud, CNRS/IN2P3, Université Paris-Saclay, Orsay, France
- ¹²⁰ Graduate School of Science, Osaka University, Osaka, Japan
- ¹²¹ Department of Physics, University of Oslo, Oslo, Norway
- ¹²² Department of Physics, Oxford University, Oxford, United Kingdom
- ¹²³ ^(a) INFN Sezione di Pavia; ^(b) Dipartimento di Fisica, Università di Pavia, Pavia, Italy
- ¹²⁴ Department of Physics, University of Pennsylvania, Philadelphia PA, United States of America
- ¹²⁵ National Research Centre "Kurchatov Institute" B.P.Konstantinov Petersburg Nuclear Physics Institute, St. Petersburg, Russia
- ¹²⁶ ^(a) INFN Sezione di Pisa; ^(b) Dipartimento di Fisica E. Fermi, Università di Pisa, Pisa, Italy
- ¹²⁷ Department of Physics and Astronomy, University of Pittsburgh, Pittsburgh PA, United States of America
- ¹²⁸ ^(a) Laboratório de Instrumentação e Física Experimental de Partículas - LIP, Lisboa; ^(b) Faculdade de Ciências, Universidade de Lisboa, Lisboa; ^(c) Department of Physics, University of Coimbra, Coimbra; ^(d) Centro de Física Nuclear da Universidade de Lisboa, Lisboa; ^(e) Departamento de Física, Universidade do Minho, Braga; ^(f) Departamento de Física Teórica y del Cosmos, Universidad de Granada, Granada; ^(g) Dep Física and CEFITEC of Faculdade de Ciências e Tecnologia, Universidade Nova de Lisboa, Caparica, Portugal
- ¹²⁹ Institute of Physics, Academy of Sciences of the Czech Republic, Praha, Czech Republic
- ¹³⁰ Czech Technical University in Prague, Praha, Czech Republic
- ¹³¹ Charles University, Faculty of Mathematics and Physics, Prague, Czech Republic
- ¹³² State Research Center Institute for High Energy Physics (Protvino), NRC KI, Russia
- ¹³³ Particle Physics Department, Rutherford Appleton Laboratory, Didcot, United Kingdom
- ¹³⁴ ^(a) INFN Sezione di Roma; ^(b) Dipartimento di Fisica, Sapienza Università di Roma, Roma, Italy
- ¹³⁵ ^(a) INFN Sezione di Roma Tor Vergata; ^(b) Dipartimento di Fisica, Università di Roma Tor Vergata, Roma, Italy

- 136 (a) INFN Sezione di Roma Tre; (b) Dipartimento di Matematica e Fisica, Università Roma Tre, Roma, Italy
- 137 (a) Faculté des Sciences Ain Chock, Réseau Universitaire de Physique des Hautes Energies - Université Hassan II, Casablanca; (b) Centre National de l'Énergie des Sciences Techniques Nucleaires, Rabat; (c) Faculté des Sciences Semlalia, Université Cadi Ayyad, LPHEA-Marrakech; (d) Faculté des Sciences, Université Mohamed Premier and LTPM, Oujda; (e) Faculté des sciences, Université Mohammed V, Rabat, Morocco
- 138 DSM/IRFU (Institut de Recherches sur les Lois Fondamentales de l'Univers), CEA Saclay (Commissariat à l'Énergie Atomique et aux Énergies Alternatives), Gif-sur-Yvette, France
- 139 Santa Cruz Institute for Particle Physics, University of California Santa Cruz, Santa Cruz CA, United States of America
- 140 Department of Physics, University of Washington, Seattle WA, United States of America
- 141 Department of Physics and Astronomy, University of Sheffield, Sheffield, United Kingdom
- 142 Department of Physics, Shinshu University, Nagano, Japan
- 143 Department Physik, Universität Siegen, Siegen, Germany
- 144 Department of Physics, Simon Fraser University, Burnaby BC, Canada
- 145 SLAC National Accelerator Laboratory, Stanford CA, United States of America
- 146 (a) Faculty of Mathematics, Physics & Informatics, Comenius University, Bratislava; (b) Department of Subnuclear Physics, Institute of Experimental Physics of the Slovak Academy of Sciences, Kosice, Slovak Republic
- 147 (a) Department of Physics, University of Cape Town, Cape Town; (b) Department of Physics, University of Johannesburg, Johannesburg; (c) School of Physics, University of the Witwatersrand, Johannesburg, South Africa
- 148 (a) Department of Physics, Stockholm University; (b) The Oskar Klein Centre, Stockholm, Sweden
- 149 Physics Department, Royal Institute of Technology, Stockholm, Sweden
- 150 Departments of Physics & Astronomy and Chemistry, Stony Brook University, Stony Brook NY, United States of America
- 151 Department of Physics and Astronomy, University of Sussex, Brighton, United Kingdom
- 152 School of Physics, University of Sydney, Sydney, Australia
- 153 Institute of Physics, Academia Sinica, Taipei, Taiwan
- 154 Department of Physics, Technion: Israel Institute of Technology, Haifa, Israel
- 155 Raymond and Beverly Sackler School of Physics and Astronomy, Tel Aviv University, Tel Aviv, Israel
- 156 Department of Physics, Aristotle University of Thessaloniki, Thessaloniki, Greece
- 157 International Center for Elementary Particle Physics and Department of Physics, The University of Tokyo, Tokyo, Japan
- 158 Graduate School of Science and Technology, Tokyo Metropolitan University, Tokyo, Japan
- 159 Department of Physics, Tokyo Institute of Technology, Tokyo, Japan
- 160 Tomsk State University, Tomsk, Russia
- 161 Department of Physics, University of Toronto, Toronto ON, Canada
- 162 (a) INFN-TIFPA; (b) University of Trento, Trento, Italy
- 163 (a) TRIUMF, Vancouver BC; (b) Department of Physics and Astronomy, York University, Toronto ON, Canada
- 164 Faculty of Pure and Applied Sciences, and Center for Integrated Research in Fundamental Science and Engineering, University of Tsukuba, Tsukuba, Japan
- 165 Department of Physics and Astronomy, Tufts University, Medford MA, United States of America
- 166 Department of Physics and Astronomy, University of California Irvine, Irvine CA, United States of

America

¹⁶⁷ (a) INFN Gruppo Collegato di Udine, Sezione di Trieste, Udine; (b) ICTP, Trieste; (c) Dipartimento di Chimica, Fisica e Ambiente, Università di Udine, Udine, Italy

¹⁶⁸ Department of Physics and Astronomy, University of Uppsala, Uppsala, Sweden

¹⁶⁹ Department of Physics, University of Illinois, Urbana IL, United States of America

¹⁷⁰ Instituto de Fisica Corpuscular (IFIC), Centro Mixto Universidad de Valencia - CSIC, Spain

¹⁷¹ Department of Physics, University of British Columbia, Vancouver BC, Canada

¹⁷² Department of Physics and Astronomy, University of Victoria, Victoria BC, Canada

¹⁷³ Department of Physics, University of Warwick, Coventry, United Kingdom

¹⁷⁴ Waseda University, Tokyo, Japan

¹⁷⁵ Department of Particle Physics, The Weizmann Institute of Science, Rehovot, Israel

¹⁷⁶ Department of Physics, University of Wisconsin, Madison WI, United States of America

¹⁷⁷ Fakultät für Physik und Astronomie, Julius-Maximilians-Universität, Würzburg, Germany

¹⁷⁸ Fakultät für Mathematik und Naturwissenschaften, Fachgruppe Physik, Bergische Universität Wuppertal, Wuppertal, Germany

¹⁷⁹ Department of Physics, Yale University, New Haven CT, United States of America

¹⁸⁰ Yerevan Physics Institute, Yerevan, Armenia

¹⁸¹ Centre de Calcul de l'Institut National de Physique Nucléaire et de Physique des Particules (IN2P3), Villeurbanne, France

¹⁸² Academia Sinica Grid Computing, Institute of Physics, Academia Sinica, Taipei, Taiwan

^a Also at Department of Physics, King's College London, London, United Kingdom

^b Also at Institute of Physics, Azerbaijan Academy of Sciences, Baku, Azerbaijan

^c Also at Novosibirsk State University, Novosibirsk, Russia

^d Also at TRIUMF, Vancouver BC, Canada

^e Also at Department of Physics & Astronomy, University of Louisville, Louisville, KY, United States of America

^f Also at Physics Department, An-Najah National University, Nablus, Palestine

^g Also at Department of Physics, California State University, Fresno CA, United States of America

^h Also at Department of Physics, University of Fribourg, Fribourg, Switzerland

ⁱ Also at II Physikalisches Institut, Georg-August-Universität, Göttingen, Germany

^j Also at Departament de Fisica de la Universitat Autònoma de Barcelona, Barcelona, Spain

^k Also at Departamento de Fisica e Astronomia, Faculdade de Ciencias, Universidade do Porto, Portugal

^l Also at Tomsk State University, Tomsk, and Moscow Institute of Physics and Technology State University, Dolgoprudny, Russia

^m Also at The Collaborative Innovation Center of Quantum Matter (CICQM), Beijing, China

ⁿ Also at Università di Napoli Parthenope, Napoli, Italy

^o Also at Institute of Particle Physics (IPP), Canada

^p Also at Horia Hulubei National Institute of Physics and Nuclear Engineering, Bucharest, Romania

^q Also at Department of Physics, St. Petersburg State Polytechnical University, St. Petersburg, Russia

^r Also at Borough of Manhattan Community College, City University of New York, New York City, United States of America

^s Also at Department of Financial and Management Engineering, University of the Aegean, Chios, Greece

^t Also at Centre for High Performance Computing, CSIR Campus, Rosebank, Cape Town, South Africa

^u Also at Louisiana Tech University, Ruston LA, United States of America

^v Also at Institutio Catalana de Recerca i Estudis Avancats, ICREA, Barcelona, Spain

^w Also at Department of Physics, The University of Michigan, Ann Arbor MI, United States of America

- ^x Also at Graduate School of Science, Osaka University, Osaka, Japan
- ^y Also at Fakultät für Mathematik und Physik, Albert-Ludwigs-Universität, Freiburg, Germany
- ^z Also at Institute for Mathematics, Astrophysics and Particle Physics, Radboud University Nijmegen/Nikhef, Nijmegen, Netherlands
- ^{aa} Also at Department of Physics, The University of Texas at Austin, Austin TX, United States of America
- ^{ab} Also at Institute of Theoretical Physics, Iliia State University, Tbilisi, Georgia
- ^{ac} Also at CERN, Geneva, Switzerland
- ^{ad} Also at Georgian Technical University (GTU), Tbilisi, Georgia
- ^{ae} Also at Ochadai Academic Production, Ochanomizu University, Tokyo, Japan
- ^{af} Also at Manhattan College, New York NY, United States of America
- ^{ag} Also at The City College of New York, New York NY, United States of America
- ^{ah} Also at Departamento de Fisica Teorica y del Cosmos, Universidad de Granada, Granada, Portugal
- ^{ai} Also at Department of Physics, California State University, Sacramento CA, United States of America
- ^{aj} Also at Moscow Institute of Physics and Technology State University, Dolgoprudny, Russia
- ^{ak} Also at Departement de Physique Nucleaire et Corpusculaire, Université de Genève, Geneva, Switzerland
- ^{al} Also at Institut de Física d'Altes Energies (IFAE), The Barcelona Institute of Science and Technology, Barcelona, Spain
- ^{am} Also at School of Physics, Sun Yat-sen University, Guangzhou, China
- ^{an} Also at Institute for Nuclear Research and Nuclear Energy (INRNE) of the Bulgarian Academy of Sciences, Sofia, Bulgaria
- ^{ao} Also at Faculty of Physics, M.V.Lomonosov Moscow State University, Moscow, Russia
- ^{ap} Also at National Research Nuclear University MEPhI, Moscow, Russia
- ^{aq} Also at Department of Physics, Stanford University, Stanford CA, United States of America
- ^{ar} Also at Institute for Particle and Nuclear Physics, Wigner Research Centre for Physics, Budapest, Hungary
- ^{as} Also at Giresun University, Faculty of Engineering, Turkey
- ^{at} Also at CPPM, Aix-Marseille Université and CNRS/IN2P3, Marseille, France
- ^{au} Also at Department of Physics, Nanjing University, Jiangsu, China
- ^{av} Also at Institute of Physics, Academia Sinica, Taipei, Taiwan
- ^{aw} Also at University of Malaya, Department of Physics, Kuala Lumpur, Malaysia
- ^{ax} Also at LAL, Univ. Paris-Sud, CNRS/IN2P3, Université Paris-Saclay, Orsay, France
- * Deceased